Sjournals
Scientific Journals
Scientific Journal of Pure and Applied Sciences (2013) 2(12) 401-460
ISSN 2322-2956
doi: 10.14196/sjpas.v2i12.1117

Contents lists available at Sjournals
Scientific Journal of
Pure and Applied Sciences
Journal homepage: www.Sjournals.com

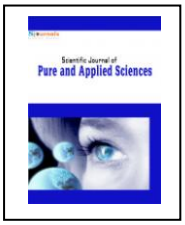

Original article

Definiability of combinatorial functions and their linear recurrence relationships within a polylogarithmic triangularizable matrix employing surjective bilipschitz functions and other isomorphisms of metric spaces for forecasting seasonal endemic onchocerciasis transmission zones in Burkina Faso

B.G. Jacob[a,*], R.J. Novak[a], L. Toe[b], M.S. Sanfo[b], S. Caliskhan[a], R. Tingueria[e], A. Pare[d], M. Noma[b], L. Yameogo[c], T.R. Unnasch[a]

[a]*Global Infectious Disease Research Program, Department of Public Health, College of Public Health, University of South Florida, 3720 Spectrum Blvd, Suite 304, Tampa, Florida, USA 33612.*
[b]*MultiDisease Surveillance Centre (MDSC) 1473, Avenue Naba Zombre, 01 B.P 549 Ouagadougou 01 Burkina Faso.*
[c]*African Programme for Onchocerciasis Control (APOC)1473, Avenue Naba Zombre, 01 B.P 549 Ouagadougou 01 Burkina Faso.*
[d]*Ministere de la Sante Ouagadougou Burkina Faso.*
[e]*School of Economic, Political and Policy Sciences. The University of Texas at Dallas, 800 West Campbell Road, Richardson, TX 75080-302.*

*Corresponding author; Global Infectious Disease Research Program, Department of Public Health, College of Public Health, University of South Florida, 3720 Spectrum Blvd, Suite 304, Tampa, Florida, USA 33612.

ARTICLE INFO

Article history:
Received 02 November 2013
Accepted 20 November 2013
Available online 31 December 2013

Keywords:
Prevalence
Random effects
Onchocerciasis
Autocorrelation

ABSTRACT

In this research, prevalence values based on Monthly Biting Rates (MBR) were employed as a response variable in a Poisson probability model framework for quantitatively regressing multiple georefernced explanatory environmental-related explanatory covariates of seasonally-sampled larval habitat of Similium damnosum s.l.a black fly vector of Onchocerciasis in a riverine study site in Burkina Faso. Results from both a Poisson and then a negative binomial (i.e., a Poisson random variable with a gamma distrusted mean) revealed that the covariates rendered from the model were significant, but furnished virtually no predictive power for mapping endemic transmission zones. Inclusion of indicator variables denoting the time sequence and the locational spatial structure was then articulated with Thiessen polygons which also failed to reveal

meaningful covariates. Thereafter, a spatiotemporal autocorrelation analyses was performed and an Autoregressive Integrated Moving Average (ARIMA) model was constructed which revealed a prominent first-order temporal autoregressive structure in the sampled covariate coefficients. A random effects term was then specified which included a specific intercept term that was a random deviation from the overall intercept term based on a draw from a normal frequency distribution. The specification revealed a non-constant mean across the riverine study site. This random intercept represented the combined effect of all omitted covariates that caused the sampled georeferenced riverine –based villages at the study site to be more prone to onchocerciasis based on regressed seasonal prevalence rates. Additionally, inclusion of a random intercept assumed random heterogeneity in the propensity or, underlying risk of onchocerciasis which persisted throughout the entire duration of the time sequence under study. This random effects term displayed serial correlation, and conformed closely to a bell-shaped curve. The model's variance implied a substantial variability in the prevalence of onchocerciasis across the study site based on the spatiotemporal-sampled covariates. The model contained considerable overdispersion (i.e., excess Poisson variability): quasi-likelihood scale = 69.565. The following equation was then used to translate and forecast the expected classification value of the prevalence of onchocerciasis into hyperendemic(0-km), (5km to 10 km) mesoendemic,(10-15km) hypoendemic transmission zones at the study site based on the sampled S. damnosum s.l. prevalence rate = exp[-2.9147 + (random effect)i]. Seasonally quantitating random effects term estimates, allowing research intervention teams to improve the quality of the forecasts for future onchocerciasis-related predictive autoregressive regression risk-based modeling efforts based on field-sampled S. damnosums.l. explanatory covariates.

1. Introduction

Onchocerciasis is one of the most important causes of blindness worldwide. The disease is caused by the filarial nematode parasite Onchocerca volvulus (www.who.com). The parasite is transmitted by black flies (Similium damnosum s.l.) that develops as larvae in fast running rivers and streams. As such, disease transmission is most intense in and around the river basins, rendering many such areas uninhabitable by migrating human populations. Unfortunately, the areas bordering the river basins contain much of the fertile land in sub-Saharan African savanna ecosystems. This means that these flies are quite localized within lotic ecosystems in sub-Saharan Africa. This also means that unlike malaria and many other tropical diseases, the distance that an adult black fly can disperse from its riverine origin in search of a blood meal can be employed as an explanatory covariate coefficient to delineate the geographic distribution of onchocerciasis in a regression- based model to forecast endemic (e.g., hyperendemic, mesoendemic, hypoendemic) transmission zones.

Historically, regression modeling spatiotemporal-sampled S. damnosum s.l.riverine larval habitats has been based on a Poisson distributions in SAS (e.g., PROC GEN MOD) using a single seasonal-sampled dataset of density-related count data (e.g., larval, adult) for simulating and forecasting endemic transmission-oriented linear-related probability risk mapping regions (Jacob et al., 2012; Toe et al., 1997; Boatin et al., 1997). In probability theory and

statistics, the Poisson distribution in SAS is a discrete probability distribution that expresses the probability of a given number of events occurring in a fixed interval of time and/or space if, these events occur with a known average rate and are independent of any previous time series related similar sampling events. Given an empirical spatiotemporal dataset of S. damnosum s.l. –related explanatory covariate coefficients θ and an input vector x, the mean of the predicted Poisson distribution can then be provided by $\mathrm{E}(Y|x) = e^{\theta' x}$ (Haight, 1967). Thereafter, the Poisson distribution's probability mass function can be calculated by $p(y|x;\theta) = \frac{[\mathrm{E}(Y|x)]^y \times e^{-\mathrm{E}(Y|x)}}{y!} = \frac{e^{y\theta' x} e^{-e^{\theta' x}}}{y!}$. For example, if a vector ecologist is given an empirical spatiotemporal dataset consisting of m vectors $x_i \in \mathbb{R}^{n+1}$, $i = 1, ..., m$, along with a set of m geosampled S. damnosum s.l. explanatory covariate coefficient values $y_1, \ldots, y_m \in \mathbb{R}$ (e.g., prevalence rates Monthly biting rates,) then, for the given parameters estimators θ, the probability of attaining a particular optimal empirical-based subset of hierarchically forecasted covariates of significance can be parsimoniously rendered by $p(y_1, \ldots, y_m | x_1, \ldots, x_m; \theta) = \prod_{i=1}^{m} \frac{e^{y_i \theta' x_i} e^{-e^{\theta' x_i}}}{y_i!}$. (McCulloch and Searle, 2005). By then employing a method of maximum likelihood, the empirical dataset of θ would the predicted probability as large as possible to seasonally quantitate Euclidean distance-based thresholds of endemic regions. To do this, the time series dependent linear S. damnosum s.l.-related predictive regression equation must be first written as a likelihood function in terms of θ: $L(\theta|X,Y) = \prod_{i=1}^{m} \frac{e^{y_i \theta' x_i} e^{-e^{\theta' x_i}}}{y_i!}$. Note, the expression on the right hand side of the equation has not actually changed in this expression thus, any sampled explanatory covariate coefficient variability may be mispecified. As such, any residually forecasted estimates from any time series dependent regression-based endemic transmission-oriented formula would be impossible to work with.

A log-likelihood [e.g., $\ell(\theta|X,Y) = \log L(\theta|X,Y) = \sum_{i=1}^{m} \left(y_i \theta' x_i - e^{\theta' x_i} - \log(y_i!) \right)$] [1.1]may then be employed for accurately regressing spatiotemporal geopredictive S. damnosum s.l.-related endemic transmission-oriented parameter estimators. In such circumstances the estimator θ would only appear in the first two terms of each term in the summation. Given that generally an infectious disease vector ecologist is usually only interested in finding the optimal covariate coefficient value for θ ,associated to a productive seasonal- sampled riverine habitats [1,2,3]based on spatiotemporal field-sampled count data $\ell(\theta|X,Y) = \sum_{i=1}^{m} \left(y_i \theta' x_i - e^{\theta' x_i} \right)$ .may be instead employed by dropping the yi! The only requirement to quantitate a robust maximum threshold, thereafter, would be to insert an additional estimator [e.g., $\frac{\partial \ell(\theta|X,Y)}{\partial \theta} = 0$] in the predictive regression-based equation. After doing so, the negative log-likelihood, $-\ell(\theta|X,Y)$, would be represented as a convex function, and so standard convex optimization techniques such as gradient descent may then be applied to find the optimal value of θ in a seasonal geopredictive map targeting onchocerciasis endemic transmission zones.

In gradient-descent methods, the parameter vector is a column vector with a fixed number of real-valued components, $\vec{\theta}_t = (\theta_t(1), \theta_t(2), \ldots, \theta_t(n))^T$ (the `T' here denotes transpose), and $V_t(s)$ is a smooth differentiable function of $\vec{\theta}_t$ for all $s \in \mathcal{S}$ (Haight, 1967). This first-order optimization algorithm may solve a system of linear geopredictive onchocerciasis endemic transmission regression-based equations in a robust spatiotemporal model by reformulating the model within a quadratic minimization framework (e.g., least squares). Solution of $A\mathbf{x} - \mathbf{b} = 0$ in the sense of linear least squares can then be defined by minimizing the function $F(x) = \|A\mathbf{x} - \mathbf{b}\|^2$ in the model. In traditional linear least squares for real A and b, the Euclidean norm is commonly applied in which case $\nabla F(\mathbf{x}) = 2A^T(A\mathbf{x} - \mathbf{b})$ (McCulloch and Searle, 2005). In this case, the line search minimization for locating the locally optimal step size γ on every iteration in the spatiotemporal geopredictive onchocerciasis endemic transmission-oriented model, can be calculated analytically utilizing explicit formulas for seasonally quantitating the locally known optimal γ sampled values associated to endemic

transmission sites. To find a local minimum of a function in the spatiotemporal endemic transmission-oriented onchocerciasis-related gradient descent predictive model thereafter, would require simply taking steps proportional to ascertaining the negative of the gradient or, of the approximate gradient of the function at a specific ground control point (e.g., capture point). Gradient descent is based on the observation that if the multivariable function $F(\mathbf{x})$ is defined and differentiable in a neighborhood of a point $\mathbf{a}$, then $F(\mathbf{x})$ decreases fastest if, the computation goes from $\mathbf{a}$ in the direction of the negative gradient of F at $\mathbf{a}$, [i.e., $-\nabla F(\mathbf{a})$](McCulloch and Searle, 2005). It thus, follows that if, $\mathbf{b} = \mathbf{a} - \gamma \nabla F(\mathbf{a})$ for $\gamma \to 0$ varying ArcGIS Euclidean-distance based seasonal-sampled endemic transmission-oriented measurements in the empirical sampled time-series dependent S. damnosum s.l. observational dataset then the significance of the explanatory covariates can be determined then $F(\mathbf{a}) \geq F(\mathbf{b})$.

With this observation in mind, any infectious disease vector ecologist could quantitate $\mathbf{x}_0$ for a local minimum of F, and then consider the sequence $\mathbf{x}_0, \mathbf{x}_1, \mathbf{x}_2, \cdots$ such that $\mathbf{x}_{n+1} = \mathbf{x}_n - \gamma_n \nabla F(\mathbf{x}_n),\ n \geq 0$ based on seasonal sampled. onchocerciasis endemic-related transmission-oriented ArcGIS-Euclidean distance-based estimators. Thereafter, the series $F(\mathbf{x}_0) \geq F(\mathbf{x}_1) \geq F(\mathbf{x}_2) \geq \cdots$, can be employed so the sequence $(\mathbf{x}_n)$ can converge to the desired local minimum for comparing the distance-based measurements. Note, that the value of the step size γ can be allowed to change at every iteration during the endemic transmission risk model construction phase. With certain assumptions, however, on the function F, F convex and ∇F, Lipschitz and particular choices of γ (e.g., a line search that satisfies the Wolfe conditions) the sampled S. damnosum s.l. riverine larval habitat explanatory covariate coefficients would converge to a local minimum. In the unconstrained minimization problem, the Wolfe conditions are a set of inequalities for performing inexact line search, especially in quasi-Newton methods whereby, a univariate function ϕ is restricted to the direction $\mathbf{p}_k$ as $\phi(\alpha) = f(\mathbf{x}_k + \alpha \mathbf{p}_k)$ (McCulloch and Searle, 2005). In optimization, quasi-Newton methods (i.e., a special case of variable metric techniques) quantitate local maxima and minima of functions based on assumptions that function are locally approximated as a quadratic in the region around the optimum employing first and second derivatives (Nielsen, 1897). Therefore, hypothetically, a step length α_k could satisfy the Wolfe conditions in a spatiotemporal geopredictive onchocerciasis endemic transmission-oriented ArcGIS/SAS based model if, the following two inequalities hold: $f(\mathbf{x}_k + \alpha_k \mathbf{p}_k) \leq f(\mathbf{x}_k) + c_1 \alpha_k \mathbf{p}_k^{\mathrm{T}} \nabla f(\mathbf{x}_k)$ and $\mathbf{p}_k^{\mathrm{T}} \nabla f(\mathbf{x}_k + \alpha_k \mathbf{p}_k) \geq c_2 \mathbf{p}_k^{\mathrm{T}} \nabla f(\mathbf{x}_k)$ with $0 < c_1 < c_2 < 1$; whereby, $\mathbf{p}_k$ would be a descent direction of forecasted onchocerciasis endemic transmission zones based on $\mathbf{p}_k^{\mathrm{T}} \nabla f(\mathbf{x}_k) < 0\, c_1$. Subsequently, Gradient descent can also be employed to solve a system of nonlinear onchocerciasis. endemic transmission-oriented predictive regression-based equations (e.g., spatial autocovariate).

Unfortunately, gradient descent has problems with pathological functions such as the Rosenbrock function [i.e, $f(x_1, x_2) = (1 - x_1)^2 + 100(x_2 - x_1^2)^2$]. Commonly, the Rosenbrock function has a narrow curved valley which contains the minimum values. Therefore, the "bottom of the valley" in the spatiotemporal geopredictive onchocerciasis endemic transmission ArcGIS/SAS-based model may be very flat regardless of regression outcomes. Because of the curved flat valley, the optimization would then "zig-zag": slowly with small step sizes in the endemic transmission–oriented risk model towards the minimum threshold values for delineating the transmission-oriented explanatory covariate coefficients. The global minimum would therefore be inside a long, narrow, parabolic shaped flat valley. Regardless, to find the valley in a robust predictive onchocerciasis endemic transmission-oriented model would still be rather difficult. For example, to converge to the global minimum may require employing another a spatial autocorrelation algorithm (e.g., eigenfunction decomposition). Other limitations for employing gradient descent for constructing a robust spatiotemporal geopredictive endemic transmission-oriented onchocerciasis model would be that the residuals would be relatively slow close and, as such, the asymptotic rate of convergence in the model residual forecasts would be of inferior quality. For example, suppose that the sequence {X} converges to the number L in the model. This sequence would then converge linearly to L, if there exists sampled endemic transmission-oriented explanatory covariates μ ∈ (0, 1) such that $\lim_{k \to \infty} \frac{|x_{k+1} - L|}{|x_k - L|} = \mu.$ The number μ in the geopredictive ArcGIS/SAS-based risk model would then represent

the rate of convergence. If the sequence converges, and μ = 0, then the sequence would converge superlinearly and if μ = 1, then the sequence is said to converge sublinearly. If the sequence converges sublinearly in the ArcGIS/SAS-based onchocerciasis endemic transmission-oriented riverine model and additionally $\lim_{k\to\infty} \frac{|x_{k+2} - x_{k+1}|}{|x_{k+1} - x_k|} = 1,$ then the sequence {xk} would converge logarithmically to L thus indicating prolific endemic areas on a risk map. A vector ecologist may also distinguish super linear rates of convergence. As such, in the time series onchocerciasis endemic transmission -oriented model the sequence could be understood to converge with order q to L for q>1 $\lim_{k\to\infty} \frac{|x_{k+1} - L|}{|x_k - L|^q} = \mu \,|\, \mu > 0$ which would then indicate all Euclidean-distance based thresholds. This may however require convergence with order 2 (i.e., quadratic convergence)or 3 (e.g., cubic convergence) such as commonly encountered in Q-linear convergence and Q-quadratic convergence.

For poorly conditioned convex problems in the time series onchocerciasis endemic transmission oriented model, the gradient descent would then increasingly zigzag as the gradients point (e.g., georefernced stratified village boundaries) then would be nearly orthogonal to the shortest direction to a minimum point (e.g., georeferenced epidemiological riverine capture point). Although locally Lipschitz problems and convex minimization problems can render bundle methods of descent which could be well-defined unfortunately, the forecasted residual non-differentiable functions would be ill-defined. A function which jumps is not differentiable at the jump nor is one which has a cusp, like |x| has at x = 0 (Toe et al., 1997).

Given two metric spaces (X, dX) and (Y, dY), where dX denotes the metric on the set X and dY is the metric on set Y (for example, Y might be the set of real numbers R with the metric dY(x, y) = |x − y|, and X might be a subset of R), a function f : X → Y is called Lipschitz continuous if there exists a real constant K ≥ 0 such that, for all x1 and x2 in X, $d_Y(f(x_1), f(x_2)) \leq K d_X(x_1, x_2)$, 92]Any such K is referred to as a Lipschitz constant for the function f. The smallest constant is sometimes called the (best) Lipschitz constant; however in most cases the latter notion is less relevant. If K = 1 the function is called a short map, and if 0 ≤ K < 1 the function is called a contraction. The inequality is (trivially) satisfied if x1 = x2. Otherwise, one can equivalently define a function to be Lipschitz continuous if and only if there exists a constant K ≥ 0 such that, for all x1 ≠ x2, $\frac{d_Y(f(x_1), f(x_2))}{d_X(x_1, x_2)} \leq K.$ For real-valued functions of several real variables, this holds if and only if the absolute value of the slopes of all secant lines are bounded by K. The set of lines of slope K passing through a point on the graph of the function forms a circular cone, and a function is Lipschitz if and only if the graph of the function everywhere lies completely outside of this cone.

Further a function is called locally Lipschitz continuous, if for every x in X there exists a neighborhood U of x such that f restricted to U is Lipschitz continuous(McCulloch and Searle, 2005). Equivalently, if X is a locally compact metric space, then f is locally Lipschitz if and only if it is Lipschitz continuous on every compact subset of X. In spaces that are not locally compact, this is a necessary but not a sufficient condition. More generally, a function f defined on X is said to be Hölder continuous or to satisfy a Hölder condition of order α > 0 on X if there exists a constant M > 0 such that $d_Y(f(x), f(y)) \leq M d_X(x, y)^\alpha$ for all x and y in X.

Hölder spaces consist of functions satisfying a Hölder condition that are basic in areas of functional analysis relevant to solving partial differential equations in dynamical systems (Toe et al., 1997). The Hölder space Ck, α(Ω), is where Ω is an open subset of some Euclidean space and k ≥ 0 an integer, consisting of those functions on Ω having continuous derivatives up to order k, such that the kth partial derivatives are Hölder continuous with exponent α, where 0 < α ≤ 1(McCulloch and Searle, 2005). Sometimes a Hölder condition of order α is also called a uniform Lipschitz condition of order α > 0.Therefore , in a spatiotemporal geopredictive onchocerciasis endemic transmission model, a Hölder space would be a locally convex topological vector space.

The category of topological vector spaces over a given topological field K can then commonly denoted TVSK or TVectK. The objects would then be the topological vector spaces over K and the morphisms which would be the continuous K-linear predictive time series dependent onchocerciasis endemic transmission-oriented ArcGIS/SAS-based risk maps. For example, if the Hölder coefficient $|f|_{C^{0,\alpha}} = \sup_{x,y\in\Omega,\ x\neq y} \frac{|f(x) - f(y)|}{|x - y|^\alpha},$ is finite, in the endemic transmission model residual forecasts, then the function f would be said to be uniformly Hölder

continuous with exponent α in Ω. In such circumstances, the Hölder coefficients would serve as a seminorm in the endemic transmission-oriented model residual forecasts targeting the statistically significant endemic transmission-oriented explanatory covariate coefficients. If the Hölder coefficient was merely bounded on compact subsets of Ω, then the function f could be categorized locally into Hölder continuous variables with exponent α in Ω. Additionally, if the function f and its derivatives up to order k are bounded on the closure of Ω in the spatiotemporal onchocerciasis endemic transmission model residuals, then the Hölder space $C^{k,\alpha}(\bar{\Omega})$could be assigned the norm $\|f\|_{C^{k,\alpha}} = \|f\|_{C^k} + \max_{|\beta|=k} |D^\beta f|_{C^{0,\alpha}}$when β ranges over the multi-indices in the model and $\|f\|_{C^k} = \max_{|\beta|\le k} \sup_{x\in\Omega} |D^\beta f(x)$.These norms and seminorms could then be theoretically denoted simply $|f|_{0,\alpha}$ and $\|f\|_{k,\alpha}$or, also $|f|_{0,\alpha,\Omega}$and $\|f\|_{k,\alpha,\Omega}$in order to stress the dependence on the domain of f in the geopredictive endemic transmission-oriented risk model residual forecasts .

Further, if Ω is open and bounded, then $C^{k,\alpha}(\bar{\Omega})$would be a Banach space in the predictive S. endemic transmission risk model with respect to the norm $\|\cdot\|_{C^{k,\alpha}}$. A normed space X is said to be a Banach space if, for every Cauchy sequence $\{x_n\}_{n=1}^{\infty} \subset X$there exists an element x in X such that $\lim_{n\to\infty} x_n = x$(McCulloch and Searle, 2005). A sequence$x_1, x_2, x_3, \cdots$of real numbers is called Cauchy, if for every positive real number ε, there is a positive integer N such that for all natural numbers m, n > N$|x_m - x_n| < \varepsilon$,where the vertical bars denote the absolute value (Toe et al., 1997). Therefore, a Cauchy sequence would be q sequence in a predictive spatiotemporal geopredictive onchocerciasis endemic transmission model whose elements become arbitrarily close to each other as the sequence progression for classifying endemic transmission zones based on spatiotemporal field-sampled count data. More precisely, given any small distance (e.g., Euclidean distance ArcGIS/SAS-based measurement from a prevalence stratified village), all but a finite number of sampled elements of the sequence would be spatiotemporally quantitated employing the aggregated seasonal-sampled measurements.

In terms of Lipschitz and Hölder continuous functions in a predictive spatiotemporal riverine larval habitat endemic transmission-oriented model, the argument rendered may prove slightly more efficient, especially if ,{fn} is a uniformly bounded sequence of real-valued functions on [a,b] such that each ƒ is Lipschitz continuous with the same Lipschitz constant K: $|f_n(x) - f_n(y)| \le K|x - y|$whereby all x, y ∈[a,b] and all fn, represent a subsequence residual forecast that converges uniformly on [a,b]. The limit function in the endemic transmission-oriented risk model would thereafter render Lipschitz continuous with the same value K for the Lipschitz constant. A slight refinement in the seasonal predictive model may be also then attained by employing a set F of functions ƒ on [a, b] that are uniformly bounded for satisfying a Hölder condition of order α, 0 < α ≤ 1, within a fixed constant M, $|f(x) - f(y)| \le M\,|x - y|^\alpha, \quad x, y \in [a, b]$. The onchocerciasis endemic transmission-oriented model then would be relatively compact in C([a, b]). In particular, the unit ball of the Hölder space C 0, α([a, b]) would be compact in C([a, b]). Unfortunately, sometimes a Hölder condition of order α like a uniform Lipschitz condition of order α > 0 may not exist in the predictive residuals as a K ≥ 1 wit $\frac{1}{K} d_X(x_1, x_2) \le d_Y(f(x_1), f(x_2)) \le K d_X(x_1, x_2)$. In such circumstances ƒ would then be a bilipschitz.

Another alternative for non-differentiable functions in an endemic transmission-oriented model would be to "smooth" the function, or bound the function by a smooth function.. Many attempts already exists, in particular,the so-called fractional derivative of Riemann–Liouville, Liouville Weyl, and Marchaud [1, 16]. The Riemann–Liouville integral is defined by $$I^\alpha f(x) = \frac{1}{\Gamma(\alpha)} \int_a^x f(t)(x - t)^{\alpha-1}\, dt$$ where Γ is the Gamma function and a is an arbitrary but fixed base point. The integral is well-defined provided ƒ is a locally integrable function, and α is a complex number in the half-plane re(α) > 0(McCulloch and Searle, 2005). The dependence on the base-point a is often suppressed, and represents a freedom in constant of integration. Clearly I1ƒ is an antiderivative of ƒ (of first order), and for positive integer values of α, Iαƒ is an antiderivative of order α by Cauchy formula for repeated integration. Another notation, which emphasizes the basepoint, is[

$$ {}_aD_x^{-\alpha} f(x) = \frac{1}{\Gamma(\alpha)} \int_a^x f(t)(x-t)^{\alpha-1}\, dt. $$

This also makes sense if a = −∞, with suitable restrictions on f.

The fundamental relations hold $\frac{d}{dx} I^{\alpha+1} f(x) = I^{\alpha} f(x), \quad I^{\alpha}(I^{\beta} f) = I^{\alpha+\beta} f,$ the latter of which is a semigroup property (Jacob, et., 2012). These properties make possible not only the definition of fractional integration, but also of fractional differentiation, by taking enough derivatives of Iαf.

Unfortuntely Riemann–Liouville integral are based on a generalization of the Cauchy formula. Hence, there is no geometric idea supporting these generalizations for, explaining the difficulties of using it in order to obtain information about the structure of non-differentiable objects in a geopredictive onchocerciasis endemic trasnmission oriented model. Moreover, fractional derivatives are all non-local on the contrary of the classical derivative. For example, the Riemann–Liouville for a onchocerciasis endemic transmission oriented model derivative would depend on a free parameter which relies on a global information on the function. The study of non-differentiable functions via these operators would then be difficult. Although Kolvankar and Gangal developed the notion of local fractional derivative by allowing a fine study of the local structure of irregular (i.e., fractal) functions this tool would not extend classical theorems of analysis (e.g., extrema, Rolle) for quantitating non-differentiable functions in a onchocerciasis sis geopredictive endemic transmission oriented model. Thus the local fractional derivative would not allow us to obtain precise results on the behavior of non-differentiable functions in the risk model

Further, probability statistics in the endemic. transmission-oriented ArcGIS/SAS-based model can be rendered by the limit of a binomial distribution $P_p(n \mid N) = \frac{N!}{n!\,(N-n)!}\, p^n\, (1-p)^{N-n}.$. In these models the binomial distribution can provide the discrete probability distribution $P_p(n \mid N)$ for obtaining exactly n successes (e.g., predicted and field-validated prolific sampled larval habitat areas based on seasonal-sampled count data) out of N Bernoulli trials but, only when the result of each Bernoulli trial is true and when the probability p is false whereby, the probability $q = 1 - p$ is mandated in the regression estimation procedure. Bernoulli trials consists of independent trials with two outcomes with constant probabilities from trial to trial which can lead to generating several important probability distributions: (e.g., binomial, geometric, and negative binomial) (Toe et al., 1997). A discrete S. damnosum s.l. –related probability distribution derived from regressing time series dependent Euclidean distance based measurements can then be derived as a probability distribution characterized by a probability mass function (pmf). In probability theory and statistics, a probability mass function is a function that provides the probability that a discrete random variable is exactly equal to some value (Boatin et al., 1997).The pmf may thus be the primary means for defining a discrete geopredicted probability distribution in a spatiotemporal regression equation where functions exist for either scalar or multivariate random variables, given that the distribution is discrete (Jacob, et., 2012).

Further, this spatiotemporal quantitated pmf would allow a randomly forecasted single seasonal- sampled onchocerciasis endemic transmission-oriented model explanatory observational geopredictor variable to assume only a finite or count ably infinite number of the sampled values. The pmf is often the primary means of defining a discrete infectious disease arthropod--borne time series –related probability distribution, and such functions exist for either scalar or multivariate random variables, given that the distribution is discrete (Toe et al., 1997). For example, Jacob et al. (2012) supposed that X: S → A (A $\subseteq$ R) was a discrete random variable in a robust seasonal sampled ArcGIS/SAS-based risk model which was defined on a sample space S where the pmf fX: A → [0, 1] for X was defined as $f_X(x) = \Pr(X = x) = \Pr(\{s \in S : X(s) = x\})$:for forecasting prolific habitats in a stochastic interpolator. Note that fX in the model was defined for all the sampled riverine larval habitat sampled values including those not in X therefore , fX(x) = 0 represented x $\notin$ X(S) in the residual forecasts. The same definition was applied for a discrete multivariate random variable dataset where X: S → An in a field validation model which was derived in a similar fashion from the seasonal-sampled S. damnosum s.l. riverine larval habitat empirical dataset but employing only that scalar values which the authors replaced by vector values. In their research the probability values for all X were equal to 1 [i.e., $\sum_{x \in A} f_X(x) = 1$]. Since X was countable, the pmf fX(x) in the model

was zero, thereafter, for all but a few explanatory endemic transmission-oriented covariate coefficients values of x. The discontinuity of pmf was then found to be related to the fact that the cumulative distribution function of a discrete random variable was also discontinuous in the model residuals. Thereafter, the authors noted that the seasonal sampled S. damnosum s.l. riverine larval habitat model derivative was zero also when the residual estimates were differentiable and the pmf was zero for all sampled larval habitat points. The binomial distribution was then provided by $P_p(n \mid N) = \binom{N}{n} p^n q^{N-n} = \frac{N!}{n!\,(N-n)!} p^n (1-p)^{N-n}$, where $\binom{N}{n}$ was a binomial coefficient. This procedure allowed parsimonious derivation of robust non-biased linear residual estimators. The final seasonal geopredictive model revealed areas of abundant habitats based on spatiotemporal field-sampled count data.

Note, this parameter estimation regression procedure would have to be statistically altered and expanded for accommodating and regressing a large spatiotemporal-dependent dataset of S. damnosum s.l. riverine larval habitat explanatory covariate coefficients in order to delineate onchocerciasis endemic trasnmission zones. Fortunately, however, the binomial coefficient $\binom{n}{k}$ has a number of ways of selecting k unordered outcomes from n possibilities, also known as a combination or combinatorial number which can help render a suitable matrix and error estimator for an empirical seasonal sampled dataset of explanatory onchocerciasis transmission-oriented regressors. This family of numbers arises in many other areas than algebra, notably in combinatorics. For any empirical dataset containing n elements of seasonal-sampled ArcGIS/SAS-based Euclidean-based measurements, the number of distinct k-element subsets may then be formed by the k-combinations of its elements given by the binomial coefficient $\binom{n}{k}$ [5] Fortunately, the properties of binomial coefficients have led to extending the meaning of the symbol $\binom{n}{k}$ beyond the basic case where n and k are nonnegative integers with k ≤ n; such expressions are then still called binomial coefficients (Haight, 1967). A such, a robust multi-seasonal-sampled onchocerciasis endemic transmission model dataset may then be tested to determine whether C(n, k), nCk, nCk, Ckn, Cnk, may be employed for suitable parameter estimation and residual quantitation of any uncertainty estimates whereby, all the C stands for combinations or various distant based choices georeferenced from a capture point (S. damnosum s.l. riverine larval habitat) 0km to 5km, 5 km to 10km etc.].

For example, the symbols ${}_nC_k$ and $\binom{n}{k}$ may denote a multi-seasonal customized binomial coefficient. For this in a time series empirical dataset the number of k-subsets possible outcomes from a set of n distinct items can be regressed. Thereafter, the number of lattice paths from the origin $(0, 0)$ to a point (a, b) in the forecasted model distribution would then be a family of positive integers that occur as coefficients [i.e., the binomial coefficient $\binom{a+b}{a}$]. The value of the binomial coefficient for nonnegative n and k in the model may then be theoretically rendered explicitly by ${}_nC_k \equiv \binom{n}{k} \equiv \frac{n!}{(n-k)!\,k!}$, in PROC REG, for example, where $z!$ denotes a factorial (wwwsas.edu). Writing the factorial as a gamma function $z! = \Gamma(z+1)$ would then allow the time-series dependent binomial coefficient to be generalized to non-integer arguments including complex x and y as $\binom{x}{y} = \frac{\Gamma(x+1)}{\Gamma(y+1)\,\Gamma(x-y+1)}$. For nonnegative integer arguments, the gamma function would then reduce to $\binom{n}{k} = \begin{cases} \frac{n!}{k!\,(n-k)!} \\ 0 \end{cases}$ factorials, leading to when 0<k<n or, otherwise to Pascal's triangle in the onchocerciasis endemic transmission model resdiual forecast targeting the endemic trasnmission-oriented explanatory covariate coefficients .

Pascal's triangle is a number triangle with numbers arranged in staggered rows such that $a_{nr} \equiv \frac{n!}{r!\,(n-r)!} \equiv \binom{n}{r}$, where $\binom{n}{r}$ is a binomial coefficient (Nielsen, 1897) Pascal's triangle contains the figurate

numbers along its diagonals, as can be seen from the identity $\sum_{i=1}^{n}\binom{i}{j}\frac{n+1}{j+1}\binom{n}{j}=\binom{n+1}{j+1}$.In addition, the sum of the elements of the i th row in a time series dependent model (e.g., multivariate seasonal S. riverine endemic transmission-oriented ArcGIS/SAS-based regression matrix) would be $\sum_{j=0}^{i}\binom{i}{j}=2^i,$ so the sum of the first $k$rows (i.e., rows 0 to $k-1$) would be the Mersenne number$\sum_{i=0}^{k-1}2^i=2^k-1.$ Mersenne number is a number of the form $M_n \equiv 2^n-1,$ where n is an integer consisting of all 1s in base-2, and are therefore binary repunits (Boatin et al., 1997).

The characteristic function for the binomial distribution in the onchcerciasis endemic transmission-oriented regression Euclidean distance –based risk model can then be linearly adjusted and thereafter be represented as $\phi(t)=\left(q+p\,e^{i\,t}\right)^N$ employing the Mersenne number. This linearization would involve viewing the distribution as a function of the expected number of successes $\nu \equiv N\,p$ instead of the sample size $N$for a fixed $p$in the endemic transmission-oriented model. An estimation model that initially is expressed as: $P=\sum_{k=n+1}^{N}\binom{N}{k}p^k\,(1-p)^{N-k}=I_p\,(n+1,N-n),$ would then subsequently transformed, for example, to $P_{\nu/N}\,(n\,|\,N)=\frac{N!}{n!\,(N-n)!}\left(\frac{\nu}{N}\right)^n\left(1-\frac{\nu}{N}\right)^{N-n}$. By so doing, this would allow expanding the multi-seasonal S. damnosum s.l. model sample size quantitation capability. Further, As t N becomes large, the distribution would approach $P_\nu\,(n)=\lim_{N\to\infty}P_p\,(n\,|\,N)$ (i.e., the Poisson distribution). It is important to mention that the sample size N would completely drop out of the probability function in the lineally transformed endemic transmission-oriented model but, it would still have the same functional form for all the spatiotemporally-sampled values of v. Thereafter, the Poisson distribution can be normalized so that the sum of probabilities in the multi-multiseasonal onchocerciasis endemic trasnmission-oriented model equals 1, since $\sum_{n=0}^{\infty}P_\nu\,(n)=e^{-\nu}\sum_{n=0}^{\infty}\frac{\nu^n}{n!}=e^{-\nu}\,e^{\nu}=1.$ (Toe et al., 1997). The ratio of probabilities of the sampled Euclidean-based ArcGIS/SAS-based explanatory regression-based explanatory covariate coefficients could then be rendered by $\frac{P_\nu\,(n=i+1)}{P\,(n=i)}=\frac{\frac{\nu^{i+1}\,e^{-\nu}}{(i+1)!}}{\frac{e^{-\nu}\,\nu^i}{i!}}=\frac{\nu}{i+1}.$ .The Poisson distribution would however would reach a maximum when $\frac{d\,P_\nu\,(n)}{d\,n}=\frac{e^{-\nu}\,n\,(\gamma-H_n+\ln\nu)}{n!}=0,$ where γ would eventually become the Euler-Mascheroni constant .

The Euler-Mascheroni constant γcan be defined in the onchocerciasis endemic transmission-oriented regression Euclidean distance –based ArcGIS/SAS-based risk model as the limit of the sequence $\gamma=\lim_{n\to\infty}\left(\sum_{k=1}^{n}\frac{1}{k}-\ln n\right)_{=}\lim_{n\to\infty}(H_n-\ln n),$ where $H_n$is a harmonic number. In mathematics, the n-th harmonic number is the sum of the reciprocals of the first n natural numbers: $H_n=1+\frac{1}{2}+\frac{1}{3}+\cdots+\frac{1}{n}=\sum_{k=1}^{n}\frac{1}{k}.$ which intresetingly also equals n times the inverse of the harmonic mean (i.e., t (M−1) of the power mean) of natural numbers (i.e.,multi-seasonal sampled Euclidean-distance based S. damnosum s.l. endemic transmission-oriented explanatory covariate coefficients) (Toe et al., 1997). The constant can be implemented in Mathematica as Euler Gamma for quantitating the spatiotemporal-sampled S endemic transmission-oriented explanatory covariate

coefficients. Although developmental versions of Mathematica can compute $\gamma$to 10^8digits in 2.7 CPU-hours and 10^9digits in 1.9 CPU-days on modern hardware, no quadratically converging algorithm for computing $\gamma$is presently known for accommodating multi-seasonal onchocerciasis geopredictive regression-based modeling or, for that matter any time series dependent vector arthropod-borne disease empirical-sampled distribution .By definition the Euler-Mascheroni constant may be defined, however also as the limit of the sequence $\gamma = \lim_{n\to\infty}\left(\sum_{k=1}^{n}\frac{1}{k} - \ln n\right) = \lim_{n\to\infty}(H_n - \ln n)$, where $H_n$is a harmonic number (Toe et al., 1997). By so doing, the correct number of the form $H_n = \sum_{k=1}^{n}\frac{1}{k}$ would arise from truncation of the harmonic series leading to the transcendental equation $\gamma - H_n + \ln \nu = 0$ which may then be employed thereafter to robustly quantitate multi-seasonal onchocerciasis endemic transmission-oriented model parameter estimators.

Although the nth factorial moment of the Poisson distribution in the spatiotemporal onchocerciasis endemic transmission-oriented risk model would be λn, the higher moments mk of the Poisson distribution about the origin would be expressed as Touchard polynomials λ: [i.e., $m_k = \sum_{i=0}^{k}\lambda^i S_{i:k},$] in order to effectively determine prolific areas of disease transmission (e.g., hyperendemic transmission zones). The Touchard polynomials comprise a polynomial sequence of binomial type defined by S(n, k) where is a Stirling number of the second kind. In combinatorics, Stirling numbers of the second kind S(n,k) count the number of equivalence relations having k equivalence classes defined on a set with n elements. Thus, if X is a random variable with a Poisson distribution in a robust spatiotemporal S. damnosum s.l. riverine larval habitat linear geopredictive model with expected value λ, then its nth moment is E(Xn) = Tn(λ). Furthermore, if X is a random sampled explanatory predictor variable in the multi-seasonal endemic transmission-oriented risk model with a Poisson distribution with expected value λ, then its nth moment would be E(Xn) = Tn(λ), leading to the definition: $T_n(x) = e^{-x}\sum_{k=0}^{\infty}\frac{x^k k^n}{k!}$. Thereafter, if so desired, the infectious disease vector ecologist can quickly prove that this polynomial sequence is of a binomial type in a robust linear-dependent geopredictive seasonal S. damnosum-related regression -based ArcGIS/SAS-based risk model by determining first if the regression residuals rendered satisfies the sequence of identities: [e.g., $T_n(\lambda+\mu) = \sum_{k=0}^{n}\binom{n}{k}T_k(\lambda)T_{n-k}(\mu).$] [see 6]. The Touchard polynomials make up the only polynomial sequence of binomial type in a time series-dependent linear hierarchical risk model in which the coefficient of the 1st-degree term of every polynomial is 1 using $T_{n+1}(x) = x\sum_{k=0}^{n}\binom{n}{k}T_k(x).$ (Toe et al., 1997). Further, the Touchard polynomials may also satisfy the recursion using $T_{n+1}(x) = x\left(1+\frac{d}{dx}\right)T_n(x).$ and $T_{n+1}(x) = x\sum_{k=0}^{n}\binom{n}{k}T_k(x).$ in a spatiotemporal geopredictive onchocerciasis endemic transmission-oriented risk model.

However, in computing Touchard polynomials for a robust spatiotemporal geopredictive onchocerciasis endemic transmission-oriented risk model, the equation $S_{n:s} = \frac{1}{n!}\sum_{i=0}^{n}(-1)^{n-i}$ would have to be employed initially for accurately determining the significance of the spatiotemporal sampled endemic transmission-oriented explanatory covariate coefficients [see 2] which would then require Stirling numbers of the second kind. [see 5]. In mathematics, particularly in combinatorics, a Stirling number of the second kind is the number of ways to partition a set of n objects into k non-empty subsets and is denoted by $S(n,k)$or $\left\{ {n \atop k} \right\}$(Toe et al., 1997). Stirling numbers of the second kind occur in the field of mathematics called combinatorics and the study of partitions .Stirling numbers of the second kind is one of two kinds of Stirling numbers, the other kind being called Stirling numbers of the first kind. Mutually inverse (i.e., finite or infinite) triangular matrices can then be formed by arranging the Stirling numbers of the first respectively second kind according to the parameters n, k generated for attaining an optimal endemic transmission-oriented geopredictive time series dependent model residual forecast.

A triangular matrix is a special kind of square matrix and a square matrix is called lower triangular if all the entries above the main diagonal are zero (Toe et al., 1997). Conversely a square matrix in a multi-seasonal geopredictive onchocerciasis endemic transmission-oriented ArcGIS/SAS-based risk model would be an "upper triangular" if all the entries (i.e., sampled georeferenced explanatory predictor covariate coefficients) below the main diagonal are zero. A triangular matrix is one that is either lower triangular or upper triangular (Haight, 1967).Therefore, ideally riverine endemic transmission-oriented regression-based predictive matrix that is both upper and lower triangular would have a diagonal matrix of the form

[i.e., a lower triangular matrix or left triangular matrix], and analogously a matrix of the form

$$U = \begin{bmatrix} u_{1,1} & u_{1,2} & u_{1,3} & \dots & u_{1,n} \\ & u_{2,2} & u_{2,3} & \dots & u_{2,n} \\ & & \ddots & \ddots & \vdots \\ & & & \ddots & u_{n-1,n} \\ 0 & & & & u_{n,n} \end{bmatrix}$$

{i.e., an upper triangular matrix or right triangular matrix]. The variable L (standing for lower or left)would then represent a lower triangular spatiotemporal matrix, while the variable U (standing for upper) or R (standing for right) would be used for upper triangular matrix. A matrix that is both upper and lower triangular is diagonal (Toe et al., 1997). Thereafter, all these ways of partitioning a set of n elements into m nonempty sets (i.e., $m$set blocks) collectively could be considered when rendering a Stirling set number for constructing a robust spatiotemporal geopredictive onchocerciasis endemic transmission-oriented model. The Stirling numbers of the second kind is commonly implemented in Mathematica as StirlingS2[n, m], and then denoted $S_n^{(m)}$ (http://mathworld.wolfram.com/Euler-MascheroniConstant.html).

When the response variable in the geopredictive spatiotemporal onchocerciasis riverine endemic transmission-oriented model has a Normal distribution, however, the mean may be linked to a set of predictor variables employing a linear function like Y = β0 + β1X1 + β2X2 …….+βk Xk. .Unfortunately, in the case of binary regression the fact that probability lies between 0-1 imposes a constraint. The normality assumption of multiple linear regression of the sampled explanatory covariates would be then lost, and so would the assumption of constant variance in the model residual forecast. Without these assumptions the F and t tests will have no basis in an endemic transmission-oriented model. One solution is to use the logistic transformation of the probability p or logit p, such that loge(p/1− p) = β0 + β1X1 + β2X2…….βnXn. The β coefficients could then be interpreted as increasing or decreasing the log odds of a seasonal tabulated event, and expβ (i.e., the odds multiplier) could then be used as the odds ratio for a unit increase or decrease in the sampled explanatory variable. Further, when the response variable is in the form of a seasonal count a different constraint in the predictive endemic model may be encountered. Counts are all positive integers and for rare events the Poisson distribution (rather than the Normal) is more appropriate since the Poisson mean > 0(Toe et al., 1997). So the logarithm of the response variable in the predictive spatiotemporal S. damnosum s.l. predictive model would then be linked to a linear function of the sampled endemic transmission-oriented explanatory covariate coefficients such that loge (Y) = β0 + β1X1 + β2X2 … etc. and so Y = (eβ0) (eβ1X1) (eβ2X2) .. etc. In other words, the typical Poisson regression endemic transmission-oriented model would express the log outcome rate as a linear function of an empirical dataset of observational predictors. The assumptions in the endemic transmission-oriented model would then include: 1). logarithm of the Onchocerciasis rate changes linearly with equal increment increases in the exposure variable. 2). changes in the rate from combined effects of different exposures or risk factors are multiplicative 3). at each level of the regressed explanatory covariate coefficients and the number of cases has variance equal to the mean. 4). observations are independent (Toe et al., 1997) Methods to identify violations of assumption (i.e. to determine whether variances are too large or too small include plots of residuals versus the mean at different levels) of the predictor variable could also be determined. Recall that in the case of normal linear regression, diagnostics of the model employ plots of residuals against fits (fitted values). This means that the same diagnostics can be used in the case of Poisson regression of an empirical spatiotemporal dataset of geopredictive onchocerciasis endemic transmission-oriented explanatory predictor covariate coefficients for targeting onchocerciasis endemicity.

On occasion, however, the negative binomial distribution can be used as an alternative to the Poisson distribution especially in its alternative parameterization state. This distribution is especially useful for discrete

data over an unbounded positive range whose sample variance exceeds the sample mean. In such cases, the spatiotemporal-sampled observations [e.g., time series S. damnosum s.l. explanatory covariate coefficients] are overdispersed with respect to a Poisson distribution for which the mean is equal to the variance. Since the negative binomial distribution has one more parameter than the Poisson (Toe et al., 1997), the second parameter can be used to adjust the variance independently of the mean in a regression-based predictive risk model. Furthermore, since in probability theory and statistics, the negative binomial distribution is a discrete probability distribution of the number of successes in a sequence of Bernoulli trials before a specified non-random number of failures denoted r (Boatin et al., 1997), the pmf of the negative binomial distribution with a non-homogenous gamma distributed mean can be subsequently expressed as $f(k) \equiv \Pr(X = k) = \binom{k+r-1}{k}(1-p)^r p^k \quad \text{for } k = 0, 1, 2, \ldots$ [see 2]. In this linear based equation, the quantity in parentheses would be the binomial coefficient, and hence would then be equivalent to $\binom{k+r-1}{k} = \frac{(k+r-1)!}{k!\,(r-1)!} = \frac{(k+r-1)(k+r-2)\cdots(r)}{k!}$. This quantity can alternatively be written as $\frac{(k+r-1)\cdots(r)}{k!} = (-1)^k \frac{(-r)(-r-1)(-r-2)\cdots(-r-k+1)}{k!} = (-1)^k \binom{-r}{k}$ for explaining "negative binomialness' in a linearly dependent spatiotemporal geopredictive onchocerciasis-related regression –based linear ArcGIS/SAS-based risk model. In ecological-based empirical analysis related to the spatiotemporal predictive arthropod-borne infectious disease regression-based risk mapping data, the sampled explanatory covariate coefficients usually exhibit overdispersion which justifies the use of a negative binomial regression with a non-homogenous gamma distributed mean [see 10].

In this research we proposed the use of a Poisson- gamma model for relative risks based on ArcGIS/SAS-based -based Euclidean distances from an S. damnosum s.l. epidemiological capture point using an empirical Bayesian approach. This model was generalized into a fully Bayesian paradigm using a hierarchical generalized probabilistic regression –based framework. Our assumption was that inferences from hierarchical generalized Bayesian probabilistic estimation matrices could generate unbiased seasonally-dependent geopredictive onchocerciasis. -related linear risk mapping variables for spatially targeting endemic transmission areas. In these model the conjugate prior for the rate parameter λ of the Poisson distribution was the gamma distribution. Additionally, in these model if $\lambda \sim \text{Gamma}(\alpha, \beta)$ denoted whether λ was distributed according to the gamma density, g which was parameterized in terms of a shape parameter α and an inverse scale parameter β employing $g(\lambda \mid \alpha, \beta) = \frac{\beta^\alpha}{\Gamma(\alpha)}\, \lambda^{\alpha-1}\, e^{-\beta\lambda} \text{ for } \lambda > 0.$. Then, given the same sample of n independent S. damnosum s.l. riverine larval habitat spatiotemporally measured explanatory covariate coefficients values ki and a prior of Gamma(α, β), $\lambda \sim \text{Gamma}(\alpha + \sum_{i=1}^{n} k_i, \beta + n).$ the posterior distribution was quantitatively assessed using . Our assumption was that by constructing such a model, the posterior mean E[λ] would approach the maximum likelihood estimate (i.e., $\widehat{\lambda}_{\text{MLE}}$) and the limit in the residual parameters which would then be expressed as $\alpha \to 0,\ \beta \to 0$. The posterior predictive distribution for a single additional observation\ employed in predictive spatiotemporal regression-based risk map can detect spatial outliers using a binomial distribution (i.e., a Gamma-Poisson distribution) (Toe et al., 1997). Thereafter, general categories of space–time autoregressive models, [e.g., autoregressive-integrated-moving-average models (ARIMA), eigenvector mapping, 3-dimensional geostatistical models] were constructed in. SAS for forecasting endemic transmission-oriented unbiased estimators and quantitating uncertainty-based residual explanatory covariate coefficients. Our assumption was that by regressing specific geographical locational covariates (e.g., Euclidean distance from a georeferenced riverine- village community to a capture point) endemicity as determined by spatial aggregation of prolific seasonal habitats could be targeted efficiently in a stochastically interpolated autoregressive risk map.

In order to compute robust eigenvectors from the spatiotemporal-sampled S.damnosum s.l. observational explanatory covariate coefficients, in this research, we also employed an eigenfunction decomposition algorithm based on geographic connectivity matrices. Geographic Connectivity/Weights Matrix are spatially represented by an n-by-n matrix with the same sequence of row and column location labels, whose entries can indicate which pairs of sampled data pairs are neighbors (Toe et al., 1997). By so doing, we were able to generate a Moran's Coefficient (MC). The MC is an index of spatial autocorrelation, involving the computation of cross-products of

mean adjusted values that are geographic neighbors (i.e., covariations), that ranges from roughly (–1, –0.5) to nearly 0 for negative, and nearly 0 to approximately 1 for positive, spatial autocorrelation, with an expected value of –1/(n – 1) for zero spatial autocorrelation, where n denotes the number of areal units. The 'MC' was then employed as a covariation index (i.e., pairwise products of the spatiotemporal-sampled geopredictive onchocerciasis endemic transmission-oriented regression coefficients deviations from the mean). The sampling distribution was constructed in SAS/ArcGIS using a stratified randomly sampled riverine–based time encompassing regression-based framework. A probability distribution was then rendered from regressing the observed endemic transmission-oriented explanatory covariate coefficients. Thereafter, by constructing all possible permutations of the spatiotemporal-sampled count values a riverine –based surface partitioned map was generated. Thereafter, we attempted to describe the residual autocorrelation error coefficients in the spatiotemporal-dependent empirical S. damnosum s.l. –oriented empirical datasets employing terms of the calculated product moment correlation coefficient and their spatially associated neighboring time series sampled village parameter estimators (prevalence rates) (i.e., y) replacing the value of the predictor variable x in the autoregressive matrix.

In the seasonal S. damnosum s.l. –oriented spatial autoregressive matrix we employed the expression $\frac{\sum_{i=1}^{n}(x_i-\bar{x})(y_i-\bar{y})/n}{\sqrt{\sum_{i=1}^{n}(x_i-\bar{x})^2/n}\sqrt{\sum_{i=1}^{n}(y_i-\bar{y})^2/n}}$ which was then transformed to $\frac{\sum_{i=1}^{n}(y_i-\bar{y})\sum_{j=1}^{n}c_{ij}(y_j-\bar{y})/\sum_{i=1}^{n}\sum_{j=1}^{n}c_{ij}}{\sqrt{\sum_{i=1}^{n}(y_i-\bar{y})^2/n}\sqrt{\sum_{i=1}^{n}(y_i-\bar{y})^2/n}}$. In this research the left-hand expression converted to the right side in the equation, by substituting the numerator term but only when a 1 appeared in the estimation matrix. We were then able to compute the numerator cross-product terms over the total spatiotemporal-sampled spatial data in the matrix (i.e., $\sum_{i=1}^{n}\sum_{j=1}^{n}c_{ij}$). The denominator of the revised expression of the sample variance was Y, s_Y^2. Our assumption was that we could couple this value with part of the accompanying numerator term in the autoregressive seasonal gropredictive autoregressive risk model which then would render $\frac{(y_i-\bar{y})}{s_Y}\sum_{j=1}^{n}c_{ij}\frac{(y_j-\bar{y})}{s_Y}=z_{Y,i}\sum_{j=1}^{n}c_{ij}z_{Y,j}$ Generally, a standardized normal deviate (i.e. Z score) notation z_Y can be calculated using $\frac{(y_i-\bar{y})}{s_Y}\sum_{j=1}^{n}c_{ij}\frac{(y_j-\bar{y})}{s_Y}=z_{Y,i}\sum_{j=1}^{n}c_{ij}z_{Y,j}$ (McCulloch and Searle, 2005). Therefore, in this research, the right hand expression of the geopredictive autoregressive S.damnosum s.l. risk model was the MC derived from the spatiotemporal sampled explanatory covariates.

A second measure of spatial autocorrelation, used in this research, was Geary's Ratio which was a paired comparison similarity index for spatially calculating neighboring sampled count values, based upon the unbiased sample variance (i.e., division by n-1 rather than n), which was expressed in this research in terms of the MC as : $\frac{\sum_{i=1}^{n}\sum_{j=1}^{n}c_{ij}(y_i-y_j)^2/\left(z\sum_{i=1}^{n}\sum_{j=1}^{n}c_{ij}\right)}{\sqrt{\sum_{i=1}^{n}(y_i-\bar{y})^2/(n-1)}\sqrt{\sum_{i=1}^{n}(y_i-\bar{y})^2/(n-1)}}=\frac{\sum_{i=1}^{n}\frac{(y_i-\bar{y})^2}{s_y^2}\sum_{j=1}^{n}c_{ij}}{\sum_{i=1}^{n}\sum_{j=1}^{n}c_{ij}}-\frac{n-1}{n}MC$. Geary Ratio, an index of spatial autocorrelation, involving the computation of squared differences of values were geographic neighbors (i.e., paired comparisons of spatiotemporal–sampled S.damnosum s.l. observations), that ranged from 0 to 1 for negative, and 1 to approximately 2 for positive, spatial autocorrelation, with an expected value of 1 for zero spatial autocorrelation. The expected value in the spatiotemporal predictive autoregressive model then became $E(GR)=\frac{\sum_{i=1}^{n}E(z_{Y,i}^2)\sum_{j=1}^{n}c_{ij}}{\sum_{i=1}^{n}\sum_{j=1}^{n}c_{ij}}-\frac{n-1}{n}E(MC)=\left(1-\frac{1}{n}\right)\times 1-\frac{n-1}{n}\left(-\frac{n}{n-1}\right)=1$. This output allowed an asymptotic

standard error to be computed as $\sqrt{\frac{2}{\sum_{i=1}^{n}\sum_{j=1}^{n} c_{ij}}}\sqrt{1+\frac{\sum_{i=1}^{n}\left(\sum_{j=1}^{n} c_{ij}\right)^2}{\sum_{i=1}^{n}\sum_{j=1}^{n} c_{ij}}}$ under the assumption of normality within a geographically weighted regression(GWR). Geographically weighted regression (GWR) can identify surface heterogeneities in predictive risk models by quantifying the spatial variability of the estimated local regression coefficients (McCulloch and Searle, 2005). In most cases these attributes in a predictive spatiotemporal autoregressive model exhibits local deviations from a global regression model.

We used spatiotemporal-sampled data obtained from the African Programme for Onchocerciasis Control (APOC, 1974–2002) for remotely constructing our seasonally-based geopredictive onchocerciasis risk -oriented endemic transmission oriented model. Large-scale control of Onchocerciasis commenced over three decades ago, initially through the Onchocerciasis Control Programme in West Africa (OCP, 1974–2002), and more recently by the African Programme for Onchocerciasis Control (APOC, 1995–2010). The goals of OCP were to eliminate onchocerciasis as a public health problem and to mitigate its negative impact on the social and economic development of affected regions. The strategic objective of APOC is to permanently protect the remaining 120 million people at risk of this debilitating and disfiguring disease in 19 countries in Africa through the establishment of community-directed treatment with ivermectin (CDTI) that is capable of being sustained by the communities after APOC financing has ended. As such , another of our assumptions was we could generate cost-effective regiments of treatment within the riverine-based communities by remotely quantifying endemic transmission zones based on the time-series dependent empirical ecological datasets, their georeferenced data feature attributes and their Euclidean-distance based covariate coefficient values. Therefore, the objectives of this research were to: (1) generate a backward Poisson stepwise regression model using multiple field and remote georeferenced seasonal-sampled predictor variables; (2) filter all latent autocorrelation error coefficients in the variance estimates using an eigenfunction spatial filter decomposition algorithm; and, 3) construct a hierarchical linear random effects model to forecast prevalence rates and eliminate uncertainty estimates (e.g., perfect multicolinearity) in multiple empirical ecological datasets of S.damnosum s.l.–related explanatory covariate coefficients spatiotemporally sampled from 2009 to 2012 in a riverine ecosystem in Burkina Faso.

2. Materials and methods

2.1. Study site

Burkina Faso is a landlocked country in West Africa It is surrounded by six countries: Mali to the north, Niger to the east, Benin to the southeast, Togo and Ghana to the south, and Côte d'Ivoire to the southwest. Its size is 274,200 km2 (105,900 sq. mi.) with an estimated population of more than 15,757,000. Water covers approximately 400 km² of the country. Burkina Faso has three distinct seasons: warm and dry (November–March), hot and dry (March–May), and hot and wet (June–October). Annual rainfall varies from about 250 mm to 1,000 mm . The terrain is mostly flat with undulating plains and hills. The study site was in the western part of the Burkina Faso within a riverine ecosystem called Chutes-Dienkoa village.

2.2. Remote sensing data

Raster image data from the DigitalGlobe QuickBird satellite service were acquired for the riverine study site for the periods of: 15 October 2009, 11 February 2010, 13 October 2010, 15 February 2011, 1 October 2011, 17 February 2012, 15 October 2012. The Order Polygon contained 5 vertices consisting of longitude/ latitude (decimal degrees) geographic coordinates using a WGS-84 ellipsoid. The satellite data contained 64 km2 of the land cover in the study site. The QuickBird imagery was classified using the Iterative Self-Organizing Data Analysis Technique (ISODATA) unsupervised routine in ERDAS Imagine v.8.7™ (ERDAS, Inc., Atlanta, Georgia). Unsupervised classifications are commonly used for the identification of sub-meter resolution-derived LULC classes associated with prolific vector arthropod-related immature habitats based on spatiotemporal-field-sampled count data [14]. QuickBird collected the data used an 11-bit dynamic range. This allowed 211or 2,048 possible intensity values for each pixel. Because computers cannot read 11-bit data, we compressed the QuickBird 11-bit data into 8-bit data. As such, QuickBird data spanning 2,048 pixel values was rescaled to 256 values. The QuickBird image data were

delivered as pan-sharpened composite products in infra-red (IR) colors. The clearest, cloud-free images available of the contiguous sub-areas of the riverine study site were used to identify LULC covariates and other spatial data feature attributes associated with the georeferenced S.damnosum s.l. habitat breeding capture point.

A base map of the riverine study site was then generated in ArcGIS using the QuickBird visible and near (IR) data using differentially corrected global positioning systems (DGPS) ground coordinates of the spatiotemporal-sampled S. damnosum s.l. habitat breeding capture point and the surrounding georeferenced villages. The DGPS were acquired from a CSI max receiver which has a positional accuracy of +/- .178. Using a local DGPS broadcaster can compensate for ionospheric and ephemeris effects which can improve horizontal accuracy significantly and can bring altitude error down in a predictive vector arthropod-related larval habitat model (Gosper et al., 1972). Each georeferenced S. damnosum s.l. habitat was then entered into the VCMS™ relational database software product (Clarke Mosquito Control Products, Roselle, IL). The VCMS™ database supported a mobile field data acquisition component module, called Mobile VCMS™ that synchronized the field sampled data from industry standardized Microsoft Windows Mobile™ devices while supporting add-on DGPS data collection By so doing multiple spatiotemporal base maps were generated for the study site.(Figure 2).

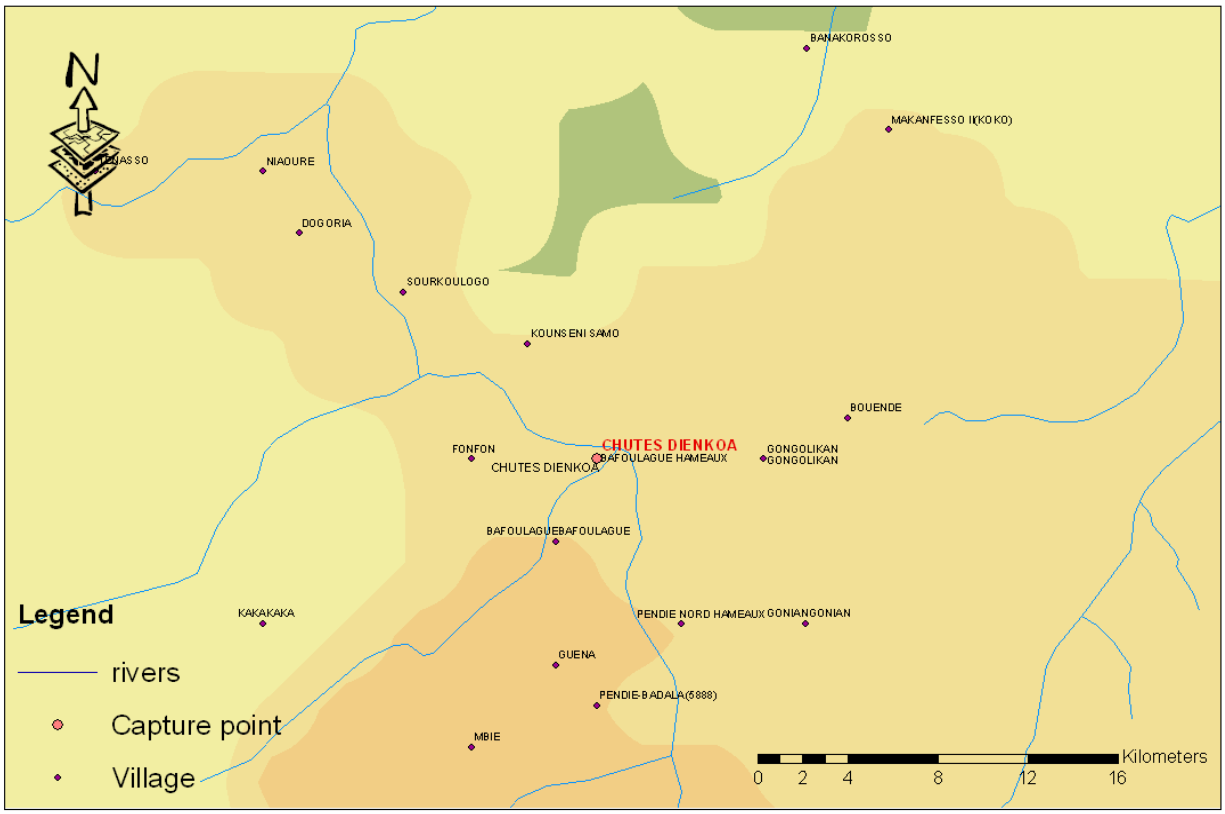

Fig. 1. Base map of the Chutes Dienkoa study site capture point and surrounding epidemiological villages as entered into the VCMS repository database.

2.3. Environmental parameters

Multiple georeferenced explanatory covariates were then examined extensively using: longitude, latitude, and altitude data (see Table 1). The criteria involved the centrographic measures of spatial mean and distance between the riverine-based villages and the georeferenced larval habitat distance from the sampled site to the breeding capture point. The data was also comprised of individual spatiotemporal-sampled observations of

S.damnsoum s.l. habitat capture point together with a battery of categorical attribute measures which were expanded into multiple coefficient estimate.

In this research, the riverine -village's distances were measured as Euclidean distances using ArcGIS projection units of the raster which also computed the digitized grid cell matrix. The Euclidean distance output raster contained the measured distances. The Euclidean Distance functions provided information according to Euclidean or, straight-line, distance between the georeferenced villages and from the remotely-sampled riverine capture point to the villages (i.e., geometric distances in the multidimensional space). In this research the Euclidean distances were computed as: distance(x,y) = { $\sum$i (xi - yi)2 }½. Every cell in the Euclidean allocation output raster was the then assigned the value of the source to which it was closest. The nearest source was then determined by the Euclidean Distance function in ArcGIS. This function assigned space between the georeferenced S. damnosum s.l. riverine habitat capture point and the villages with their stratified prevalence rates. The Euclidean direction output raster contained the azimuth direction from each digitized grid cell centroid to the nearest source. The Euclidean Allocation function identified the nearest human habitation center closest to each grid cell. The distance between sampled and human habitation areas were then categorized into numerous classes (e.g., 1: 0–5 km, 2: 5–10 km and 10-15km)

Table 1
Environmental predictor variables sampled at the epidemiological capture point.

Variable	Description	Units
GCP	Ground control points	Decimal-degrees
FlOW	flowing water	Presence or absence
HGHT	Height of water	
TURB	Turbidity of water	Formazin Turbidity Unit
AQVEG	Aquatic vegetation	Percentage
HGVEG	Hanging vegetation	Percentage
DDVEG	Dead vegetation	Perecentage
RCKS	Rocks	Perecentage
MMB	Man-made barriers	Type (e.g.,damns, bridges)
DISHAB	Distance between epidemiological villages	meters
DISCAP	Distance between capture point and epidemiological villages	meters

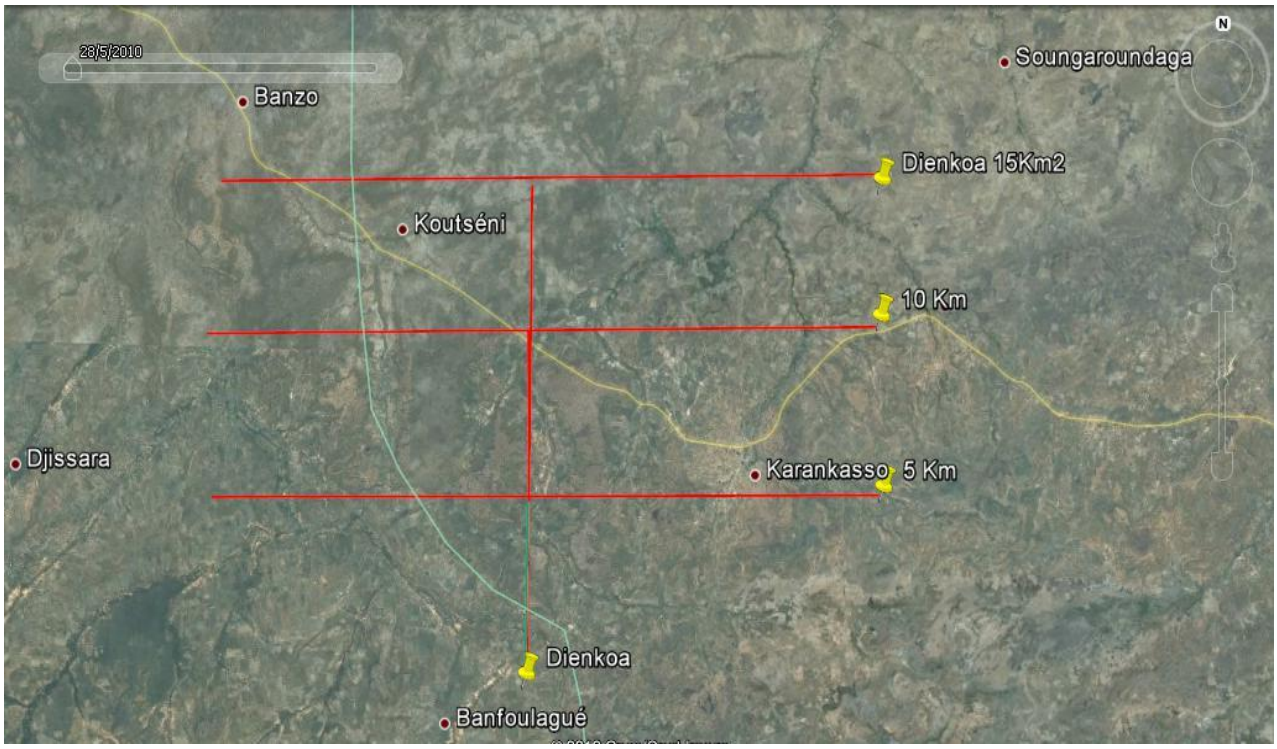

Fig. 4. An Euclidean-distance-based matrix overlaid onto the georeferenced spatiotemporal-sampled S. damnosum s.l. riverine habitat capture point

2.4. Regression Model

We then constructed a Poisson model in SAS GEN MOD. The Poisson process in our analyses was provided by the limit of a binomial distribution based on the spatiotemporal-sampled covariate coefficient estimates using $P_p(n \mid N) = \frac{N!}{n!\,(N-n)!}\, p^n (1-p)^{N-n}$. (2.1). We viewed the distribution as a function of the expected number of time series-dependent larval count predictor variables using the sample size N for quantifying the fixed p in equation (2.1), which then was then transformed into the linear equation: $P_{\nu/N}(n \mid N) = \frac{N!}{n!\,(N-n)!}\left(\frac{\nu}{N}\right)^n \left(1-\frac{\nu}{N}\right)^{N-n}$, Based on the sample size N, the distribution approached $P_\nu(n)$ which in this research was expressed by $= \lim_{N\to\infty} P_p(n \mid N) \lim_{N\to\infty} \frac{N(N-1)\cdots(N-n+1)}{n!}\frac{\nu^n}{N^n}\left(1-\frac{\nu}{N}\right)^N \left(1-\frac{\nu}{N}\right)^{-n} =$ $\lim_{N\to\infty} \frac{N(N-1)\cdots(N-n+1)}{N^n}\frac{\nu^n}{n!}\left(1-\frac{\nu}{N}\right)^N \left(1-\frac{\nu}{N}\right)^{-n} = 1\cdot\frac{\nu^n}{n!}\cdot e^{-\nu}\cdot 1 = \frac{\nu^n e^{-\nu}}{n!}$,

The GENMOD procedure then fit a generalized linear model (GLM) to the sampled data by MLE of the parameter vector β. In this research the GENMOD procedure estimated the parameters of the S. damnosum s.l.regression-based risk model numerically through an iterative fitting process. The dispersion parameter was then estimated by the residual deviance and by Pearson's chi-square divided by the degrees of freedom (d.f.). Covariances, standard errors, and p-values were then computed for the estimated covariate coefficients based on the asymptotic normality of the model residuals derived from the MLE .

Interestingly, our model revealed that the sample size N completely dropped out of the probability function, which in this research had the same functional form for all the spatiotemporal-sampled parameter estimator measurement values (i.e., ν). As expected, the Poisson distribution was normalized so that the sum of

probabilities equaled 1. The ratio of probabilities was then $\sum_{n=0}^{\infty} P_{\nu}(n) = e^{-\nu} \sum_{n=0}^{\infty} \frac{\nu^n}{n!} = e^{-\nu} e^{\nu} = 1.$ which in this research was provided by $\frac{P_{\nu}(n=i+1)}{P(n=i)} = \frac{\frac{\nu^{i+1} e^{-\nu}}{(i+1)!}}{\frac{e^{-\nu} \nu^i}{i!}} = \frac{\nu}{i+1}.$ .The Poisson distribution then revealed that the covariate coefficients reached a maximum when $\frac{d P_{\nu}(n)}{d n} = \frac{e^{-\nu} n (\gamma - H_n + \ln \nu)}{n!} = 0,$ where γ was the Euler-Mascheroni constant and H_n was a harmonic number, leading to the transcendental equation $\gamma - H_n + \ln \nu = 0$. The linear model also revealed that the Euler-Mascheroni constant arose in the integrals as $\gamma = -\int_0^{\infty} e^{-x} \ln x \, dx = -\int_0^1 \ln \ln \left(\frac{1}{x}\right) dx = \int_0^{\infty} \left(\frac{1}{1-e^{-x}} - \frac{1}{x}\right) e^{-x} \, dx = \int_0^{\infty} \frac{1}{x} \left(\frac{1}{1+x} - e^{-x}\right) dx$ (2 .2). The Euler–Mascheroni constant is a mathematical constant recurring in analysis and number theory, usually denoted by γ (Toe et al., 1997). Commonly, integrals that render γ in combination with temporal constants include $\int_0^{\infty} e^{-x^2} \ln x \, dx = -\frac{1}{4} \sqrt{\pi} \, (\gamma + 2 \ln 2)$ and $\int_0^{\infty} e^{-x} (\ln x)^2 \, dx = \gamma^2 + \frac{1}{6} \pi^2$. (Boatin et al., 1997).

Thereafter, the double integrals in the spatiotemporal S. damnosum s.l. regression model included $\gamma = \int_0^1 \int_0^1 \frac{x-1}{(1-x\,y) \ln (x\,y)} \, dx \, dy$. An interesting analog of equation (2.2) in our seasonal predictive regression risk model was then provided by $\ln \left(\frac{4}{\pi}\right) = \sum_{n=1}^{\infty} (-1)^{n-1} \left[\frac{1}{n} - \ln \left(\frac{n+1}{n}\right)\right] = \int_0^1 \int_0^1 \frac{x-1}{(1+x\,y) \ln (x\,y)} \, dx \, dy = e^{\gamma} = \lim_{n \to \infty} \frac{1}{\ln p_n} \prod_{i=1}^{n} \frac{1}{1 - \frac{1}{p_i}},$ $0.241564 \ldots \gamma$. This solution was also provided by incorporating Mertens theorem [i.e.,] where the product was aggregated over the spatiotemporal-sampled S. damnosum s.l-related values found in the ecological empirical datasets. The Mertens' 3rd theorem, $\lim_{n \to \infty} \ln n \prod_{p \le n} \left(1 - \frac{1}{p}\right) = e^{-\gamma},$ is related to the density of prime numbers where γ is the Euler–Mascheroni constant(Boatin et al., 1997).By taking the logarithm of both sides in the regression risk-based model, an explicit formula for γI was then obtained using $\gamma = \lim_{x \to \infty} \left[\sum_{p \le x} \ln \left(\frac{1}{1 - \frac{1}{p}}\right) - \ln \ln x\right].$. This product was also given by series due to Euler, which followed from equation (2.2) by first replacing $\ln n$b$\ln (n+1)$, in the regression equation using $\gamma = \sum_{k=1}^{\infty} \left[\frac{1}{k} - \ln \left(1 + \frac{1}{k}\right)\right]$ and then generating $\lim_{n \to \infty} [\ln (n+1) - \ln n] = \lim_{n \to \infty} \ln \left(1 + \frac{1}{n}\right) = 0,$ .We then substituted the telescoping sum $\sum_{k=1}^{n} \ln \left(1 + \frac{1}{k}\right)$ for $\ln (n+1)$ which then rendered $\ln \left(1 + \frac{1}{k}\right) = \ln (k+1) - \ln k$ .Thereafter, we obtained $\lim_{n \to \infty} \left[\sum_{k=1}^{n} \frac{1}{k} - \sum_{k=1}^{n} \ln \left(1 + \frac{1}{k}\right)\right]_{\gamma} = \lim_{n \to \infty} \sum_{k=1}^{n} \left[\frac{1}{k} - \ln \left(1 + \frac{1}{k}\right)\right]$.

Additionally, other series in the spatiotemporal predictive S. damnosum s.l.regression-based risk model included the equation (◇) where $\gamma=\sum_{n=2}^{\infty}(-1)^n\frac{\zeta(n)}{n}=\ln\left(\frac{4}{\pi}\right)+\sum_{n=1}^{\infty}\frac{(-1)^{n-1}\zeta(n+1)}{2^n(n+1)}$ and where $\zeta(z)$ was $\gamma=\sum_{n=1}^{\infty}(-1)^n\frac{\lfloor \lg n\rfloor}{n}$ and the Riemann zeta function. The Riemann zeta function ζ(s), is a function of a complex variables that analytically continues the sum of the infinite series $\sum_{n=1}^{\infty}\frac{1}{n^s}$, which converges when the real part of s is greater than 1 where lg is the logarithm to base 2 and $\lfloor x\rfloor$ is the floor function (Toe et al., 1997). Nielsen (Nielsen, 1897) earlier gave a series equivalent to $\gamma=1-\sum_{n=1}^{\infty}\sum_{k=2^{n-1}}^{2^n-1}\frac{n}{(2k+1)(2k+2)}$. and thereafter $\frac{1}{(2k+1)(2k+2)}=\frac{1}{2k+1}-\frac{1}{2k+2}$ was then added $0=-\frac{1}{2}+\frac{1}{4}+\frac{1}{8}+\frac{1}{16}+\cdots$ to render Vacca's formula. Gosper et al. (1897) used the sums $\gamma=\sum_{n=1}^{\infty}\sum_{k=2^n}^{\infty}\frac{(-1)^k}{k}=\sum_{k=1}^{\infty}\frac{1}{2^{k+1}}\sum_{j=0}^{k-1}\binom{2^{k-j}+j}{j}^{-1}$ with $k-j$ by replacing the undefined I and then rewrote the equation as a double series for applying the Euler's series transformation which we then employed to each of the sampled time-series dependent S. damnosum s.l explanatory covariate coefficient estimates.

In this research $\binom{n}{k}$ was used as a binomial coefficient, rearranged to achieve the conditionally convergent series in the predictive autoregressive spatiotemporal onchocerciasis -related linear endemic transmission-oriented model as the plus and minus terms were first grouped in pairs of the sampled covariate coefficient estimates employing the resulting series of the actual sampled measurement indicator values. The double series was thereby equivalent to Catalan's integral: $\gamma=\int_0^1\frac{1}{1+x}\sum_{n=1}^{\infty}x^{2^n-1}\,dx.$ Catalan's integrals are a special case of general formulas due to $J_0\left(\sqrt{z^2-y^2}\right)=\frac{1}{\pi}\int_0^{\pi}e^{y\cos\theta}\cos(z\sin\theta)\,d\theta,$ where $J_0(z)$ is a Bessel function of the first kind(Boatin et al., 1997). The Bessel function is a function $Z_n(x)$ defined in a robust regression model by employing the recurrence relations $Z_{n+1}+Z_{n-1}=\frac{2n}{x}Z_n$ and $Z_{n+1}-Z_{n-1}=-2\frac{dZ_n}{dx}.$ (Toe et al., 1997) which Jacob et al. [15] recently defined as solutions in a West Nile Virus (WNV) related mosquito (i.e., Culex quinquefasciatus) regression models in a district in Birmingham, Alabama using the differential equation $x^2\frac{d^2y}{dx^2}+x\frac{dy}{dx}+\left(x^2-n^2\right)y=0.$. Thereafter, analytical approaches based on the eigenfunctions of spatial uncertainty configuration matrices were proposed in order to consider explicitly spatial explanatory covariates of Cx. quinquefasciatus habitat suitability. The products were distance-based (DB) topological ArcGIS/SAS-based eigenvector maps based upon geographic connectivity matrices. Thus, $x^2\frac{d^2y}{dx^2}+x\frac{dy}{dx}+\left(x^2-n^2\right)y=0.$ helped create predictors that could be easily incorporated into conventional WNV mosquito regression- based risk models. The equation helped provide a flexible tool (i.e., second-order autocorrelation) that allowed the full range of general and generalized linear modeling theory to be applied to WNV mosquito risk modeling in the presence of nonzero spatial autocorrelation.

In this research the Bessel function $J_n(z)$ was defined by the contour integral $J_n(z)=\frac{1}{2\pi i}\oint e^{(z/2)(t-1/t)}\,t^{-n-1}\,dt,$ where the contour enclosed the origin and was traversed in a counterclockwise direction. This function render :

$J_0\left(2\,i\,\sqrt{z}\right)=\frac{1}{\pi}\int_0^{\pi}e^{(1+z)\cos\theta}\cos\left[(1-z)\sin\theta\right]d\,\theta.$ Thereafter, to quantify the equivalence in the spatiotemporal ecological empirical dataset of the S. damnosum s.l.regression-based risk-oriented parameter estimators, we expanded $1/(1+x)$into a geometric series and multiplied the sampled data attribute features by x^{2^n-1}, and integrated the term wise as in Sondow and Zudilin (de la Vallée Poussin, 1989). Other series for γ then included $\gamma=\frac{3}{2}-\ln 2-\sum_{m=2}^{\infty}(-1)^m\frac{m-1}{m}\left[\zeta\,(m)-1\right]$ and $\gamma=\frac{2^n}{e^{2^n}}\sum_{m=0}^{\infty}\frac{2^{m\,n}}{(m+1)!}\sum_{t=0}^{m}\frac{1}{t+1}-n\ln 2+O\left(\frac{1}{2^n\,e^{2^n}}\right),$ .A rapidly converging limit for γ was then provided by $\gamma=\lim_{n\to\infty}\left[\frac{2\,n-1}{2\,n}-\ln n+\sum_{k=2}^{n}\left(\frac{1}{k}-\frac{\zeta\,(1-k)}{n^k}\right)\right]=\lim_{n\to\infty}\left[\frac{2\,n-1}{2\,n}-\ln n+\sum_{k=2}^{n}\frac{1}{k}\left(1+\frac{B_k}{n^k}\right)\right],$ where B_k was a Bernoulli number. Another limit formula was then provided by the equation $\gamma=-\lim_{n\to\infty}\left[\frac{\Gamma\left(\frac{1}{n}\right)\Gamma\,(n+1)\,n^{1+1/n}}{\Gamma\left(2+n+\frac{1}{n}\right)}-\frac{n^2}{n+1}\right]$. Limits to the spatiotemporal-sampled S. damnosums.l. riverine habitat regression-based risk model was then rendered by $\gamma=\lim_{x\to\infty}\zeta\,(\zeta\,(z))-2^x+\left(\frac{4}{3}\right)^x+1$ where $\zeta\,(z)$was the Riemann zeta function.

Another connection with the primes was provided by $d\,(n)=\sigma_0\,(n)$for the spatiotemporal -sampled explanatory covariate coefficient numerical values from 1 to nI in the ecological empirical dataset which in this research was found to be asymptotic to $\frac{\sum_{k=1}^{n}d\,(k)}{n}\sim\ln n+2\,\gamma-1$. De laValléePoussin (Griffith, 1897) proved that if a large number n is divided by all primes $\leq n$, then the average amount by which the quotient is less than the next whole number is γ. An elegant identity for γ in our seasonal predictive S. damnosum s.l. regression-based risk model was then provided by $\gamma=\frac{S_0\,(z)-K_0\,(z)}{I_0\,(z)}-\ln\left(\frac{1}{2}\,z\right),$ where $I_0\,(z)$was a modified Bessel function of the first kind, $K_0\,(z)$was a modified Bessel function of the second kind, and $S_0\,(z)\equiv\sum_{k=0}^{\infty}\frac{\left(\frac{1}{2}\,z\right)^{2\,k}H_k}{(k!)^2},$ where H_n was a harmonic number. This provided an efficient iterative algorithm for γ by computing $B_k=\frac{B_{k-1}\,n^2}{k^2}$,$A_k=\frac{1}{k}\left(\frac{A_{k-1}\,n^2}{k}+B_k\right)$,$U_k V_k=U_{k-1}+A_k$ and $V_k=V_{k-1}+B_k$with $A_0=-\ln nB_0=1U_0=A_0$and $V_0=1$. Reformulating this identity rendered the limit $\lim_{n\to\infty}\left[\sum_{k=0}^{\infty}\frac{\left(\frac{n^k}{k!}\right)^2H_k}{\sum_{k=0}^{\infty}\left(\frac{n^k}{k!}\right)^2}-\ln n\right]=\gamma$ .Infinite products involving γalso arose from the Barnes G-function using the positive integer n. In mathematics, the Barnes G-functionG(z) is a function that is an extension of superfactorials to the complex numbers which is related to the Gamma function (Toe et al., 1997). In this research, this function provided $\prod_{n=1}^{\infty}e^{-1+1/(2\,n)}\left(1+\frac{1}{n}\right)^n=\frac{e^{1+\gamma/2}}{\sqrt{2\,\pi}}$ and $\prod_{n=1}^{\infty}e^{-2+2/n}\left(1+\frac{2}{n}\right)^n=\frac{e^{3+2\,\gamma}}{2\,\pi}$. As such, the Barnes G-function was linearly defined in our time-series dependent S. damnosum s.l. regression-based risk model. The model was defined by

$G(z+1) = (2\pi)^{z/2} \exp(-(z(z+1)+\gamma z^2)/2) \times \prod_{n=1}^{\infty} \left[\left(1+\frac{z}{n}\right)^n \exp(-z+z^2/(2n))\right]$, where γ was the Euler–Mascheroni constant, exp(x) = ex, and ∏ was capital pi notation. The Euler-Mascheroni constant was then rendered by the expressions $\gamma = -\Gamma'(1) = -\psi_0(1)$, where $\psi_0(x)$ was the digamma function $\gamma = \lim_{s\to 1}\left[\zeta(s) - \frac{1}{s-1}\right]$ and the asymmetric limit form of $\gamma = \lim_{s\to 1^+} \sum_{n=1}^{\infty}\left(\frac{1}{n^s} - \frac{1}{s^n}\right)$ and $\gamma = \lim_{x\to\infty}\left[x - \Gamma\left(\frac{1}{x}\right)\right]$. In mathematics, the digamma function is defined as the logarithmic derivative of the gamma function: $\psi(x) = \frac{d}{dx}\ln\Gamma(x) = \frac{\Gamma'(x)}{\Gamma(x)}$. where it is commonly the first of the polygamma functions. The digamma function, in this research was denoted as ψ0(x), which was then related to the harmonic numbers in that $\psi(n) = H_{n-1} - \gamma$ where Hn is the nth harmonic number, and γ was the Euler-Mascheroni constant. The difference between the nth convergent in equation (◇) and γ in our spatiotemporal-sampled predictive S. damnosums.l. regression-based risk model was then rendered by $\sum_{k=1}^{n}\frac{1}{k} - \ln n - \gamma = \int_n^{\infty}\frac{x-\lfloor x\rfloor}{x^2}\,dx,$ where $\lfloor x\rfloor$ was the floor function which satisfied the inequality $\frac{1}{2(n+1)} < \sum_{k=1}^{n}\frac{1}{k} - \ln n - \gamma < \frac{1}{2n}$.The symbol γ was then $\gamma' \equiv e^{\gamma} \approx 1.781072$. This led to the radical representation of the spatiotemporal-sampled explanatory observational covariate coefficients as $e^{\gamma} = \left(\frac{2}{1}\right)^{1/2}\left(\frac{2^2}{1\cdot 3}\right)^{1/3}\left(\frac{2^3\cdot 4}{1\cdot 3^3}\right)^{1/4}\left(\frac{2^4\cdot 4^4}{1\cdot 3^6\cdot 5}\right)^{1/5}\cdots$, which in this research was related to the double series $\gamma = \sum_{n=1}^{\infty}\frac{1}{n}\sum_{k=0}^{n-1}(-1)^{k+1}\binom{n-1}{k}\ln(k+1)$ and $\binom{n}{k}$ a binomial coefficient. Thereafter, another proof of product in the seasonal predictive S.damnosums.l.regression risk model was then provided by the equation $\frac{\pi}{2} = \left(\frac{2}{1}\right)^{1/2}\left(\frac{2^2}{1\cdot 3}\right)^{1/4}\left(\frac{2^3\cdot 4}{1\cdot 3^3}\right)^{1/8}\left(\frac{2^4\cdot 4^4}{1\cdot 3^6\cdot 5}\right)^{1/16}$ ….The solution was then made even clearer by changing $n \to n+1$. In this research, both these regression-based risk-based formulas were also analogous to the product for e which then rendered: $e = \left(\frac{2}{1}\right)^{1/1}\left(\frac{2^2}{1\cdot 3}\right)^{1/2}\left(\frac{2^3\cdot 4}{1\cdot 3^3}\right)^{1/3}\left(\frac{2^4\cdot 4^4}{1\cdot 3^6\cdot 5}\right)^{1/4}$ …

In this research, the Touchard polynomials (i.e., S. damnosum s.l. exponential polynomials), comprised a polynomial sequence of a binomial type as defined by the equation $T_0(x) = 1, \qquad T_n(x) = \sum_{k=1}^{n} S(n,k)x^k = \sum_{k=1}^{n}\left\{{n \atop k}\right\}x^k, \quad n > 0,$ where S(n, k) was a Stirling number of the second kind, (i.e., the number of partitions of the empirical ecological-sampled dataset based on the size n into k disjoint non-empty subsets.) The value at 1 of the nth Touchard polynomial in this research was the nth Bell number,(i.e., the number of partitions of the sampled larval habitat dataset based on size n: $T_n(1) = B_n$.) If X is a random variable with a Poisson distribution with expected value λ, then its nth moment is E(Xn) = Tn(λ), leading to the definition: $T_n(x) = e^{-x}\sum_{k=0}^{\infty}\frac{x^k k^n}{k!}$. (Jacob, et., 2012). By so doing, we were able to quickly prove that this polynomial sequence in the predictive regression based equation was of abinomial type, [i.e., it satisfied the sequence of identities:($T_n(\lambda+\mu) = \sum_{k=0}^{n}\binom{n}{k}T_k(\lambda)T_{n-k}(\mu).$)]. In this research, the Touchard polynomials made up the only polynomial sequence of binomial type in which the coefficient of the 1st-degree term of every polynomial was 1 [i.e., $T_{n+1}(x) = x\sum_{k=0}^{n}\binom{n}{k}T_k(x).$]. We also noticed that the Touchard polynomials satisfied the the Rodrigues-like

formula[i.e., $T_n\left(e^x\right) = e^{-e^x}\frac{d^n}{dx^n}\left(e^{e^x}\right)$]. Furthermore, the Touchard polynomials satisfied the recursion $T_{n+1}(x) = x\left(1+\frac{d}{dx}\right)T_n(x)$. and $T_{n+1}(x) = x\sum_{k=0}^{n}\binom{n}{k}T_k(x)$. in the geopredictive seasonal S.damnosum s.l. riverine regression-based risk model. Using the Umbral notation Tn(x)=Tn(x),these formulas become: $T_n(\lambda+\mu) = (T(\lambda)+T(\mu))^n$. and $T_{n+1}(x) = x\left(1+T(x)\right)^n$. The generating function of the Touchard polynomials was then $\sum_{n=0}^{\infty}\frac{T_n(x)}{n!}t^n = e^{x\left(e^t-1\right)}$. and a contour-integral representation was $T_n(x) = \frac{n!}{2\pi i}\oint\frac{e^{x(e^t-1)}}{t^{n+1}}\,dt$. The Touchard polynomials (and thereby the Bell numbers) was then generalized, using the real part of the above integral, to non-integer order: thus, $T_n(x) = \frac{n!}{\pi}\int_0^{\pi} e^{x\left(e^{\cos(\theta)}\cos(\sin(\theta))-1\right)}\cos\left(xe^{\cos(\theta)}\sin(\sin(\theta))-n\theta\right)\mathrm{d}\theta$.

2.5. Negative binomial regression

Unfortunately, extra-Poisson variation was detected in the variance estimates in our model. A modification of the iterated re-weighted least square scheme and/or a negative binomial non-homogenous regression-based framework conveniently accommodates extra-Poisson variation when constructing seasonal log-linear models employing frequencies or prevalence rates as dependent/response variables (Toe et al., 1997). Operationally these models consists of making iterated weighted least square fit to approximately normally distributed time series-dependent explanatory predictor covariate coefficients based on observed prevalence rates or their logarithm. Unfortunately, the variances of the S.damnosum s.l. regression-related observations in the log-linear equations were assumed to be constant. Subsequently, we introduced an extra-binomial variation scheme into the linear-logistic model which was fitted by a Poisson procedure.

We then constructed a robust negative binomial regression model in SAS with non-homogenous means and a gamma distribution by incorporating $\alpha = \frac{1}{\theta}(\alpha > 0)$ in equation (2.1) .The distribution in the linear regression was then rewritten $f(y_i|\mathbf{x}_i) = \frac{\Gamma(y_i+\alpha^{-1})}{y_i!\Gamma(\alpha^{-1})}\left(\frac{\alpha^{-1}}{\alpha^{-1}+\mu_i}\right)^{\alpha^{-1}}\left(\frac{\mu_i}{\alpha^{-1}+\mu_i}\right)^{y_i},\quad y_i = 0,1,2,\ldots$ for quantifying the spatiotemporal-sampled S. damnosum s.l. parameter estimators. The negative binomial distribution was thus derived as a gamma mixture of Poisson-derived random variables. The conditional mean in the model was then $E(y_i|\mathbf{x}_i) = \mu_i = e^{\mathbf{x}_i'\boldsymbol{\beta}}$ and the variance was. $V(y_i|\mathbf{x}_i) = \mu_i[1+\frac{1}{\boldsymbol{\theta}}\mu_i] = \mu_i[1+\alpha\mu_i] > E(y_i|\mathbf{x}_i)$

To further estimate the S. damnosum s.l. regression based risk model, we specified DIST=NEGBIN (p=1) in the MODEL statement in PROC REG. The negative binomial model NEGBIN1 was setp=1 , which revealed the variance function $V(y_i|\mathbf{x}_i) = \mu_i + \alpha\mu_i$ which was found to be linear in the mean of the risk model. The log-likelihood function of the NEGBIN1 regression model was then provided by the following equation $\mathscr{L} = \sum_{i=1}^{N}\left\{\sum_{j=0}^{y_i-1}\ln\left(j+\alpha^{-1}\exp(\mathbf{x}_i'\boldsymbol{\beta})\right)\right.$ where $\left. -\ln(y_i!) - \left(y_i+\alpha^{-1}\exp(\mathbf{x}_i'\boldsymbol{\beta})\right)\ln(1+\alpha) + y_i\ln(\alpha)\right\}$.The gradient for the model was then expressed as $\frac{\partial\mathscr{L}}{\partial\boldsymbol{\beta}} = \sum_{i=1}^{N}\left\{\left(\sum_{j=0}^{y_i-1}\frac{\mu_i}{(j\alpha+\mu_i)}\right)\mathbf{x}_i - \alpha^{-1}\ln(1+\alpha)\mu_i\mathbf{x}_i\right\}$ and $\frac{\partial\mathscr{L}}{\partial\alpha} = \sum_{i=1}^{N}\left\{-\left(\sum_{j=0}^{y_i-1}\frac{\alpha^{-1}\mu_i}{(j\alpha+\mu_i)}\right) - \alpha^{-2}\mu_i\ln(1+\alpha) - \frac{(y_i+\alpha^{-1}\mu_i)}{1+\alpha} + \frac{y_i}{\alpha}\right\}$.

In this research, the negative binomial regression model with variance function $V(y_i|\mathbf{x}_i) = \mu_i + \alpha\mu_i^2$, was referred to as the NEGBIN2 model. To estimate this model, we specified DIST=NEGBIN (p=2) in the model statements. A test of the Poisson distribution was then performed by examining the hypothesis that $\alpha = \frac{1}{\theta_i} = 0$. A Wald test of this hypothesis was also provided which were the reported t statistics for the estimates in the

negative binomial S. damnosum s.l. geopredictive regression model. The log-likelihood function of the regression model (i.e., NEGBIN2) was then generated by the equation $\mathscr{L} = \sum_{i=1}^{N} \left\{ \sum_{j=0}^{y_i-1} \ln(j+\alpha^{-1}) - \ln(y_i!) = -(y_i+\alpha^{-1})\ln(1+\alpha\exp(\mathbf{x}_i'\boldsymbol{\beta})) + y_i\ln(\alpha) + y_i\mathbf{x}_i'\boldsymbol{\beta} \right\}$ where y was an integer when the gradient was $\frac{\partial \mathscr{L}}{\partial \boldsymbol{\beta}} = \sum_{i=1}^{N} \frac{y_i-\mu_i}{1+\alpha\mu_i}\mathbf{x}_i$. The variance in the S. damnosum s.l. model was then assessed by: $\frac{\partial \mathscr{L}}{\partial \alpha} = \sum_{i=1}^{N} \left\{ -\alpha^{-2}\sum_{j=0}^{y_i-1} \frac{1}{(j+\alpha^{-1})} + \alpha^{-2}\ln(1+\alpha\mu_i) + \frac{y_i-\mu_i}{\alpha(1+\alpha\mu_i)} \right\}$.

2.5 Autocorrelation model: A spatial autoregressive model was then generated that used a variable Y, as a function of nearby sampled S..damnosums.l.-related geopredictive covariate coefficients at the riverine study site. In this research, Y had an indicator value 1 (i.e., an autoregressive response) and/or the residuals of Y which were values of nearby sampled Y residuals (i.e., an SAR or spatial error specification). For the time series-dependent -related parameter estimators, the SAR model furnishes an alternative specification that frequently is written in terms of matrix W (Boatin et al., 1997). A misspecification perspective was then used for performing a spatial autocorrelation error estimation analysis using the seasonal-sampled predictor covariate coefficients. The model was generated using they = Xβ + ε* (i.e. regression equation) assuming the sampled S.damnosum s.l data had autocorrelated disturbances. The model also assumed that the sampled data could be decomposed into a white-noise component, ε, and a set of unspecified sub-district level regression models that had the structure $y = XB + \underbrace{E\gamma + \varepsilon}_{=\varepsilon^*}$. White noise in a seasonal -based regression model is a univariate or multivariate discrete-time stochastic process whose terms are independent and independent (i.i.d) with a zero mean (Jacob, et., 2012). In this research, the misspecification term wasE_Y.

Distance between the S.damnosum s.l.-related parameter estimators was then defined in terms of an n-by-n geographic weights matrix, C, whose cijvalues were 1 if the sampled geolocationsi and j were deemed nearby, and 0 otherwise. Adjusting this matrix by dividing each row entry by its row sum, with the row sums given by C1, converted this matrix to matrix W. The n-by-1 vector $x = \left[x_1 \cdots x_n\right]^T$ contained measurements of a quantitative variable for n (i.e., georeferenced sampled S.damnosum s.l.geopredictor covariate μ) within the n-by-n spatial weighting matrix. The formulation for the Moran's index of spatial autocorrelation used in this research was: $I(x) = \frac{n\sum_{(2)} w_{ij}(x_i-\bar{x})(x_j-\bar{x})}{\sum_{(2)} w_{ij}\sum_{i=1}^{n}(x_i-\bar{x})^2}$ where $\sum_{(2)} = \sum_{i=1}^{n}\sum_{j=1}^{n}$ with $i \neq j$. The values w_{ij} were the spatial weights (i.e., sampled S.damnosum s.l. endemic transmission-oriented covariate coefficients) stored in the symmetrical matrix W [i.e., $\left(w_{ij} = w_{ji}\right)$] that had a null diagonal $\left(w_{ii} = 0\right)$. The matrix was initially generalized to an asymmetrical matrix W. Matrix W can be generalized by a non-symmetric matrix W^* by using $W = \left(W^* + W^{*T}\right)/2$ (McCulloch and Searle, 2005). Moran's I was then rewritten using matrix notation: $I(x) = \frac{n}{1^t W 1}\frac{x^T HHWHHx}{x^T HHx} = \frac{n}{1^T W 1}\frac{x^T HWHx}{x^T Hx}$ where $H = \left(I - 11^T/n\right)$ was an orthogonal projector verifying that $H = H^2$ (i.e., H was independent). The spatial error model in the disturbance was then revealed in the seasonal predictive S.damnosum s.l. model residuals using an alternate form of the model: y= X βW+ (1-λW2)-1. The concentrated log-likelihood equation then estimated λ which in this research was obtained by substituting the GLS estimators of β and σ2as functions of λ into the likelihood equation of the spatial error model. The likelihood equation used the simplification for the Jacobian term.

In this research the Jacobian was the derivative of a multivariate function. In vector calculus, the Jacobian matrix is the matrix of all first-order partial derivatives of a vector- or scalar-valued function with respect to another vector; therefore, if F : Rn → Rm is a function from Euclidean n-space to Euclidean m-space. In this

research this function was given by m real-valued component functions, y1(x1,...,xn), ..., ym(x1,...,xn). The partial derivatives of all these functions were organized in an m-by-n matrix, (i.e., the Jacobian matrix J of F in the S.damnosum s.l. model), as follows: $J = \begin{bmatrix} \frac{\partial y_1}{\partial x_1} & \cdots & \frac{\partial y_1}{\partial x_n} \\ \vdots & \ddots & \vdots \\ \frac{\partial y_m}{\partial x_1} & \cdots & \frac{\partial y_m}{\partial x_n} \end{bmatrix}$. The matrices were also denoted by $J_F(x_1, \ldots, x_n)$ and $\frac{\partial(y_1, \ldots, y_m)}{\partial(x_1, \ldots, x_n)}$. Since (x1,...,xn) were the usual orthogonal Cartesian coordinates, the ith row (i = 1, ..., n) of these matrices corresponded to the gradient of the ith component function yi: (∇y_i) .The model described by the JF(p) was the best linear approximation of F near the point p (i.e., sampled S. damnosum s.l ArcGIS/SAS-based Euclidean-distant-based parameter estimators) in the sense that $F(\mathbf{x}) = F(\mathbf{p}) + J_F(\mathbf{p})(\mathbf{x} - \mathbf{p}) + o(\|\mathbf{x} - \mathbf{p}\|)$for x close to p and where o was the little o-notation for $x \to p$ and $\|\mathbf{x} - \mathbf{p}\|$ was the distance between x and p. If p is a point in Rn and F is differentiable at p, then its derivative is given by JF(p) (McCulloch and Searle, 2005). The transformation from spherical coordinates (r, θ, ϕ) to Cartesian coordinates (x1, x2, x3) was then provided by the function F : R+ × [0,π] × [0,2π) → R3 with components: $x_1 = r\ \sin\theta\ \cos\phi x_2 = r\ \sin\theta\ \sin\phi$ $x_3 = r\ \cos\theta.$ The matrix for this change was then $J_F(r, \theta, \phi) = \begin{bmatrix} \frac{\partial x_1}{\partial r} & \frac{\partial x_1}{\partial \theta} & \frac{\partial x_1}{\partial \phi} \\ \frac{\partial x_2}{\partial r} & \frac{\partial x_2}{\partial \theta} & \frac{\partial x_2}{\partial \phi} \\ \frac{\partial x_3}{\partial r} & \frac{\partial x_3}{\partial \theta} & \frac{\partial x_3}{\partial \phi} \end{bmatrix} = \begin{bmatrix} \sin\theta\ \cos\phi & r\ \cos\theta\ \cos\phi & -r\ \sin\theta\ \sin\phi \\ \sin\theta\ \sin\phi & r\ \cos\theta\ \sin\phi & r\ \sin\theta\ \cos\phi \\ \cos\theta & -r\ \sin\theta & 0 \end{bmatrix}$. The determinant was r2 sin θ. Since dV = dx1dx2dx3 in the predictive seasonal autoregressive model, this determinant implied that the differential volume element dV = r2 sin θdrdθd. Nevertheless, this determinant varied the sampled coordinates. To avoid any variation the new coordinates were defined as $w_1 = \frac{r^3}{3},\ w_2 = -\cos\theta,\ w_3 = \phi.$ in the model. Thereafter, the determinant equaled to 1 and volume element became $r^2 dr\ \sin\theta\ d\theta\ d\phi = dw_1 dw_2 dw_3$. In this research, the Jacobian term appeared in the likelihood functions as a normalizing factor. This ensured that the use of our variable transformations still led to probability density functions whose complete integration yielded unity. In probability theory, a normalizing constant is a constant by which an everywhere non-negative function must be multiplied so the area under its graph is 1 to make it a probability density function(pdf) (Griffith, 1897). We then defined this function as $p(x) = e^{-x^2/2}, x \in (-\infty, \infty)$. This rendered the values had $\int_{-\infty}^{\infty} p(x)\, dx = \int_{-\infty}^{\infty} e^{-x^2/2}\, dx = \sqrt{2\pi}$, .Thereafter, we defined the function $\varphi(x)$as $\varphi(x) = \frac{1}{\sqrt{2\pi}} p(x) = \frac{1}{\sqrt{2\pi}} e^{-x^2/2}$ in the S.damnosum s.l. model so that $\int_{-\infty}^{\infty} \varphi(x)\, dx = \int_{-\infty}^{\infty} \frac{1}{\sqrt{2\pi}} e^{-x^2/2}\, dx = 1$ Function $\varphi(x)$is a pdf(Griffith, 1897). This was the density of the standard normal distribution using the means expected value as 0 and the variance as 1. In this research the constant $\frac{1}{\sqrt{2\pi}}$ was the normalizing constant of function p(x). In the models. Similarly, $\sum_{n=0}^{\infty} \frac{\lambda^n}{n!} = e^{\lambda},$ and consequently $f(n) = \frac{\lambda^n e^{-\lambda}}{n!}$ was a probability mass function on the set of all nonnegative integers in the sampled ecological empirical dataset.

A Moans scatterplot was then generated in ArcGIS. The Moran scatterplot portrays Pn j¼1 cij zj versus zi, whose trend line highlights the global trend across a given geographic landscape employing sums of neighboring values' quantities which can be visualized with a map(McCulloch and Searle, 2005). By doing so we generated local indices of spatial autocorrelation (LISA) statistics, which enabled clusterings on the S. damnosum s.l. map to become more conspicuous. LISA quantities highlight local trends across a given geographic landscape, emphasizing

any clusterings in the deviations from the global trend line (Jacob, et., 2012).These individual contributions to the MC revealed whether spatial autocorrelation essentially was the same in all demarcated zones in our study site map.

Bayesian analyses: In the Bayes formulation, the specification of the seasonal S. damnosums.l. risk model was performed by assigning priors to all unknown parameters. We used the empirical dataset of spatiotemporal-sampled observations X=[x1…,xn]; whereby, each xifor i=1…n was assumed to be distributed according to some distribution p(xi | θ). The posterior probability Pr(M|D) of the models(i.e.,M) was given by the sampled data feature attributes (i.e., D) which was given by Bayes' theorem: $\Pr(M|D) = \frac{\Pr(D|M)\Pr(M)}{\Pr(D)}.$ Given a model selection problem in which we have to choose between models, on the basis of observed data D, the plausibility of the different models M1 and M2, parameterized by the parameter vectors θ1 and θ2is assessed by the Bayes factorK commonly provided by $K = \frac{\Pr(D|M_1)}{\Pr(D|M_2)} = \frac{\int \Pr(\theta_1|M_1)\Pr(D|\theta_1, M_1)\,d\theta_1}{\int \Pr(\theta_2|M_2)\Pr(D|\theta_2, M_2)\,d\theta_2}.$ where Pr(D|Mi) is commonly called the marginal likelihood(i.e.,i.) []

In this research θ was a parameter that was unknown and thus had to be inferred from the sampled georeferenced data. Our Bayesian procedure began by assuming that θ was distributed according to some prior distribution p(θ | α), where the parameter α was a hyperparameter. The joint probability of the was then generated using: $p(\mathbf{X}|\theta) = p(x_1, \ldots, x_n|\theta) = \prod_{i=1}^{n} p(x_i|\theta)$, whereby, the equations $p(\mathbf{X}|\theta, \alpha) = p(\mathbf{X}|\theta)$ and $p(x_i|\theta, \alpha) = p(x_i|\theta)$ were conditionally independent of the hyperparameter. We assumed that the two quantities were related by their conditional probability. This conditional probability (i.e., likelihood function) was dependent on the modality in the model. The conditional probability of an event A assuming that B Bhas occurred, denotes $P(A \mid B)$, which is equivalent to $P(A \mid B) = \frac{P(A \bigcap B)}{P(B)}$, [] which in this research was proven directly employing $P(A \mid B)\,P(B) = P(A \bigcap B),$ as generalized by $P(A \bigcap B \bigcap C) = P(A)\,P(B \mid A)\,P(C \mid A \bigcap B).$

The estimate was then computed as a function of the posterior density which required the specification of a prior density in addition to the likelihood function Bayesian inference which then determined the posterior distribution of the sampled time series dependent S.damnosums.l.parameter estimators $p(\theta|\mathbf{X}, \alpha)$ using :

$$\begin{aligned} p(\theta|\mathbf{X}, \alpha) &= \frac{p(\theta, \mathbf{X}, \alpha)}{p(\mathbf{X}, \alpha)} \\ &= \frac{p(\theta, \mathbf{X}, \alpha)}{\int_\theta p(\theta, \mathbf{X}, \alpha) d\theta} \\ &= \frac{p(\mathbf{X}|\theta, \alpha)p(\theta|\alpha)}{\int_\theta p(\mathbf{X}|\theta, \alpha)p(\theta|\alpha)\,\mathrm{d}\theta} \\ &= \frac{p(\mathbf{X}|\theta)p(\theta|\alpha)}{\int_\theta p(\mathbf{X}|\theta)p(\theta|\alpha)\,\mathrm{d}\theta} \\ &= \frac{[\prod_{i=1}^{n} p(x_i|\theta)]p(\theta|\alpha)}{\int_\theta [\prod_{i=1}^{n} p(x_i|\theta)]p(\theta|\alpha)\,\mathrm{d}\theta} \end{aligned}$$

In this research we defined the deviance as $D(\theta) = -2\log(p(y|\theta)) + C$, where y was the sampled onchocerciasis endemic transmission-oriented explanatory covariate coefficients, $p(y|\theta)$ was the likelihood function and C was a constant. The expectation $\bar{D} = \mathbf{E}^{\theta}[D(\theta)]$ actually measured how well the model fit the sampled data. The residual revealed that the larger the expectation value, the worse the fit. The effective number of parameter estimators for the risk model was then computed as $p_D = \bar{D} - D(\bar{\theta})$, where $\bar{\theta}$ was the expectation of θ. In this research the DIC was calculated in the model as $DIC = p_D + \bar{D}.$

We then used PROC MCMC for generating the multivariate density functions in the Bayesian autoregressive estimation analysis. In PROC MCMC we used the logarithm of LOGMPDFWISHART for determining the Wishart distribution and the logarithm LOGMPDFIWISHART for the inverted-Wishart distribution. We let x be an n-dimensional random vector with mean vector μ and covariance matrix $\mathbf{\Sigma}$.. The density was $pdf(x;\mu,\mathbf{\Sigma}) = \frac{\exp(-\frac{1}{2}(x-\mu)^T\mathbf{\Sigma}^{-1}(x-\mu))}{\sqrt{(2\pi)^n|\mathbf{\Sigma}|}}$ where $|\mathbf{\Sigma}|$ was the determinant of the covariance matrix $\mathbf{\Sigma}$. The density function from the Wishart distribution in the model was then : $pdf(x;\mu,\mathbf{\Sigma}) = \frac{1}{C_n(\mu)}|\mathbf{\Sigma}|^{-\frac{\mu}{2}}|x|^{\frac{\mu-n-1}{2}}\exp\left(-\frac{1}{2}tr(\mathbf{\Sigma}^{-1}x)\right)$ with $\mu > n$, and the trace of the square matrices A was: $tr(A)=\sum_i a_{ii}$ $C_n(\mu) = 2^{\frac{\mu n}{2}}\Gamma_n\left(\frac{\mu}{2}\right)$ $\Gamma_n(z) = \pi^{\frac{n(n-1)}{4}}\prod_{i=1}^{n}\Gamma\left(z-\frac{i-1}{2}\right)$. Additionally, the density function from the inverse-Wishart distribution was $pdf(x;\mu,\mathbf{\Sigma}) = \frac{1}{D_n(\mu)}|\mathbf{\Sigma}|^{\frac{\mu-n-1}{2}}|x|^{-\frac{\mu}{2}}\exp\left(-\frac{1}{2}tr(\mathbf{\Sigma}x^{-1})\right)$ for $\mu > 2n$, and $D_n(\mu) = 2^{\frac{(\mu-n-1)n}{2}}\Gamma_n\left(\frac{\mu-n-1}{2}\right)$ for model.

The marginal and conditional distributions from the inverse Wishart-distributed matrix was then further quantified using $A\sim W^{-1}(\psi, m)$. We partitioned the matrices for determining if ψ was conformable with each other using: $A = \begin{bmatrix} A_{11} & A_{12} \\ A_{21} & A_{22} \end{bmatrix}$, $\psi = \begin{bmatrix} \psi_{11} & \psi_{12} \\ \psi_{21} & \psi_{22} \end{bmatrix}$ where A_{ij} and ψ_{ij} were pi x pj matrices. We then determined if A_{11} was independent of $A_{11}^{-1}A_{12}$ and $A_{22\cdot1}$, when $A_{22\cdot1} = A_{22} - A_{21}A_{11}^{-1}A_{12}$ which in this research was the Schur complementA_{11}in;ii)$A_{11}\sim W^{-1}(\psi_{11}, m - p_2)$;iii)$A_{11}^{-1}A_{12}|A_{22\cdot1}\sim MN_{p_1xp_2}(\psi_{11}^{-1}\psi_{12}, A_{22\cdot1}\otimes\psi_{11}^{-1})$when of $MN_{pxq}(\cdot,\cdot)$ was a matrix normal distribution rendered from the spatiotemporal-sampled S.damnosums.l.parameters and, $A_{22\cdot1}\sim W^{-1}(\psi_{11}, m)$.In linear algebra and the theory of matrices, the Schur complement of a matrix block (i.e., a sub-matrix within a larger matrix) commonly is defined using pop, pique, pop and q×qmatrices,whereD is invertible and $M = \begin{bmatrix} A & B \\ C & D \end{bmatrix}$ so that M is a (p+q)×(p+q) matrix (Griffith, 1897).

In this research, the sampled S.damnosum s.l. observations $X = x_1, \ldots, x_n$ were independent p-variate Gaussian variables drawn from a distribution, then the conditional distribution had a $W^{-1}(A + \psi, n + m)$ distribution, where A =XXT was n times the sample covariance matrix. Because the prior and posterior distributions are the same family(Griffith, 1897)., the inverse Wishart distribution was the conjugate to the multivariate Gaussian generated from the sampled georeferenced predictor covariate coefficient estimates.

Model data input was also conducted in PROC MCMC but the number of chains had to be specified before compilation. A Markov chain was generated using a sequence of sX1, X2, X3, ... with the Markov property, namely that, given the present state, the future and past states were independent. Both the model residual estimates revealed $\Pr(X_{n+1} = x | X_1 = x_1, X_2 = x_2, \ldots, X_n = x_n) = \Pr(X_{n+1} = x | X_n = x_n)$. In this research the probability of going from state i to state j in n time steps was $p_{ij}^{(n)} = \Pr(X_n = j \mid X_0 = i)$ and the single-step transition was $p_{ij} = \Pr(X_1 = j \mid X_0 = i)$. For quantifying the external values in the Markov chains we used $p_{ij}^{(n)} = \Pr(X_{k+n} = j \mid X_k = i)$and $p_{ij} = \Pr(X_{k+1} = j \mid X_k = i)$.The n-step transition probabilities satisfied the Chapman–Kolmogorov equation, that for any k such that 0 < k < n, $p_{ij}^{(n)} = \sum_{r\in S} p_{ir}^{(k)} p_{rj}^{(n-k)}$ When the stochastic process under consideration is Markovian, the Chapman–Kolmogorov equation is equivalent to an identity on transition densities (Jacob, et., 2012). In our Markov models we assumed that i1 < ... < in. Then, because of the Markov property our model rendered, $p_{i_1,\ldots,i_n}(f_1,\ldots,f_n) = p_{i_1}(f_1)p_{i_2;i_1}(f_2 \mid f_1)\cdots p_{i_n;i_{n-1}}(f_n \mid f_{n-1})$,where the conditional probability $p_{i;j}(f_i \mid f_j)$ was the transition probability between the times i>j. A stochastic process has the Markov property if the conditional probability distribution of future states of the process depends only upon the present state, not on the sequence of events that preceded it (Jacob, et., 2012).

In this research the Chapman–Kolmogorov equation took the form $p_{i_3;i_1}(f_3 \mid f_1) = \int_{-\infty}^{\infty} p_{i_3;i_2}(f_3 \mid f_2)p_{i_2;i_1}(f_2 \mid f_1)\,df_2$. where S was the state space of the Markov chain in the

S.damnosums.l.risk model. In mathematics, specifically in probability theory and in particular the theory of Markovian stochastic processes, the Chapman–Kolmogorov equation is an identity relating the joint probability distributions of different sets of coordinates on a stochastic process (Griffith, 1897). We used { fi } as an indexed collection of the sampled random variables, that was, a stochastic process. We let $p_{i_1,\ldots,i_n}(f_1,\ldots,f_n)$ be the joint pdf of the values of the random variables f1 to fn. Then, the Chapman–Kolmogorov equation generated by the sampled random variables was $p_{i_1,\ldots,i_{n-1}}(f_1,\ldots,f_{n-1}) = \int_{-\infty}^{\infty} p_{i_1,\ldots,i_n}(f_1,\ldots,f_n)\,df_n$ using a straightforward marginalization over the nuisance variables. Note that we did not assume anything about the temporal or any other ordering of the seasonal-sampled environmental S. damnosum s.l. variables in the equation, thus, the estimates were applied equally to the marginalization of any parameter. When the stochastic process under consideration was Markovian, the Chapman–Kolmogorov equation was equivalent to an identity on transition densities in the model. In the Markov chain setting, one assumed that i1 < ... < in. Then, because of the Markov property, $p_{i_1,\ldots,i_n}(f_1,\ldots,f_n) = p_{i_1}(f_1)p_{i_2;i_1}(f_2 \mid f_1)\cdots p_{i_n;i_{n-1}}(f_n \mid f_{n-1}),$ the conditional probability $p_{i;j}(f_i \mid f_j)$ was the transition probability between the times i>j in the model. The Chapman–Kolmogorov equation generated using the seasonal-sampled S. damnosums.l. data feature attributes then took the form $p_{i_3;i_1}(f_3 \mid f_1) = \int_{-\infty}^{\infty} p_{i_3;i_2}(f_3 \mid f_2)p_{i_2;i_1}(f_2 \mid f_1)\,df_2.$ Our model revealed that when the probability distribution on the state space of a Markov chain was discrete and the Markov chain was homogeneous, the Chapman–Kolmogorov equations could be expressed in terms of infinite-dimensional matrix multiplication, thus: $P(t+s) = P(t)P(s)$ when P(t) was the transition matrix of jump t, (i.e., P(t) was the matrix such that entry (i,j) contained the probability of the chain moving from state i to state j in t steps). Additionally, it followed that to calculate the transition matrices of jump t, it was sufficient to raise the transition matrix of jump one to the power of t, that is $P(t) = P^t$ in the seasonal endemic transmission risk model. The marginal distribution Pr(Xn = x) was the distribution over states at time n in the residuals. The initial distribution was Pr(X0 = x) in the predictive model. The evolution of the process through each step was then described by $\Pr(X_n = j) = \sum_{r\in S} p_{rj}\Pr(X_{n-1} = r) = \sum_{r\in S} p_{rj}^{(n)}\Pr(X_0 = r).$

Furthermore, in this research we extended this analyses to show that that distance between the nth step transition probability and the invariant probability measure in the time-series dependent S.damnosum s.l. model was bounded by p*[a+bg(x)] for the constant a>b>0 and p<1. The invariant was then used to obtain convergence rates to quantify the transition probabilities for autoregressive processes in the models using a random walk on a half line. In this research a random walk with reflecting zone on the nonnegative integers generated from the sampled predictor covariate coefficients was a Markov chain whose transition probabilities $q(x,y)$ were those of a random walk [i.e., q(x,y)= p(y-x)] which was outside a finite set $\{0,1,2,\ldots,K\}$. As such, that the distribution q(x) stochastically dominated p(-x) for every $x \in \{0,1,2,\ldots,K\}$. Jacob et. al. [11] has proven that when $\sum x p_x \rangle 0$, the transition probabilities satisfy $q^n(x,y) \sim C_{xy}R^{-n}n^{-\frac{3}{2}}$ as $n \to \infty$, and when $\sum x p_x \rangle = 0$, $q^n(x,y) \sim C_{xy}n^{-\frac{1}{2}}$ in an autoregressive seasonal vector arthropod-related predictive infectious disease model. In this research we did so to extend and strengthen the model residuals in countable state space. Inference for MCMC simulation techniques was then based on weighted Least Squares Regression proposals and on latent utility representations of multi-categorical S. damnosum s.l. regression-based model.

Employing the time-series S. damnosum s.l. data, a weighted autoregressive average moving model (e.g., ARIMA) was constructed in SAS using X_t where t was an integer index and the X_t were the sampled covariate coefficients. The ARMA(p,q) model was provided by: $\left(1 - \sum_{i=1}^{p} \alpha_i L^i\right) X_t = \left(1 + \sum_{i=1}^{q} \theta_i L^i\right) \varepsilon_t$ where L was the lag operator, the α_i are the parameters of the autoregressive part of the model, the θ_i was the parameters of the moving average part and the ε_t was the error terms. In time series analysis, the lag operator or back shift

operator operates on an element of a time series to produce the previous element. In mathematics, and in particular functional analysis, the shift operator or translation operator is an operator that takes a function f(·) to its translation f(·+a) (Jacob, et., 2012). In time series analysis, the shift operator is called the lag operator(Griffith, 1897). In this research, given the time series dependent observational explanatory covariates $X = \{X_1, X_2, \ldots\}$ then $LX_t = X_{t-1}$ for all $t > 1$ or equivalently $X_t = LX_{t+1}$ for all $t \geq 1$where L is the lag operator. Note that the lag operator was raised to arbitrary integer powers so that $L^{-1}X_t = X_{t+1}$ and $L^k X_t = X_{t-k}$. The error terms εt were then independent, identically distributed variables sampled from a normal distribution with zero mean. We then assumed that the polynomial $\left(1 - \sum_{i=1}^{p} \alpha_i L^i\right)$ had a unitary root of multiplicity d. The S.damnosums.l. risk model was then rewritten as: $\left(1 - \sum_{i=1}^{p} \alpha_i L^i\right) = \left(1 - \sum_{i=1}^{p-d} \phi_i L^i\right)(1 - L)^d$. An ARIMA(p,d,q) process then expressed this polynomial factorization property, and it was given by: $\left(1 - \sum_{i=1}^{p} \phi_i L^i\right)(1 - L)^d X_t = \left(1 + \sum_{i=1}^{q} \theta_i L^i\right)\varepsilon_t$.

3. Results

Initially, we constructed a Poisson regression model using the spatiotemporal-sampled S.damnosums.l covariate coefficient measurement values. Our model was generalized by introducing an unobserved heterogeneity term for each sampled observation i. The weights were then assumed to differ randomly in a manner that was not fully accounted for by the other spatiotemporal-sampled. related covariates. In this research this process was formulated as $E(y_i|\mathbf{x}_i, \tau_i) = \mu_i \tau_i = e^{\mathbf{x}_i'\boldsymbol{\beta} + \varepsilon_i}$ where the unobserved heterogeneity term$\tau_i = e^{\varepsilon_i}$ was independent of the vector of regressors $\mathbf{x}_i$. Then the distribution of y_i was conditional on $\mathbf{x}_i$ which in our model had a Poisson specification with conditional mean and conditional variance $\mu_i \tau_i$: $f(y_i|\mathbf{x}_i, \tau_i) = \frac{\exp(-\mu_i \tau_i)(\mu_i \tau_i)^{y_i}}{y_i!}$. We then let $g(\tau_i)$be the pdf of τ_i. Then, the distribution $f(y_i|\mathbf{x}_i)$ was no longer conditional on τ_i. Instead it was obtained by integrating $f(y_i|\mathbf{x}_i, \tau_i)$with respect to τ_i: $f(y_i|\mathbf{x}_i) = \int_0^\infty f(y_i|\mathbf{x}_i, \tau_i) g(\tau_i) d\tau_i$.

In the time series S. damnosum s.l. regressing of the sampled covariate coefficients, the random variable K followed the binomial distribution with the sampled parameters n and p where we wrote K ~ B(n, p). The probability of getting exactly k successes in n trials was then rendered by the pmf which in this research was provided by $f(k; n, p) = \Pr(K = k) = \binom{n}{k} p^k (1-p)^{n-k}$ for k = 0, 1, 2, ..., n, where $\binom{n}{k} = \frac{n!}{k!(n-k)!}$ was the binomial coefficient .Hence, when n chose k in there model estimation, this was denoted C(n, k), nCk, or nCk. The formula was understood as follows: k successes were represented as (pk) (i.e. tabulated seasonal village prevalence rates) which was identified employing (1 − p)n − k. In creating reference tables for our binomial distribution probability, we used n/2 values. This was because for k > n/2, the probability was calculated by its complement as $f(k, n, p) = f(n - k; n, 1 - p)$.Looking at the expression ƒ(k, n, p) as a function of k in the onchocerciasis endemic transmission model there was a k value that maximized it. This k value was then found by calculating $\frac{f(k+1, n, p)}{f(k, n, p)} = \frac{(n-k)p}{(k+1)(1-p)}$ and comparing it to 1. There is always an integer M that satisfies $(n+1)p - 1 < M \leq (n+1)p$. when ƒ(k, n, p) is monotone increasing for k < M and monotone decreasing for k > M, with the exception of the case where (n + 1)p is an integer (Toe et al., 1997). In our case, there were two seasonal-sampled S. damnosum s.l. explanatory predictor covariate coefficient values for which ƒ was maximal: (n + 1)p and (n + 1)p − 1. In this research, M was the most probable outcome of the Bernoulli trials (i.e.,mode).

A generalized hypergeometric function ${}_pF_q\left(a_1, \ldots, a_p; b_1, \ldots, b_q; x\right)$was then generated for our multiseasonal S. damnosum s.l. model. In this research, a number of generalized hypergeometric functions were used . For example, ${}_0F_1\left(; b; z\right)$, a confluent hypergeometric limit function, was implemented in Mathematica as

Hypergeometric0F1[b, z]. ${}_1F_1(a;b;z)$.Thereafter the confluent hypergeometric function of the first kind, was implemented in Mathematica in the model as Hypergeometric1F1[a, b, z]. The function ${}_2F_1(a,b;c;z)$ (i.e.,"the" hypergeometric function or Gauss's hypergeometric function) was also implemented in the model. Thereafter, the Cauchy principal value was computed in Mathematica employing Integrate[f, x, a, b], PrincipalValue -> True]. Cauchy principal values of functions with possibly nonsimple poles can be computed numerically using the "CauchyPrincipalValue" method in NIntegrate(Boatin et al., 1997). Cauchy principal values are important in the theory of generalized functions, where they allow extension of L^2 results to L^1 (Toe et al., 1997).

A generalized version of the falling factorial was then defined by $(x)_n^{(h)}(x)=x(x-h)\dots(x-(n-1)h)$ for the S. damnsoum s.l. endemic transmission-oriented model which was parsimoniously implemented in Mathematica as FactorialPower[x, n, h]. We noticed that the usual factorial was related to the falling factorial by The first few falling factorials were $(x)_0=1,(x)_1=x,(x)_2=x(x-1)=x^2-x,(x)_3=x(x-1)(x-2)=x^3-3x^2+2x,(x)_4$ $=x(x-1)(x-2)(x-3)=x^4-6x^3+11x^2-6x$ The derivatives were then given by $\frac{d}{dz}(z)_n=(H_z-H_{z-n})(z)_n$, where H_z was the harmonic number. A sum formula connecting the falling factorial $(x)_n$ and rising factorial $x^{(n)}$ in $(x)_n=\sum_{k=0}^{n}c_{n\,k}\,x^{(k)}$, the model was then achieved employing $g(t)=1,f(t)e^t-1,h(t)=1,l(t)=1-e^{-t}$, where the generating function $\sum_{n=0}^{\infty}\frac{t_n(x)}{n!}t^n=\sum_{n=0}^{\infty}\frac{1}{n!}\sum_{k=0}^{n}c_{n\,k}\,x^k\,t^k=e^{t\,x/(1+t)}$ and where $1+x\,t+\frac{1}{2}(x^2-2x)t^2+\frac{1}{6}(x^3-6x^2+6x)t^3+\frac{1}{24}(x^4-12x^3+36x^2-24x)t^4+\dots,$ In this research, the falling factorial was associated with $f(t)=e^t-1$ and had a generating function $\sum_{k=0}^{\infty}\frac{(x)_k}{k!}t^k=e^{x\ln(1+t)}=(1+t)^x$, which was equivalent to $\sum_{k=0}^{\infty}\binom{x}{k}t^k=(1+t)^x.$ The binomial identity of our predictive linear onchocerciasis endemic transmission-oriented model was $(x+y)_n=\sum_{k=0}^{n}\binom{n}{k}(x)_k\,(y)_{n-k},$ when $\binom{n}{k}$ was the binomial coefficient, which we re-wrote $\binom{x+y}{n}=\sum_{k=0}^{n}\binom{x}{k}\binom{y}{n-k},$ We found that the falling factorial in the riverine model followed the relation $x(x)_n=(x)_{n+1}+n(x)_n$ and $n!=(n)_n$

The cumulative distribution function in the S. damnosum s.l. riverine larval habitat model distribution was then expressed as: $F(x;n,p)=\Pr(X\le x)=\sum_{i=0}^{\lfloor x\rfloor}\binom{n}{i}p^i(1-p)^{n-i}$ where $\lfloor x\rfloor$ was the "floor" under x, (i.e. the greatest integer less than or equal to x in the empirical dataset) . The function was represented in terms of the regularized incomplete beta function, as follows: $F(k;n,p)=\Pr(X\le k)=I_{1-p}(n-k,k+1)=$ $(n-k)\binom{n}{k}\int_0^{1-p}t^{n-k-1}(1-t)^k\,dt.$ for each 5km delineated in the ArcGIS risk map from the capture point. For k ≤ np, upper bounds for the lower tail of the distribution function was then derived for each sub-section.. In particular, Hoeffding's inequality yielded the bound $F(k;n,p)\le\frac{1}{2}\exp\left(-2\frac{(np-k)^2}{n}\right),$ and Chernoff's inequality derived the bound $F(k;n,p)\le\exp\left(-\frac{1}{2p}\frac{(np-k)^2}{n}\right).$ In probability theory, Hoeffding's inequality provides an upper bound on the probability that the sum of random variables deviates from its expected

value while, Chebyshev's inequality guarantees that in any probability distribution,"nearly all" values are close to the mean — the precise statement being that no more than 1/k2 of the distribution's values can be more than k standard deviations away from the mean or, equivalently, at least 1 - 1/k2 of the distribution's values are within k standard deviations of the mean (Toe et al., 1997).These bounds were reasonably tight when p = 1/2, since the following expression held in the riverine ArcGIS/SAS-based model for all k ≥ 3n/8 $F(k;n,1/2) \geq \frac{1}{15}\exp\left(-\frac{16(n/2-k)^2}{n}\right)$. Thereafter, it was possible to expand any power of x + y in the model into a sum of the form $(x+y)^n = \binom{n}{0}x^n y^0 + \binom{n}{1}x^{n-1}y^1 + \binom{n}{2}x^{n-2}y^2 + \cdots + \binom{n}{n-1}x^1 y^{n-1} + \binom{n}{n}x^0 y^n$, where each $\binom{n}{k}$ was a binomial coefficient . This binomial identity used a summation notation, which in this research was written as $(x+y)^n = \sum_{k=0}^{n}\binom{n}{k}x^{n-k}y^k = \sum_{k=0}^{n}\binom{n}{k}x^k y^{n-k}$. The final expression in the model followed the symmetry of x and y. A variant of the binomial formula was also obtained for each sub-classified area by substituting 1 for y, so that it involves only a single sampled variable. This formula in the model was $(1+x)^n = \binom{n}{0}x^0 + \binom{n}{1}x^1 + \binom{n}{2}x^2 + \cdots + \binom{n}{n-1}x^{n-1} + \binom{n}{n}x^n$, where $(1+x)^n = \sum_{k=0}^{n}\binom{n}{k}x^k$.

We then investigated generalized binomial expansions that arose our two-dimensional S.damnsoum s.l. sequences for satisfying a broad generalization of the triangular recurrence for binomial coefficients. In particular, we generated new combinatorial formula for the sequences in terms of a 'shift by rank' quasi-expansion based on an ordered set partitions. We used Dilcher's formula[i.e., $\sum_{1\leq k\leq n}\binom{n}{k}\frac{(-1)^{k-1}}{k^m} = \sum_{1\leq i_1\leq i_2\leq\ldots i_m\leq n}\frac{1}{i_1\, i_2\cdots i_m}$,] for expressing generalized Bernoulli polynomials in terms of classical Bernoulli polynomials. where $\binom{n}{k}$ is a binomial coefficient. An inverted version was then given by $\sum_{1\leq k\leq n}\binom{n}{k}(-1)^{k-1}\sum_{1\leq i_1\leq i_2\ldots\leq i_m=k}\frac{1}{i_1\, i_2\cdots i_m} = \sum_{1\leq k\leq n}\frac{1}{k^m} = H_n^{(m)}$, where $H_n^{(k)}$ was a harmonic number of order m. A q-analog was then provided by $\sum_{1\leq k\leq n}\begin{bmatrix}n\\k\end{bmatrix}_q(-1)^{k-1}\frac{q^{\binom{k+1}{2}+(m-1)k}}{(1-q^k)^m} = \sum_{1\leq i_1\leq i_2\leq\ldots\leq i_m\leq n}\frac{q^{i_1}}{1-q^{i_1}}\cdots\frac{q^{i_m}}{1-q^{i_m}}$, where $\begin{bmatrix}n\\k\end{bmatrix}_q$ was a q-binomial coefficient.

In this research, the Hurwitz zeta function in our geopredictive obchocerciasis endemic transmission-oriented ArcGIS/SAS-based model satisfied $\zeta(-n,a) = -\frac{B_{n+1}(a)}{n+1}$ for $n \geq 0$ where $B_k(a)$ was a Bernoulli polynomial, given $\zeta(0,a) = \frac{1}{2} - a.$ The Hurwitz zeta function was then given by the functional equation $\zeta\left(s,\frac{p}{q}\right) = 2\,\Gamma(1-s)\,(2\pi q)^{s-1}\sum_{n=1}^{q}\sin\left(\frac{\pi s}{2}+\frac{2\pi n p}{q}\right)\zeta\left(1-s,\frac{n}{q}\right)$ and by the integral $\zeta(s,a) = \frac{1}{2}a^{-s} + \frac{a^{1-s}}{s-1} + 2\int_0^{\infty}(a^2+y^2)^{-s/2}\left\{\sin\left[s\tan^{-1}\left(\frac{y}{a}\right)\right]\right\}\frac{dy}{e^{2\pi y}-1}$. In our model we noted that if, $\Re[z] < 0$ and $0 < a \leq 1$, then $\zeta(z,a) = \frac{2\,\Gamma(1-z)}{(2\pi)^{1-z}}\left[\sin\left(\frac{\pi z}{2}\right)\sum_{n=1}^{\infty}\frac{\cos(2\pi a n)}{n^{1-z}} + \cos\left(\frac{\pi z}{2}\right)\sum_{n=1}^{\infty}\frac{\sin(2\pi a n)}{n^{1-z}}\right]$. In addition we found that

$\zeta\left(s,\frac{1}{2}\right)=\sum_{k=0}^{\infty}\left(k+\frac{1}{2}\right)^{-s}=2^{s}\sum_{k=0}^{\infty}(2k+1)^{-s}=2^{s}\left[\zeta(s)-\sum_{k=1}^{\infty}(2k)^{-s}\right]=2^{s}\left(1-2^{-s}\right)\zeta(s)=\left(2^{s}-1\right)\zeta(s)$ in the model residuals. The residual derivative identities included $\frac{d}{ds}\zeta(0,a)=\ln\left[\Gamma(a)\right]-\frac{1}{2}\ln(2\pi)=\frac{d}{ds}\zeta(0,0)=-\frac{1}{2}\ln(2\pi)$, where $\Gamma(z)$ was the gamma function The implied that $\frac{d}{da}\zeta(s,a)=-s\,\zeta(s+1,a)$ in our model when $s\neq 0,1$ In the limit, $\lim_{s\to 1}\left[\zeta(s,a)-\frac{1}{s-1}\right]=-\psi_0(a)$ where $\psi_0(z)$ was the digamma function.

The polygamma function $\psi_m(z)$ was then expressed in the spatiotemporal geopredictive onchocerciasis endemic transmission-oriented ArcGIS/SAS-based model in terms of the Hurwitz zeta function by $\psi_m(z)=(-1)^{m+1}\,m!\,\zeta(1+m,z)$. For positive integers k, p, and $q>p$, $\zeta'\left(-2k+1,\frac{p}{q}\right)=\frac{[\psi(2k)-\ln(2\pi q)]\,B_{2k}(p/q)}{2k}$ which was then subtracted from the geopredictive regression equation $\frac{[\psi(2k)-\ln(2\pi)]\,B_{2k}}{q^{2k}\,2k}+\frac{(-1)^{k+1}\,\pi}{(2\pi q)^{2k}}\sum_{n=1}^{q-1}\sin\left(\frac{2\pi pn}{q}\right)\psi_{(2k-1)}\left(\frac{n}{q}\right)+\frac{(-1)^{k+1}\,2\,(2k-1)!}{(2\pi q)^{2k}}\sum_{n=1}^{q-1}\cos\left(\frac{2\pi pn}{q}\right)\zeta'\left(2k,\frac{n}{q}\right)+\frac{\zeta'(-2k+1)}{q^{2k}}$ when B_n was a Bernoulli number, $B_n(x)$ wasa Bernoulli polynomial, $\psi_n(z)$ was a polygamma function, and $\zeta(z)$ was the Riemann zeta function which in this research also rendered the following closed-form expressions: $\zeta'\left(1-2k,\frac{1}{2}\right)=-\frac{B_{2k}\ln 2}{4^k\,k}-\frac{\left(2^{2k-1}-1\right)\zeta'(-2k+1)}{2^{2k-1}}$, $\zeta'\left(1-2k,\begin{matrix}1/3\\2/3\end{matrix}\right)=\mp\frac{\sqrt{3}\,\left(9^k-1\right)B_{2k}\,\pi}{8k\cdot 9^k}-\frac{3\,B_{2k}\ln 3}{4k\cdot 9^k}\mp\frac{(-1)^k\,\psi_{2k-1}\left(\frac{1}{3}\right)}{2\sqrt{3}\,(6\pi)^{2k-1}}-\frac{\left(9^k-1\right)\zeta'(1-2k)}{2\cdot 9^k}=\zeta'\left(1-2k,\begin{matrix}1/4\\3/4\end{matrix}\right)=\mp\frac{\left(4^k-1\right)B_{2k}\,\pi}{4^{k+1}\,k}+\frac{\left(4^{k-1}-1\right)B_{2k}\ln 2}{k\cdot 2^{4k-1}}\mp\frac{(-1)^k\,\psi_{2k-1}\left(\frac{1}{4}\right)}{4\,(8\pi)^{2k-1}}-\frac{\left(4^k-2\right)\zeta'(1-2k)}{2^{4k}}$, $\zeta'\left(1-2k,\begin{matrix}1/6\\5/6\end{matrix}\right)=\mp\frac{\left(9^k-1\right)\left(2^{2k-1}+1\right)B_{2k}\,\pi}{8\sqrt{3}\,k\cdot 6^{2k-1}}+\frac{B_{2k}\left(3^{2k-1}-1\right)\ln 2}{4k\cdot 6^{2k-1}}+\frac{B_{2k}\left(2^{2k-1}-1\right)\ln 3}{4k\cdot 6^{2k-1}}\mp\frac{(-1)^k\left(2^{2k-1}+1\right)\psi_{2k-1}\left(\frac{1}{3}\right)}{2\sqrt{3}\,(12\pi)^{2k-1}}+\frac{\left(2^{2k-1}-1\right)\left(3^{2k-1}-1\right)\zeta'(1-2k)}{2\cdot 6^{2k-1}}$

where $\zeta'(z_0,a)$ means $d\,\zeta(z,a)/d\,z\,|_{z=z_0}$, $\zeta'(z_0)$ means $d\,\zeta(z)/d\,z\,|_{z=z_0}$, and the upper and lower fractions on the left side of the equations correspond to the plus and minus signs, respectively, on the right side. Further, on the real line with $x>1$, the Riemann zeta function in the spatiotemporal onchocerciasis endemic transmission-oriented model was defined by the integral $\zeta(x)\equiv\frac{1}{\Gamma(x)}\int_0^{\infty}\frac{u^{x-1}}{e^u-1}\,d\,u$, where $\Gamma(x)$ is the gamma function. Since x was an integer n , then we had the identity $\frac{u^{n-1}}{e^u-1}=\frac{e^{-u}\,u^{n-1}}{1-e^{-u}}=e^{-u}\,u^{n-1}\sum_{k=0}^{\infty}e^{-k\,u}=\sum_{k=1}^{\infty}e^{-k\,u}\,u^{n-1}$, so $\int_0^{\infty}\frac{u^{n-1}}{e^u-1}\,d\,u=\sum_{k=1}^{\infty}\int_0^{\infty}e^{-k\,u}\,u^{n-1}\,d\,u.$

To evaluate $\zeta(n)$, we let $y\equiv k\,u$ so that $d\,y=k\,d\,u$ and plugged in the identity we obtained which rendered $\zeta(n)=\frac{1}{\Gamma(n)}\sum_{k=1}^{\infty}\int_0^{\infty}e^{-k\,u}\,u^{n-1}\,d\,u=\frac{1}{\Gamma(n)}\sum_{k=1}^{\infty}\int_0^{\infty}e^{-y}\left(\frac{y}{k}\right)^{n-1}\frac{d\,y}{k}=\frac{1}{\Gamma(n)}\sum_{k=1}^{\infty}\frac{1}{k^n}\int_0^{\infty}e^{-y}\,y^{n-1}\,d\,y.$ Integrating the final expression gave $\Gamma(n)$, which in this research canceled the factor $1/\Gamma(n)$ and provided the Riemann zeta

$$\zeta(n) = \sum_{k=1}^{\infty} \frac{1}{k^n},$$

function[i.e.,](i.e.,a p-series). The p-series is shorthand name for a series with the variable taken to a negative exponent, (e.g., , where . -series are given in closed form by the Riemann zeta function in a S. damnosum s.l. transmission-oriented ArcGIS/SAS-based geopredictive model).

In our geopredictive onchocerciasis endemic transmission-oriented model the Riemann zeta function was

$$\zeta(n) = \underbrace{\int_0^1 \cdots \int_0^1}_{n} \frac{\prod_{i=1}^{n} d\,x_i}{1 - \prod_{i=1}^{n} x_i},$$

also defined in terms of multiple integrals by and as a Mellin transform by $\int_0^{\infty} \text{frac}\left(\frac{1}{t}\right) t^{s-1}\, d\,t = -\frac{\zeta(s)}{s}$ for $0 < \Re[s] < 1$, where $\text{frac}(x)$ was the fractional part The integral transform in the model was then defined by $\phi(z) = \int_0^{\infty} t^{z-1} f(t)\, d\,t$, $f(t) = \frac{1}{2\pi i} \int_{c-i\infty}^{c+i\infty} t^{-z} \phi(z)\, d\,z.$ We noticed the transform $\phi(z)$existed in the model if the integral $\int_0^{\infty} |f(x)|\, x^{k-1}\, d\,x$ was bounded for some $k > 0$, in which case the inverse $f(t)$existed with $c > k$. Table 2 gives Mellin transforms of common functions in the geopredictive onchocerciasis endemic transmission-oriented model. Here, δ was the delta function, $H(x)$ was the Heaviside step function, $\Gamma(z)$was the gamma function, $B(z; a, b)$ was the incomplete beta function, $\text{erfc}\, z$ was the complementary error function erfc, and $\text{Si}(z)$was the sine integral.

Table 2
Mellin Functions for the spatiotemporal S. damnosum s.l. riverine larval habitat model.

$f(t)$	$\phi(z)$	convergence
$\delta(t-a)$	a^{z-1}	
$H(t-a)$	$-\frac{a^z}{z}$	$a > 0, z < 0$
$H(a-t)$	$\frac{a^z}{z}$	$a > 0, z > 0$
$t^n H(t-a)$	$-\frac{a^{n+z}}{n+z}$	$a > 0, \Re[z+n] < 0$
$t^n H(a-t)$	$\frac{a^{n+z}}{n+z}$	$a > 0, \Re[n+z] > 0$
e^{-at}	$a^{-z}\Gamma(z)$	$\Re[a], \Re[z] > 0$
e^{-t^2}	$\frac{1}{2}\Gamma\left(\frac{1}{2}z\right)$	$\Re[z] > 0$
$\sin t$	$\Gamma(z)\sin\left(\frac{1}{2}\pi z\right)$	$-1 < \Re[z] < 1$
$\cos t$	$\Gamma(z)\cos\left(\frac{1}{2}\pi z\right)$	$0 < \Re[z] < 1$
$\frac{1}{1+t}$	$\pi \csc(\pi z)$	$0 < \Re[z] < 1$
$\frac{1}{(1+t)^a}$	$\frac{\Gamma(a-z)\Gamma(z)}{\Gamma(a)}$	$\Re[a-z] > 0, \Re[z] > 0$
$\frac{1}{1+t^2}$	$\frac{1}{2}\pi \csc\left(\frac{1}{2}\pi z\right)$	$0 < \Re[z] < 2$

$(1-t)^{a-1} H(1-t)$	$\frac{\Gamma(a)\Gamma(z)}{\Gamma(a+z)}$	$\Re[a], \Re[z] > 0$
$(t-1)^{-a} H(t-1)$	$\frac{\Gamma(1-a)\Gamma(a-z)}{\Gamma(1-x)}$	$\Re[a-z] > 0, \Re[a] < 1$
$\ln(1+t)$	$\frac{\pi \csc(\pi z)}{z}$	$-1 < \Re[z] < 0$
$\frac{1}{2}\pi - \tan^{-1} t$	$\frac{\pi \sec\left(\frac{1}{2}\pi z\right)}{2z}$	$0 < \Re[z] < 1$
erfc t	$\frac{\Gamma\left(\frac{1}{2}(1+z)\right)}{\sqrt{\pi}\, z}$	$\Re[z] > 0$
Si (t)	$-\frac{1}{z}\Gamma(z)\sin\left(\frac{1}{2}\pi z\right)$	$\Re[z] > -1$
$\frac{t^a}{1-t} H(t-a)$	$-B\left(a^{-1}; 1-a-z; 0\right)$	$a > 1, \Re[a+z] < 1$

We found another example of a Mellin transform in our predictive spatiotemporal onchocerciasis endemic transmission-oriented ArcGIS/SAS-based model based on the relationship between the Riemann function $f(x)$ and the Riemann zeta function $\zeta(s)$ It appeared in the unit square integral $\int_0^1 \int_0^1 \frac{[-\ln(x\,y)]^s}{1-x\,y}\, dx\, dy = \Gamma(s+2)\,\zeta(s+2),$ valid for $\Re[s] > 1$. Note that the zeta function $\zeta(s)$ had a singularity at $s = 1$, where it reduced to the divergent harmonic series. The Riemann zeta function in our S. damnosum s.l. riverine larval habitat model satisfied the reflection functional equation $\zeta(1-s) = 2(2\pi)^{-s} \cos\left(\frac{1}{2}s\pi\right)\Gamma(s)\,\zeta(s)$ .In this research a symmetrical form of this functional equation was provided by $\Gamma\left(\frac{s}{2}\right)\pi^{-s/2}\,\zeta(s) = \Gamma\left(\frac{1-s}{2}\right)\pi^{-(1-s)/2}\,\zeta(1-s)$

As defined above, the zeta function $\zeta(s)$ with $s = \sigma + i\,t$ was a complex number in this research which was then defined for $\Re[s] > 1$. However, $\zeta(s)$ had a unique analytic continuation to the entire complex plane, excluding the point $s = 1$, which corresponded to a simple pole with a al of 1 In particular, we noticed as $s \to 1$, $\zeta(s)$ the residual rendered obeid $\lim_{s\to 1}\left[\zeta(s) - \frac{1}{s-1}\right] = \gamma,$ where γ was the Euler-Mascheroni constant. To perform the analytic continuation for $\Re[s] > 0$, we then re-wrote $\sum_{n=1}^{\infty}\frac{(-1)^n}{n^s} + \sum_{n=1}^{\infty}\frac{1}{n^s} - 2\sum_{n=2,4,\ldots}^{\infty}\frac{1}{n^s} = 2\sum_{k=1}^{\infty}\frac{1}{(2k)^s} = 2^{1-s}\sum_{k=1}^{\infty}\frac{1}{k^s},$ which rendered $\sum_{n=1}^{\infty}\frac{(-1)^n}{n^s} + \zeta(s) = 2^{1-s}\,\zeta(s).$ in terms of $\zeta(s)$ Therefore, $\zeta(s) = \frac{1}{1-2^{1-s}}\sum_{n=1}^{\infty}\frac{(-1)^{n-1}}{n^s}.$ Here, the sum on the right-hand side in the predictive spatiotemporal onchocerciasis endemic transmission-oriented ArcGIS/SAS-based model was exactly the Dirichlet eta function $\eta(s)$ While this formula defined $\zeta(s)$ for only the right half-plane $\Re[s] > 0$, equation (◇) was employed to analytically continue it to the rest of the complex plane. In this research, analytic continuation was also performed using Hankel functions. These functions were defined by the contour integral $H_\epsilon(z) = \int_{C_\epsilon}\frac{(-w)^{z-1}\,e^{-w}}{1-e^{-w}}\, dw$ for $\Im[w] < 0$, $|\arg(-w)| < \pi$, $\epsilon \neq 2\pi k > 0$, where C_ϵ was a Hankel contour. The Riemann zeta function was then expressed in terms of $H_\epsilon(z)$ as $\zeta(z) = -\frac{H_\epsilon(z)}{2i\sin(\pi z)\,\Gamma(z)}$ for $0 < \epsilon < 2\pi$ and $\Re[z] > 1$, where $\Gamma(z)$ was the gamma function in the multivariate onchocerciasis endemic transmission –oriented model distribution.

A globally convergent series for the Riemann zeta function then provided the analytic continuation of $\zeta(s)$ to the entire complex plane except $s=1$ which was provided by

$$\zeta(s)=\frac{1}{1-2^{1-s}}\sum_{n=0}^{\infty}\frac{1}{2^{n+1}}\sum_{k=0}^{n}(-1)^k\binom{n}{k}(k+1)^{-s}$$

where $\binom{n}{k}$ was a binomial coefficient. This equation was related to renormalization and random variates derived from the regression of the seasonal-sampled onchocerciasis endemic transmission-oriented explanatory predictor covariate coefficients which in this research was derived by applying Euler's series transformation whereby $n=0$ to equation. By so doing, we proved the related globally convergent series

$$\zeta(s)=\frac{1}{s-1}\sum_{n=0}^{\infty}\frac{1}{n+1}\sum_{k=0}^{n}(-1)^k\binom{n}{k}(k+1)^{1-s}$$

can be extended to a generalization of the Riemann zeta function in a robust spatiotemporal onchocerciasis endemic transmission model such that $\zeta(s)\equiv\zeta(s,1)$. Further, if the singular term was excluded from the sum definition of $\zeta(s,a)$ in the model, then $\zeta(s)=\zeta(s,0)$ as well. Expanding $\zeta(s)$ about $s=1$ then rendered

$$\zeta(s)=\frac{1}{s-1}+\sum_{n=0}^{\infty}\frac{(-1)^n}{n!}\gamma_n(s-1)^n,$$

where γ_n were Stieltjes constants.

Expanding the Riemann zeta function about $z=1$ thereafter rendered

$$\zeta(z)=\frac{1}{z-1}+\sum_{n=0}^{\infty}\frac{(-1)^n}{n!}\gamma_n(z-1)^n$$

where the constants

$$\gamma_n\equiv\lim_{m\to\infty}\left[\sum_{k=1}^{m}\frac{(\ln k)^n}{k}-\frac{(\ln m)^{n+1}}{n+1}\right]$$

(i.e., Stieltjes constants) quantitated the seasonal-sampled onchocerciasis endemic transmission-oriented explanatory predictor covariate coefficients. Another sum that was then used to define the constants which then rendered

$$\zeta(z+1)-\frac{1}{z}=\sum_{k=0}^{\infty}\frac{(-1)^k\gamma_k z^k}{k!}.$$

These constants were returned by the Mathematica function StieltjesGamma[n]. In the model construction phase a generalization $\gamma_n(a)$ took $\gamma_n(a)/n!$ as the coefficient of $(1-s)^n$ as the function $\zeta(s,a)$ about $s=1$. These generalized Stieltjes constants were implemented in Mathematica as StieltjesGamma[n, a]. Then $n=0$ generated the Euler-Mascheroni constant[i.e., $\gamma_0\equiv\gamma$.] A limit formula for γ_1 was then given by

$$\gamma_1=-\lim_{y\to\infty}y\left\{y+\mathrm{I}\left[\zeta\left(1+\frac{i}{y}\right)\right]\right\},$$

where $\zeta(z)$ was the Riemann zeta function. In this research, the Euler–Mascheroni constant denoted by the lowercase Greek letter gamma (γ) which was defined as the limiting difference between the harmonic series and the natural logarithm:

$$\gamma=\lim_{n\to\infty}\left(\sum_{k=1}^{n}\frac{1}{k}-\ln(n)\right)=\lim_{b\to\infty}\int_1^b\left(\frac{1}{\lfloor x\rfloor}-\frac{1}{x}\right)dx.$$

In our multi-seasonal predictive model $\lfloor x\rfloor$ represented the floor function.

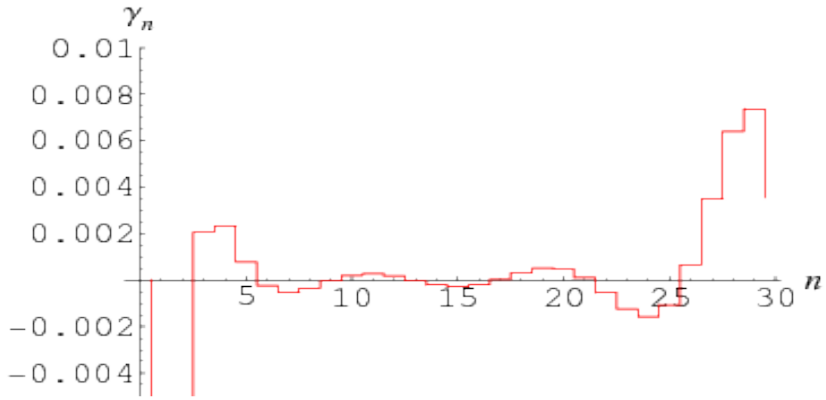

Fig. 4. A linear displayed S. damnosum s.l. riverine larval habitat model distribution renderd by by absorbing the coefficient of γ_n into the constant, $\gamma_n' \equiv \frac{(-1)^n}{n!}\gamma_n$

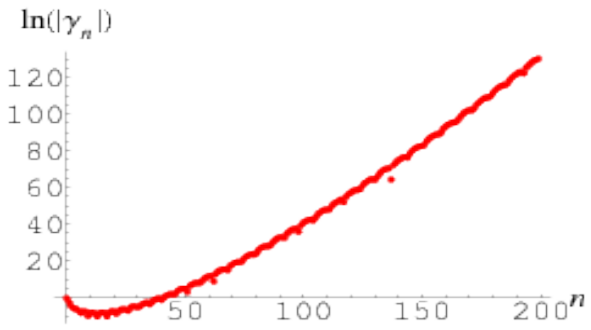

Fig. 5. The Stieltjes constants predicted larval count values where n increases seasonally to 200 as renderd by $\gamma_n = \zeta^{(n)}(z) - \left.\frac{(-1)^n\, n!}{(z-1)^{n+1}}\right|_{z=1}$.

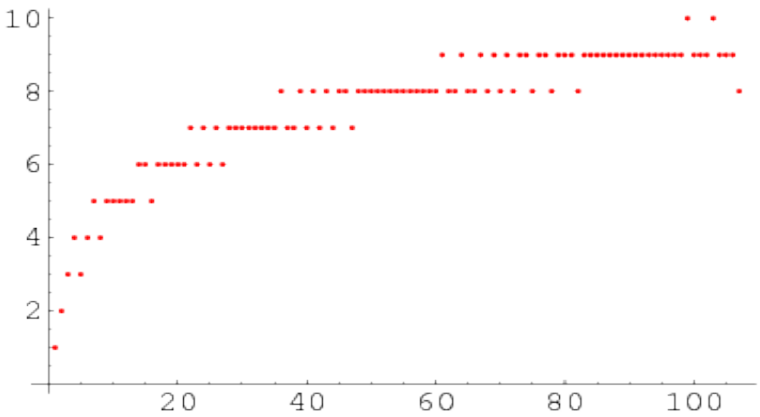

Fig. 6. Plots of the linear predicted S. values of the Stieltjes constants as a function of n as model increases to 100.

The Euler-Mascheroni constant for the geopredictive spatiotemporal onchocerciasis endemic transmission

$$\gamma = \sum_{k=1}^{\infty} \frac{(-1)^k}{k} \lfloor \lg k \rfloor,$$

ArcGIS/SAS-based model was then expressed as where $\lfloor x \rfloor$id the floor function and the log function[i.e., $\lg x \equiv \log_2 x$] was the logarithm to base 2. This calculations then rendered

$$\frac{2\,\gamma_1}{\ln 2} = \sum_{k=1}^{\infty} \frac{(-1)^k}{k} \left[2 \lg k - \lfloor \lg (2\,k) \rfloor\right] \lfloor \lg k \rfloor.$$

where γ_1 was defined by the sum $\sum_{n=1}^{x} \frac{1}{n} \ln\left(\frac{x}{n}\right) = \frac{1}{2} (\ln x)^2 + \gamma \ln x - \gamma_1 + O\left(x^{-1}\right)$ The exact form of this model was then provided by $\sum_{n=1}^{x} \frac{1}{n} \ln\left(\frac{x}{n}\right)$ = $H_x \ln x - \zeta'(1, x+1) - \gamma_1$ =$H_x \ln x + \gamma_1 (x+1) - \gamma_1$, where H_x was a harmonic number, $\zeta(s, a)$was the Hurwitz zeta function, $\zeta'(1, a)$ and $\lim_{s \to 1} d\,\zeta(s, a)/d\,z\,|_{z=s}$. Interestingly, Jacob et al. (1) provided a similar series for γ_n

$$\gamma_n = n!\,(\ln 2)^n \sum_{m=1}^{n+1} \frac{(-1)^{m-1}}{m!} \sum_{k=1}^{\infty} \frac{(-1)^k}{k\,\lfloor \lg k \rfloor^m} B_{1+n-m}\left(\frac{\ln k}{\ln 2}\right),$$

valid for all $n > 1$,employing in a spatiotemporal geopredictor risk model for immature S.damnosum s.l. where $B_n(x)$was a Bernoulli polynomial. In this research, this series converged extremely slowly, requiring multiple terms in the predictive spatiotemporal onchocerciasis endemic transmission-oriented model to get two digits of γ_1 and many more for higher order γ_n Thereafter, γ_n was

$$\gamma_n = \frac{(\ln 2)^n}{n+1} \sum_{k=1}^{\infty} \frac{(-1)^k}{k} B_{n+1}\left(\frac{\ln k}{\ln 2}\right).$$

also be expressed as a single sum using A set of constants then related to γ_n

$$\delta_n \equiv \lim_{m \to \infty} \left[\sum_{k=1}^{m} (\ln k)^n - \int_1^m (\ln x)^n\,d\,x - \frac{1}{2} (\ln m)^n\right]$$

was rendered by We noted that the endemic transmission-

$$\sum_{k=0}^{\infty} \frac{\gamma_{k+n}}{k!} = (-1)^n \left[n! + \zeta^{(n)}(0)\right]$$

oriented Stieltjes constants also satisfied

In this research, the Riemann zeta function was defined in the complex plane by the contour integral

$$\zeta(z) = \frac{\Gamma(1-z)}{2\,\pi\,i} \oint_{\gamma} \frac{u^{z-1}}{e^{-u} - 1}\,d\,u$$

for all $z \neq 1$, The Riemann zeta function is an extremely important special function of mathematics and physics that arises in definite integration and is intimately related with very deep results surrounding the prime number theorem. The prime number theorem gives an asymptotic form for the prime counting function $\pi(n)$, which counts the number of primes less than some integer n. Legendre (1808) suggested

that for large n , $\pi(n) \sim \frac{n}{\ln n + B}$, with $B = -1.08366$ where B is the Legendre's constant, a formula which is correct in the leading term only, $\frac{n}{\ln n + B} \sin \frac{n}{\ln n} - B \frac{n}{(\ln n)^2} + B^2 \frac{n}{(\ln n)^3} + \ldots$. In this research the Riemann hypothesis asserted that the nontrivial Riemann zeta function zeros of $\zeta(s)$ in the onchocerciasis endemic transmission-oriented ArcGIS/SAS-based model revealed $\sigma = \Re[s] = 1/2$, ("critical thresholds.")based on the sampled covariates coefficients.

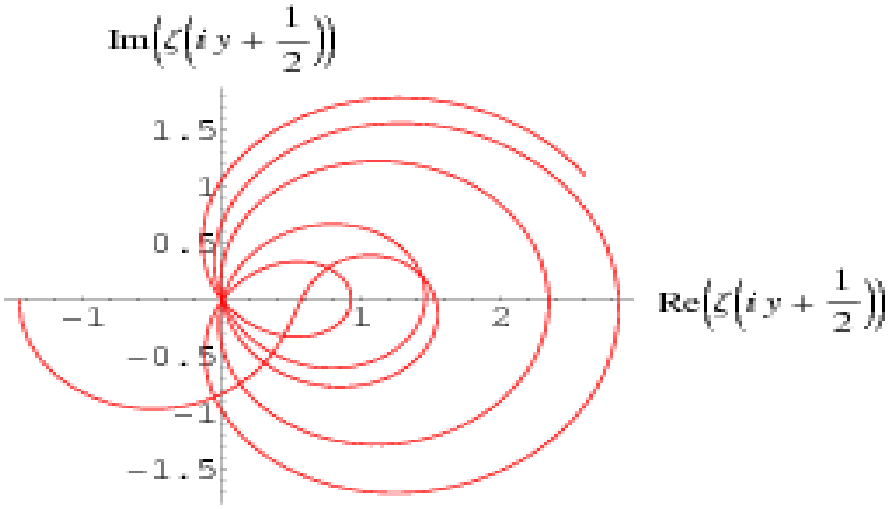

Fig. 7. Plots of the linear predicted S. damnosum s.l. values of the Stieltjes constants as a function of n as model increased to5km from the capture point.

Plots of the predicted S. values of the Stieltjes constants as a function of n plot above revealed that parts of $\zeta(1/2 + i y)$(i.e., values of $\zeta(z)$along the critical line) as y was varied from 0 to 15 km in the regressed seasonal-sampled endemic transmission data. The Riemann zeta function was split up into $\zeta\left(\frac{1}{2} + i t\right) = Z(t) e^{-i \vartheta(t)}$, where $Z(t)$and $\vartheta(t)$ (i.e., Riemann-Siegel functions) . The Riemann zeta function was then related to the Dirichlet lambda function $\lambda(\nu)$and Dirichlet beta function $\eta(\nu)$by $\frac{\zeta(\nu)}{2^\nu} = \frac{\lambda(\nu)}{2^\nu - 1} = \frac{\eta(\nu)}{2^\nu - 2}$ and $\zeta(\nu) + \eta(\nu) = 2\lambda(\nu)$. Our ArcGIS/SAS-based model estimates was also related to the Liouville function $\lambda(n)$by $\frac{\zeta(2s)}{\zeta(s)} = \sum_{n=1}^{\infty} \frac{\lambda(n)}{n^s}$. Additionally, for $n = -1, \zeta'(-1) = \frac{1}{12} - \ln A$, e A was represented in the onchocerciasis endemic transmission-oriented model as the Glaisher-Kinkelin constant. In mathematics, the Glaisher–Kinkelin constant or Glaisher's constant, typically denoted A, is a mathematical constant, related to the K-function and the Barnes G-function. In this research the approximate value was $A \approx 1.2824271291\ldots$ which was provided by the multi-seasonal S. damnosum s.l. model distribution limit: $A = \lim_{n\to\infty} \frac{K(n+1)}{n^{n^2/2+n/2+1/12} e^{-n^2/4}}$ where $K(n) = \prod_{k=1}^{n-1} k^k$ was the K-function.

In this research a n equivalent form involving the Barnes G-function was provided by

$G(n) = \prod_{k=1}^{n-2} k! = \frac{[\Gamma(n)]^{n-1}}{K(n)}$ where $\Gamma(n)$ was the gamma function rendered by $A = \lim_{n\to\infty} \frac{(2\pi)^{n/2} n^{n^2/2-1/12} e^{-3n^2/4+1/12}}{G(n+1)}$ The Glaisher-Kinkelin constant then appeared in the Riemann zeta function of the riverine spatiotemporal endemic transmission model as: $\zeta'(-1) = \frac{1}{12} - \ln A$ and $\sum_{k=2}^{\infty} \frac{\ln k}{k^2} = -\zeta'(2) = \frac{\pi^2}{6}[12\ln A - \gamma - \ln(2\pi)]$ for each km from the capture point when γ was the Euler–Mascheroni constant

Thereafter, $\zeta^{(n)}(0)$ was expressed analytically in terms of π, $\zeta(n)$, the Euler-Mascheroni constant γ, and the Stieltjes constants γ_i, [e.g., $\zeta''(0) = \gamma_1 + \frac{1}{2}\gamma^2 - \frac{1}{24}\pi^2 - \frac{1}{2}[\ln(2\pi)]^2$, $\zeta'''(0) = 3\ln(2\pi)\gamma_1 + 3\gamma\gamma_1 + \frac{3}{2}\gamma_2 - \zeta(3) - \frac{1}{2}[\ln(2\pi)]^3 - \frac{1}{8}\pi^2\ln(2\pi) + \frac{3}{2}\gamma^2\ln(2\pi) + \gamma^3$].Derivatives $\zeta^{(n)}(1/2)$ were then provided in closed form, [e.g., , $\zeta'\left(\frac{1}{2}\right) = \frac{1}{4}\left[(\pi + 2\gamma + 6\ln 2 + 2\ln\pi)\zeta\left(\frac{1}{2}\right)\right] = -3.92264613\ldots$ for ArcGIS Eulcidean-distance 0 -5m].The derivative of the Riemann zeta function for $\Re[s] > 1$ was then defined by $-\sum_{k=1}^{\infty} \frac{\ln k}{k^s} = -\sum_{k=2}^{\infty} \frac{\ln k}{k^s}$. $\zeta'(2)$ where A was the Glaisher-Kinkelin constant for multiple sampled distance based measurements from the capture point. We employed the series for $\zeta'(s)$ for $s = 1$ when $\zeta'(s) = -\frac{1}{(s-1)^2} - \gamma_1 + \gamma_2(s-1) - \frac{1}{2}\gamma_3(s-1)^2 + \ldots,$ and where γ_i were Stieltjes constants for all the sampled parameters.

For validating $S_{\pm}(n) \equiv \sum_{k=1}^{\infty} \frac{1}{k^n\left(e^{2\pi k} \pm 1\right)}$, the first few sampled onchocerciasis endemic transmission-oriented estimator values were then written as: $\zeta(3) = \frac{7}{180}\pi^3 - 2S_-(3)$, $\zeta(5) = \frac{1}{294}\pi^5 - \frac{72}{35}S_-(5) - \frac{2}{35}S_+(5)$, $\zeta(7) = \frac{19}{56\,700}\pi^7 - 2S_-(7)$, $\zeta(21)$ $\frac{68\,529\,640\,373}{1\,881\,063\,815\,762\,259\,253\,125}\pi^{21} - \frac{4\,196\,352}{2\,098\,175}S_-(21) - \frac{2}{2\,098\,175}S_+(21)$ and so on. Another set of related formulas were then generated as , $\zeta(7) = \frac{304}{13}\sum_{n=1}^{\infty}\frac{1}{n^7(e^{\pi n}-1)} - \frac{103}{4}\sum_{n=1}^{\infty}\frac{1}{n^7\left(e^{2\pi n}-1\right)} - \frac{19}{52}\sum_{n=1}^{\infty}\frac{1}{n^7\left(e^{4\pi n}-1\right)}$, $\zeta(9) = \frac{64}{3}\sum_{n=1}^{\infty}\frac{1}{n^9(e^{\pi n}-1)} + \frac{441}{20}\sum_{n=1}^{\infty}\frac{1}{n^9\left(e^{2\pi n}-1\right)} - 32\sum_{n=1}^{\infty}\frac{1}{n^9\left(e^{3\pi n}-1\right)} - \frac{4763}{60}\sum_{n=1}^{\infty}\frac{1}{n^9\left(e^{4\pi n}-1\right)} + \frac{529}{8}\sum_{n=1}^{\infty}\frac{1}{n^9\left(e^{6\pi n}-1\right)} - \frac{1}{8}\sum_{n=1}^{\infty}\frac{1}{n^9\left(e^{12\pi n}-1\right)}$

Thereafter we procured multiterm sums for odd $\zeta(n)$ which included $\zeta(5) = 2\sum_{k=1}^{\infty}\frac{(-1)^{k+1}}{k^5\binom{2k}{k}} - \frac{5}{2}\sum_{k=1}^{\infty}\frac{(-1)^{k+1}H_{k-1}^{(2)}}{k^3\binom{2k}{k}}$, $\zeta(9) = \frac{9}{4}\sum_{k=1}^{\infty}\frac{(-1)^{k+1}}{k^9\binom{2k}{k}} - \frac{5}{4}\sum_{k=1}^{\infty}\frac{(-1)^{k+1}H_{k-1}^{(2)}}{k^7\binom{2k}{k}} + 5\sum_{k=1}^{\infty}\frac{(-1)^{k+1}H_{k-1}^{(4)}}{k^5\binom{2k}{k}} + \frac{45}{4}\sum_{k=1}^{\infty}\frac{(-1)^{k+1}H_{k-1}^{(6)}}{k^3\binom{2k}{k}} - \frac{25}{4}\sum_{k=1}^{\infty}\frac{(-1)^{k+1}H_{k-1}^{(2)}H_{k-1}^{(4)}}{k^3\binom{2k}{k}}$

where $H_n^{(r)}$ was a generalized harmonic number.

In this research we noted that A number of sum identities involving $\zeta(n)$ include $\sum_{n=2}^{\infty}[\zeta(n)-1]=1$, $\sum_{n=2,4,\ldots}^{\infty}[\zeta(n)-1]=\frac{3}{4}$, $\sum_{n=3,5,\ldots}^{\infty}[\zeta(n)-1]=\frac{1}{4}$ and $\sum_{n=2}^{\infty}(-1)^n[\zeta(n)-1]=\frac{1}{2}$. Sums involving the spatiotemporal-sampled onchocerciasis integers multiples of the argument then includes $\sum_{n=1}^{\infty}[\zeta(2n)-1]=\frac{3}{4}$, $\sum_{n=1}^{\infty}[\zeta(3n)-1]=\frac{1}{3}\left[-(-1)^{2/3}H_{(3-i\sqrt{3})/2}+(-1)^{1/3}H_{(3+i\sqrt{3})/2}\right]$, $\sum_{n=1}^{\infty}[\zeta(4n)-1]=\frac{1}{8}(7-2\coth\pi)$, and so on where H_n was a harmonic number. Two surprising sums involving $\zeta(x)$ were then given by $\sum_{k=2}^{\infty}\frac{(-1)^k\zeta(k)}{k}=\gamma$ and $\sum_{k=2}^{\infty}\frac{\zeta(k)-1}{k}=1-\gamma$, where γ was the Euler-Mascheroni constant This geopredictive onchocerciasis endemic transmission-oriented endemic equation was then generalized to $\sum_{k=2}^{\infty}\frac{(-x)^k\zeta(k)}{k}=x\gamma+\ln(x!)$ for $-1<x\le 1$. Other unexpected sums in the model was then provided by $\sum_{n=1}^{\infty}\frac{\zeta(2n)}{n(2n+1)2^{2n}}=\ln\pi-1$ and $\sum_{n=1}^{\infty}\frac{\zeta(2n)}{n(2n+1)}=\ln(2\pi)-1.$ which was a special case of the $\sum_{k=1}^{\infty}\frac{\zeta(2k,z)}{k(2k+1)2^{2k}}=(2z-1)\ln\left(z-\frac{1}{2}\right)-2z+1+\ln(2\pi)-2\ln\Gamma(z),$ where $\zeta(s,a)$ is a Hurwitz zeta function. Considering the sum $S_n=\sum_{k=2}^{n-2}\frac{\zeta(k)\zeta(n-k)}{2^k},$ in the spatiotemporal onchocerciasis endemic transmission-oriented model then $\lim_{n\to\infty}S_n=\ln 2,$ where log 2 was the natural logarithm of 2, which in this research was found to be a particular case of $\lim_{n\to\infty}\sum_{k=2}^{n-2}\zeta(k)\zeta(n-k)x^{k-1}=x^{-1}-\psi_0(-x)-\gamma,$ where $\psi_0(z)$ is the digamma function and γ was the Euler-Mascheroni constant derived from $\sum_{k=2}^{\infty}\zeta(k)x^{k-1}=-\psi_0(1-x)-\gamma$ A generalization of a result of Ramanujan (who gave the $m=1$ case) was then given by $\sum_{k=1}^{\infty}\frac{1}{[k(k+1)]^{2m+1}}=-2\sum_{k=0}^{m}\zeta(2k)\frac{2m+1-2k}{2m+i-2k}$ An additional set of sums over $\zeta(n)$ in the predictive spatiotemporal onchocerciais endemic transmission-oriented ArcGIS/SAS-based model was then given by $C_1=\sum_{n=2}^{\infty}\frac{\zeta(n)}{n!}=\int_0^{\infty}\frac{I_1\left(2\sqrt{u}\right)-\sqrt{u}}{(e^u-1)\sqrt{u}}\,du=\int_0^{\infty}\frac{{}_0\tilde{F}_1(;2;u)-1}{e^u-1}\,du\approx 1.078189;C_2=\sum_{n=1}^{\infty}\frac{\zeta(2n)}{n!}\sum_{n=1}^{\infty}e^{1/n^2}-1=\int_0^{1}\frac{u\,{}_0F_2\left(;\frac{3}{2},2;\frac{1}{4}u^4\right)}{e^u-1}\,du\approx 2.407447;C_3=\sum_{n=1}^{\infty}\frac{\zeta(2n)}{(2n)!}=\int_0^{\infty}\frac{u+{}_0\tilde{F}_1(;2;-u)-{}_0\tilde{F}_1(;2;u)}{2(1-e^u)}\,du=0.869002$ where $I_n(z)$ was a modified Bessel function of the first kind, ${}_p\tilde{F}_q$ was a regularized hypergeometric function. Unfortunately, these sums had no known closed-form expression. The inverse of the Riemann zeta function $1/\zeta(p)$, was then plotted which was the asymptotic density of pth-

powerfree numbers (i.e., square free numbers, cube free numbers, etc.) in the empirical dataset of endemic transmission-oriented residual explanatory covariates. The model provided gives the number $Q_p(n)$ of pth-power free numbers $\leq n$ for several spatiotemporal-sampled coefficients values of n in the dataset.

We then found that an analytical solution to this integral existed in the linear-based S.damnosum s.l .risk model when τ_i was assumed to follow a gamma distribution. The model also revealed that y_i, was the vector of the sampled observation explanatory predictor covariate coefficients while $\mathbf{x}_i$, was independently Poisson distributed with $P(Y_i = y_i|\mathbf{x}_i) = \frac{e^{-\mu_i}\mu_i^{y_i}}{y_i!}, \quad y_i = 0, 1, 2, \ldots$ and the mean parameter — that is, the mean number of seasonal sampling events per spatiotemporal period — was rendered by $\mu_i = \exp(\mathbf{x}_i'\boldsymbol{\beta})$ where $\boldsymbol{\beta}$ was a $(k+1) \times 1$ parameter vector. The intercept in the model was then β_0 and the coefficients for the k regressors were $\beta_1, \ldots, \beta_k$. Taking the exponential of $\mathbf{x}_i'\boldsymbol{\beta}$ ensured that the mean parameter μ_i was nonnegative. Thereafter, the conditional mean was provided by $E(y_i|\mathbf{x}_i) = \mu_i = \exp(\mathbf{x}_i'\boldsymbol{\beta})$.

The seasonal-sampled S. damnosum s.l.-related geoparameter estimators were then evaluated using $\ln[E(y_i|\mathbf{x}_i)] = \ln(\mu_i) = \mathbf{x}_i'\boldsymbol{\beta}$. Note, that the conditional variance of the count random variable was equal to the conditional mean (i.e., equidispersion) in the model [e.g., $V(y_i|\mathbf{x}_i) = E(y_i|\mathbf{x}_i) = \mu_i$]. In a log-linear model the logarithm of the conditional mean is linear (Toe et al., 1997). The marginal effect of any regressor in the model was then provided by $\frac{\partial E(y_i|\mathbf{x}_i)}{\partial x_{ji}} = \exp(\mathbf{x}_i'\boldsymbol{\beta})\boldsymbol{\beta}_j = E(y_i|\mathbf{x}_i)\beta_j$. Thus, a one-unit change in the jth regressor in the model led to a proportional change in the conditional mean $E(y_i|\mathbf{x}_i)$ of β_j.

In this research, the standard estimator for our Poisson model was the maximum likelihood estimator. Since the independent-sampled observations were independent, the log-likelihood function was computed as $\mathscr{L} = \sum_{i=1}^{N}(-\mu_i + y_i \ln \mu_i - \ln y_i!) = \sum_{i=1}^{N}(-e^{\mathbf{x}_i'\boldsymbol{\beta}} + y_i\mathbf{x}_i'\boldsymbol{\beta} - \ln y_i!)$. Given the spatiotemporal-sampled dataset of parameter estimators (i.e., θ) and an input vector x, the mean of the predicted Poisson distribution was then provided by $\mathrm{E}(Y|x) = e^{\theta' x}$. By so doing, the Poisson distribution's pmf of the sampled estimators was then rendered by $p(y|x;\theta) = \frac{e^{y(\theta' x)}e^{-e^{\theta' x}}}{y!}$. The pmf in a spatiotemporal predictive seasonal autoregressive risk model is often the primary means of defining a discrete probability distribution, and, as such, functions exist for either scalar or multivariate random variables, given that the distribution is discrete (Haight, 1967).

Since in this research, the sampled S. damnosum s.l.-data consisted of m vectors $x_i \in \mathbb{R}^{n+1}$, $i = 1, \ldots, m$, along with a set of m values $y_1, \ldots, y_m \in \mathbb{R}$ then, for the sampled parameter estimators θ, the probability of attaining this particular set of the sampled observations was provided by the equation $p(y_1, \ldots, y_m|x_1, \ldots, x_m;\theta) = \prod_{i=1}^{m}\frac{e^{y_i(\theta' x_i)}e^{-e^{\theta' x_i}}}{y_i!}$.Consequently, we found the set of θ that made this probability as large as possible in the model estimates. To do this, the equation was first rewritten as a likelihood function in terms of θ: $L(\theta|X,Y) = \prod_{i=1}^{m}\frac{e^{y_i(\theta' x_i)}e^{-e^{\theta' x_i}}}{y_i!}$.Note the expression on the right hand side in the seasonal S.damnosums.l.risk model had not actually changed.

Next, we used a log-likelihood [i.e. $\ell(\theta|X,Y) = \log L(\theta|X,Y) = \sum_{i=1}^{m}\left(y_i(\theta' x_i) - e^{\theta' x_i} - \log(y_i!)\right)$]. Because the logarithm is a monotonically increasing function, the logarithm of a function achieves its maximum value at the same points as the function itself, and, hence, the log-likelihood can be used in place of the likelihood in maximum likelihood estimation and other related techniques (Toe et al., 1997). Finding the maximum of a function in a model often involves taking the derivative of a function and solving for the parameter estimator being maximized, and this is often easier when the function being maximized is a log-likelihood rather than the original likelihood function (McCulloch and Searle, 2005). We noticed that the parameters θ only appeared in the first two terms of each term

in the summation. Therefore, given that we were only interested in finding the best value for θin the geopredictive onchocerciasis endemic transmission-oriented model we dropped the yi!and simply wrote $\ell(\theta|X,Y)=\sum_{i=1}^{m}\left(y_i(\theta' x_i)-e^{\theta' x_i}\right)$. Thereafter, to find a maximum, we solved an equation $\frac{\partial \ell(\theta|X,Y)}{\partial \theta}=0$ which had no closed-form solution. However, the negative log-likelihood (LL) [i.e., $-\ell(\theta|X,Y)$] was a convex function, and so standard convex optimization was applied to find the optimal value of θ .

We found that the Poisson process in our regression model was then provided by the limit of a binomial distribution $P_p(n\,|\,N)=\frac{N!}{n!\,(N-n)!}\,p^n\,(1-p)^{N-n}.$ (3.1). Viewing the distribution as a function of the expected number of successes[i.e., $\nu \equiv N\,p$] instead of the sample size N for fixed p, then allowed equation (3.1) to become $P_{\nu|N}(n\,|\,N)=\frac{N!}{n!\,(N-n)!}\left(\frac{\nu}{N}\right)^n\left(1-\frac{\nu}{N}\right)^{N-n}$ .As the sample size N become larger, the distribution then approached P when $\lim_{N\to\infty} P_p(n\,|\,N)$, $\lim_{N\to\infty}\frac{N(N-1)\cdots(N-n+1)}{n!}\,\frac{\nu^n}{N^n}\left(1-\frac{\nu}{N}\right)^N\left(1-\frac{\nu}{N}\right)^{-n}$,, $\lim_{N\to\infty}\frac{N(N-1)\cdots(N-n+1)}{N^n}\,\frac{\nu^n}{n!}\left(1-\frac{\nu}{N}\right)^N\left(1-\frac{\nu}{N}\right)^{-n}$, $1\cdot\frac{\nu^n}{n!}\cdot e^{-\nu}\cdot 1$ and $\frac{\nu^n\,e^{-\nu}}{n!}$. We noted that the sample size N had completely dropped out of the probability function, which had the same functional form for all values of ν in our model.

Thereafter, as expected, the Poisson regression distribution was normalized so that the sum of probabilities equaled 1, since $\sum_{n=0}^{\infty}P_\nu(n)=e^{-\nu}\sum_{n=0}^{\infty}\frac{\nu^n}{n!}=e^{-\nu}\,e^{\nu}=1.$ The ratio of probabilities was then provided by the equation $\frac{P_\nu(n=i+1)}{P(n=i)}=\frac{\frac{\nu^{i+1}\,e^{-\nu}}{(i+1)!}}{\frac{e^{-\nu}\,\nu^i}{i!}}=\frac{\nu}{i+1}.$. The Poisson distribution reached a maximum when $\frac{d\,P_\nu(n)}{d\,n}=\frac{e^{-\nu}\,n\,(\gamma-H_n+\ln\nu)}{n!}=0,$ where γ was the Euler-Mascheroni constant and H_n was a harmonic number, leading to the equation $\gamma-H_n+\ln\nu=0,$ which in this research could not be solved exactly for n.

Next, the moment-generating function of the Poisson distribution was given by M = $e^{-\nu}\,e^{\nu\,e^t}=e^{\nu\left(e^t-1\right)}$,M=$\nu\,e^t\,e^{\nu\left(e^t-1\right)}$ and M=$\left(\nu\,e^t\right)^2\,e^{\nu\left(e^t-1\right)}+\nu\,e^t\,e^{\nu\left(e^t-1\right)}$, when R=$\nu\left(e^t-1\right)$, R'=$\nu\,e^t$ so R=$R'(0)=\nu$ The raw moments were also computed directly by summation, which yielded an unexpected connection with the exponential polynomial$\phi_n(x)$and Stirling numbers of the second kind[i.e. $\phi_n(x)=\sum_{k=0}^{\infty}\frac{e^{-x}\,x^k}{k!}\,k^n=\sum_{k=1}^{n}x^k\,S(n,k)$] which in this research was the Dobiński's formula. In combinatorial mathematics, Dobinski's formula states that the number of partitions of a set of n members is $\frac{1}{e}\sum_{k=0}^{\infty}\frac{k^n}{k!}$ (Haight, 1967). In this research, this number h was the nth Bell numberBn,. In the S.damnosums.l.-based regression model the formula $\phi_n(x)=\sum_{k=0}^{\infty}\frac{e^{-x}\,x^k}{k!}\,k^n=\sum_{k=1}^{n}x^k\,S(n,k)$ was then viewed as a particular case, for x = 0, employing the relation $\frac{1}{e}\sum_{k=x}^{\infty}\frac{k^n}{(k-x)!}=\sum_{k=0}^{n}\binom{n}{k}B_k x^{n-k}$

In this research, the expression given by the model's Dobinski's formula was revealed as the nth moment of the Poisson distribution with expected value 1. Dobinski's formula was then the number of partitions of the set of the sampled endemic geopredictive S. damnosum s.l. transmission-oriented parameter estimators empirical dataset size (i.e.,n) which equaled the nth moment of that distribution. We used the Pochhammer symbol (x)n to denote the falling factorial. If x and n were nonnegative integers, 0 ≤ n ≤ x, then (x)n is the number of one-to-one

functions that map a size-n set into a size-x set (Jacob, et., 2012). In this research we let ƒ be any function from a size-n set A into a size-x set B. We then let ƒ−1(u) = {v ∈ A : ƒ(v) = u}. Then {ƒ−1(u) : u ∈ B} was a partition of A. This equivalence relation was the "kernel" of the function ƒ. Any function from A into B factors into one function that maps a member of A to that part of the kernel to which it belongs, and another function, which is necessarily one-to-one, that maps the kernel into B (Toe et al., 1997). In this research the first of these two factors was completely determined by the partition π that is the kernel for deriving optimal distance from the capture point. The number of one-to-one functions from π into B was then (x)|π|, in the regression model when |π| was the number of parts in the partition π. Therefore, the total number of functions from a size-n set A into a size-x set B was $\sum_{\pi}(x)_{|\pi}$ in then model when the index π ran through the set of all partitions of A. Thereafter, we had, $E\left(X^{n}\right)=\sum_{\pi}1$, which was the number of partitions of the set A in the S . damnosum s.l. ArcGIS/SAS-based model. We noted that in the model, $\nu\,(1+\nu)$, $\nu\left(1+3\,\nu+\nu^{2}\right)$ and $\nu\left(1+7\,\nu+6\,\nu^{2}+\nu^{3}\right)$.

In this research the Stirling numbers of the second kind was variously denoted using $S\,(n,\,m)$, $\mathcal{S}_{n}^{(m)}$, $\mathfrak{S}_{n}^{m}$, $s_{n}^{(m)}$, $S_{2}\,(n,\,m)$ and Knuth's notation[i.e., $\left\{ {n \atop m} \right\}$].Thereafter a set of n elements in a robust multi-seasonal onchocerciasis endemic predictive transmission-oriented model were subsequently partitioned in n subsets, $S\,(n,\,1)=S\,(n,\,n)=1.$ and $S\,(n,\,0)=\delta_{n\,0}$, $S\,(n,\,2)=2^{n-1}-1$, $S\,(n,\,3)=\frac{1}{6}\,(3^{n}-3\cdot 2^{n}+3)$, $S\,(n,\,n-1)=\binom{n}{2}$. .This process aided in regressing the endemic transmission-oriented parameter estimation process parsimoniously. The Stirling numbers of the second kind were then computed from the sum $S\,(n,\,k)=\frac{1}{k!}\sum_{i=0}^{k}(-1)^{i}\binom{k}{i}(k-i)^{n},$ with $\binom{n}{k}$ a binomial coefficient employing generating functions $x^{n}=\sum_{m=0}^{n}S\,(n,\,m)\,(x)_{m}$ = $\sum_{m=0}^{n}S\,(n,\,m)\,x\,(x-1)\cdots(x-m+1),$ $\sum_{n=k}^{\infty}S\,(n,\,k)\,\frac{x^{n}}{n!}=\frac{1}{k!}\,(e^{x}-1)^{k},$ and $\sum_{n=1}^{\infty}S\,(n,\,k)\,x^{n}$ $\sum_{=n=k}^{\infty}S\,(n,\,k)\,x^{n}$ $=\frac{x^{k}}{(1-x)\,(1-2\,x)\cdots(1-k\,x)}=\frac{(-1)^{k}}{\left(\frac{x-1}{x}\right)_{k}}$] for $z<1/m$ and where $(x)_{m}$ was a Pochhammer symbol In mathematics, the Pochhammer symbol is the notation (x)n, where n is a non-negative integer (Boatin et al., 1997). Depending on the context the Pochhammer symbol, therefore, in the future an infectious disease vector ecologist or local abatement district manager infectious disease vector ecologist or local abatement district manager

may lineally quantitate either the rising factorial or the falling factorial in a spatiotemporal geopredictive onchocerciasis endemic transmission-oriented model. The falling factorial $(x)_{n}$, may then be defined using $(x)_{n}=x\,(x-1)\cdots(x-(n-1))$ for $n\geq 0$ in the model residuals.

Thereafter, the central moments in the model was computed as $\nu\,(1+3\,\nu)$, in the model so the mean, variance, skewness, and kurtosis were $\frac{\mu_{3}}{\sigma^{3}}=\frac{\nu}{\nu^{3/2}}=\nu^{-1/2}$, $\frac{\mu_{4}}{\sigma^{4}}-3=\frac{\nu\,(1+3\,\nu)}{\nu^{2}}-3$ and $\frac{\nu+3\,\nu^{2}-3\,\nu^{2}}{\nu^{2}}=\nu^{-1}.$,respectively. The characteristic function for the Poisson distribution in the Poisson predictive seasonal autoregressive hyperendemic model was then revealed as $\phi\,(t)=e^{\nu\,(e^{i\,t}-1)}$ and the cumulative distribution function was $K\,(h)=\nu\left(e^{h}-1\right)=\nu\left(h+\frac{1}{2!}\,h^{2}+\frac{1}{3!}\,h^{3}+\ldots\right),$ so $\kappa_{r}=\nu.$ The mean deviation of the Poisson distribution in the mode was then rendered by $\mathrm{MD}=\frac{2\,e^{-\nu}\,\nu^{\lfloor\nu\rfloor+1}}{\lfloor\nu\rfloor!}.$ The cumulative distribution functions of the Poisson and chi-squared distributions were related in the S. damnosum s.l .model in the following ways as

$F_{\text{Poisson}}(k;\lambda) = 1 - F_{\chi^2}(2\lambda; 2(k+1))$ integer k and $\Pr(X = k) = F_{\chi^2}(2\lambda; 2k) - F_{\chi^2}(2\lambda; 2(k+1))$. The Poisson distribution was then expressed in terms of $\lambda \equiv \frac{\nu}{x}$, whereby, the rate of changes were equal to the equation $P_\nu(n) = \frac{(\lambda x)^n e^{-\lambda x}}{n!}$. The moment-generating function of the Poisson distribution generated from the sampled variables was also rendered by $M(t) = e^{(\nu_1+\nu_2)(e^t-1)}$. Given a random variable x and a probability distribution function $P(x)$, if there exists an $h > 0$ such that $M(t) \equiv \langle e^{tx} \rangle$ for $|t| < h$, where $\langle y \rangle$ denotes the expectation value of y, then $M(t)$ is called the moment-generating function (Toe et al., 1997). Commonly, for a continuous distribution in a seasonal linear regression-based time-series dependent onchocerciasis endemic transmission-oriented model $\int_{-\infty}^{\infty} e^{tx} P(x)\,dx \int_{-\infty}^{\infty} \left(1 + tx + \frac{1}{2!} t^2 x^2 + \ldots\right) P(x)\,dx$ the equation $1 + t m_1' + \frac{1}{2!} t^2 m_2' + \ldots$, is employed where m_r' is the r the raw moment (Jacob, et., 2012). For quantifying independent X and Y , the moment-generating function in a robust model which satisfies $M_{x+y}(t) = \langle e^{t(x+y)} \rangle$, $\langle e^{tx} e^{ty} \rangle, \langle e^{tx} \rangle \langle e^{ty} \rangle$ and $M_x(t) M_y(t)$. if ,the independent variables x_1, x_2, ..., x_N have Poisson distributions with parameters μ_1, μ_2, ..., μ_N, and $X = \sum_{j=1}^{N} x_j$ (Boatin et al., 1997).In this research this was evident since the cumulant-generating function was $K \equiv \sum_j K_j(h) = \left(e^h - 1\right) \sum_j \mu_j = \mu\left(e^h - 1\right)$.

Many sums of reciprocal powers were then expressed in terms the cumulant-generating function in the geopredictive spatiotemporal onchocerciasis endemic transmission-oriented model. We defined these terms by $\Phi(z, s, a) \equiv \sum_{k=0}^{\infty} \frac{z^k}{(a+k)^s}$, for $|z| < 1$ and $a \neq 0, -1, \ldots$. It was implemented in this form as HurwitzLerchPhi[z, s, a] in Mathematica. A series formula for $\Phi(z, s, a)$ valid on a larger domain in the complex z-plane was then given by $(1 - z)\Phi(z, s, a)$

$= \sum_{n=0}^{\infty} \left(\frac{-z}{1-z}\right)^n \sum_{k=0}^{n} (-1)^k \binom{n}{k} (a+k)^{-s}$, for distance-based measurements from 0-15km from the capture point which would hold for all complex s and complex z with $\Re[z] < 1/2$.

In the S. damnosum s.l. model the directed Kullback-Leibler (K-L) divergence between Pois(λ) and Pois(λ0) was provided by $D_{\mathrm{KL}}(\lambda \| \lambda_0) = \lambda_0 - \lambda + \lambda \log \frac{\lambda}{\lambda_0}$. In probability theory and information theory, the Kullback–Leibler divergence along with information divergence, information gain, relative entropy are a non-symmetric measures of the difference between two probability distributions P and Q in a model (Toe et al., 1997). In this research, for quantitating the probability distributions P and Q of a sampled discrete random variable, the K–L divergence was defined by $D_{\mathrm{KL}}(P \| Q) = \sum_i P(i) \ln \frac{P(i)}{Q(i)}$. The model revealed that the average of the logarithmic difference between the probabilities P and Q was the average quantified using the probabilities P. The K-L divergence is only defined if P and Q both sum to 1 and if $Q(i) > 0$ for any i such that $P(i) > 0$ (Boatin et al., 1997).

In the seasonal onchocerciasis endemic transmission oriented model, if the quantity 0 ln 0 appeared in the formula, it was interpreted as zero. For distributions P and Q of the continuous random variable in the sampled ecological datasets KL-divergence was defined to be the integral [i.e., $D_{\mathrm{KL}}(P \| Q) = \int_{-\infty}^{\infty} p(x) \ln \frac{p(x)}{q(x)} \mathrm{d}x$] where p and q denoted the distances of P and Q. More generally, since P and Q were probability measures over the sampled dataset X, and Q was absolutely continuous with respect to P, then the K-L divergence from P to Q was

defined as $D_{\mathrm{KL}}(P\|Q) = -\int_X \ln \frac{\mathrm{d}Q}{\mathrm{d}P}\,\mathrm{d}P,$ in the seasonal model where $\frac{\mathrm{d}Q}{\mathrm{d}P}$ was the Radon–Nikodym derivative of Q with respect to P, provided the expression on the right-hand side existed. In mathematics, the Radon–Nikodym theorem is a result in measure theory that states that, given a measurable space (i.e., X,Σ), if a σ-finite measure ν on (i..e, X,Σ) is absolutely continuous with respect to a σ-finite measure μ on (X,Σ)(Boatin et al., 1997). By so doing, in this research a measurable function f was rendered on X taking values in [0,∞), such that $\nu(A) = \int_A f\,d\mu$ for any measured value which rendered statistical significance based of the seasonal- sampled covariate coefficients.

Likewise, since P was absolutely continuous with respect to Q in the S. damnosum s.l. regression model, the covariate coefficients were also defined using: $D_{\mathrm{KL}}(P\|Q) = \int_X \ln \frac{\mathrm{d}P}{\mathrm{d}Q}\mathrm{d}P = \int_X \frac{\mathrm{d}P}{\mathrm{d}Q}\ln\frac{\mathrm{d}P}{\mathrm{d}Q}\mathrm{d}Q,$ which in this research was recognized as the all distances in the empirical spatiotemporal-sampled onchocerciasis endemic transmission-oriented empirical dataset for all P relative to Q. Continuing, if μ was any measure on X in the model then $p = \frac{\mathrm{d}P}{\mathrm{d}\mu}$ and $q = \frac{\mathrm{d}Q}{\mathrm{d}\mu}$ existed, and the K-L divergence from P to Q which in this research was given as $D_{\mathrm{KL}}(P\|Q) = \int_X p \ln \frac{p}{q}\,\mathrm{d}\mu.$. The bounds for the tail probabilities of the Poisson random variable $X \sim \mathrm{Pois}(\lambda)$ were then derived in the endemic transmission-oriented model using a Chernoff bound argument as $P(X \geq x) \leq \frac{e^{-\lambda}(e\lambda)^x}{x^x},\ \text{for } x > \lambda,$ and as $P(X \leq x) \leq \frac{e^{-\lambda}(e\lambda)^x}{x^x},\ \text{for } x < \lambda.$

$$\zeta(s) = \prod_{k=1}^{\infty} \frac{1}{1 - \frac{1}{p_k^s}},$$

We then considered the Euler product where $\zeta(s)$ was the Riemann zeta function and p_k was the k th prime. $\zeta(1) = \infty$. Thereafter, by taking the finite product up to $k = n$ in the spatiotemporal S. damnosum s.l.endemic transmission model and pre-multiplying by a factor $1/\ln p_n$, we were able to employ $n \to \infty$ which rendered $\lim_{n\to\infty} \frac{1}{\ln p_n} \prod_{k=1}^{n} \frac{1}{1 - \frac{1}{p_k}} = e^{\gamma}$ which was equivalent to $1.781072\ldots$, By doing so, γ became the Euler-Mascheroni constant which represented the limit of the sequence $\gamma = \lim_{n\to\infty}\left(\sum_{k=1}^{n} \frac{1}{k} - \ln n\right) = \lim_{n\to\infty}(H_n - \ln n),$ in the model when H_n was the harmonic number which in this research had the form $H_n = \sum_{k=1}^{n} \frac{1}{k}$. A harmonic number can be expressed analytically as $H_n = \gamma + \psi_0(n+1),$ where γ was the Euler-Mascheroni constant and $\Psi(x) = \psi_0(x)$ I s the digamma function (Toe et al., 1997). Our model revealed that the Euler product attached to the Riemann zeta function $\zeta(s)$ employed the sum of the geometric series rendered from the spatiotemporal-sampled dataset of S. damnosum s.l. ArcGIS/SAS-based Euclidean distance–based explanatory covariate coefficients which was then expressed as $\prod_p (1 - p^{-s})^{-1} = \prod_p \left(\sum_{n=0}^{\infty} p^{-ns}\right) = \sum_{n=1}^{\infty} \frac{1}{n^s} = \zeta(s)$. A closely related result was also obtained by noting that $1 + \frac{1}{p_k} = \frac{1 - \frac{1}{p_k^2}}{1 - \frac{1}{p_k}}.$ .We also considered the variation of (3) with the $+$ sign changed to a $-$ sign and the $\ln p_n$ moved from the denominator to the numerator which then rendered for each km from the capture

$\lim_{n\to\infty} \ln p_n \prod_{k=1}^{n} \frac{1}{1+\frac{1}{p_k}} \lim_{n\to\infty} \ln p_n \prod_{k=1}^{n} \frac{1}{1-\frac{1}{p_k^2}}$ point . For example we noted that for 10-15km in the model $\frac{1}{1-\frac{1}{p_k}} = \frac{\prod_{k=1}^{\infty} \frac{1}{1-\frac{1}{p_k^2}}}{\lim_{n\to\infty} \frac{1}{\ln p_n} \prod_{k=1}^{n} \frac{1}{1-\frac{1}{p_k}}} = \frac{\zeta(2)}{e^{\gamma}} = \frac{\pi^2}{6\, e^{\gamma}} = 0.923563.$

We then tested the model for overdispersion with a likelihood ratio test. This test quantified the equality of the mean and the variance imposed by the Poisson distribution against the alternative that the variance exceeded the mean .For the negative binomial distribution, the variance = mean + k mean2 (k>= 0, the negative binomial distribution reduces to Poisson when k=0) (Toe et al., 1997). In this research, the null hypothesis was H0: k=0 and the alternative hypothesis was Ha : k>0 . To carry out the test, we used the following steps initially and then ran the model using negative binomial distribution and a record log likelihood (LL) value. We then recorded LL for the Poisson model. We used the likelihood ratio (LR) test, that is, we computed LR statistic, -2(LL (Poisson) – LL (negative binomial). The asymptotic distribution of the LR statistic had probability mass of one half at zero and one half – Chi-sq distribution with 1 d.f. To test the null hypothesis further at the significance level α, we then used the critical value of Chi-sq distribution corresponding to significance level 2α, that is we rejected H0 if LR statistic >χ2 (1-2α , 1 df).

Next, we assumed that the endemic transmission-oriented ArcGIS/SAS-based model explanatory covariate coefficients was based on the log of the mean, μ, which was a linear function of independent variables, log(μ) = intercept + b1*X1 +b2*X2 + ...+ b3*Xm. This log-transformation implied that μ was then the exponential function of independent variables, μ = exp(intercept + b1*X1 +b2*X2 + ...+ b3*Xm). Instead of assuming as before that the distribution of the spatiotemporal-sampled district-level covariate coefficients [i.e.,Y], was the number of sampling occurrences in a binomial distribution we were able to relax the generalized linear Poisson regression specification assumption about the equality of the mean and variance since in the model residuals. We found that the variance of negative binomial was equal to μ + kμ2 , where k>= 0 was a dispersion parameter. The maximum likelihood method was then used to estimate k as well as the parameter estimators of the model for log(μ).Fortunately, the SAS syntax for running negative binomial regression was almost the same as for Poisson regression. The only change was the dist option in the MODEL statement. Instead of dist = poisson,dist = nb was used.

The pmf of the negative binomial distribution with a gamma distributed mean was then expressed as $f(k) \equiv \Pr(X = k) = \binom{k+r-1}{k}(1-p)^r p^k \quad \text{for } k = 0, 1, 2, \ldots$ In this equation, the quantity in parentheses was the binomial coefficient, and was equal to $\binom{k+r-1}{k} = \frac{(k+r-1)!}{k!\,(r-1)!} = \frac{(k+r-1)(k+r-2)\cdots(r)}{k!}$ This quantity was also alternatively written as $\frac{(k+r-1)\cdots(r)}{k!} = (-1)^k \frac{(-r)(-r-1)(-r-2)\cdots(-r-k+1)}{k!} = (-1)^k \binom{-r}{k}$ for explaining all the “negative binomialness’ in the regression-based risk model (Toe et al., 1997).

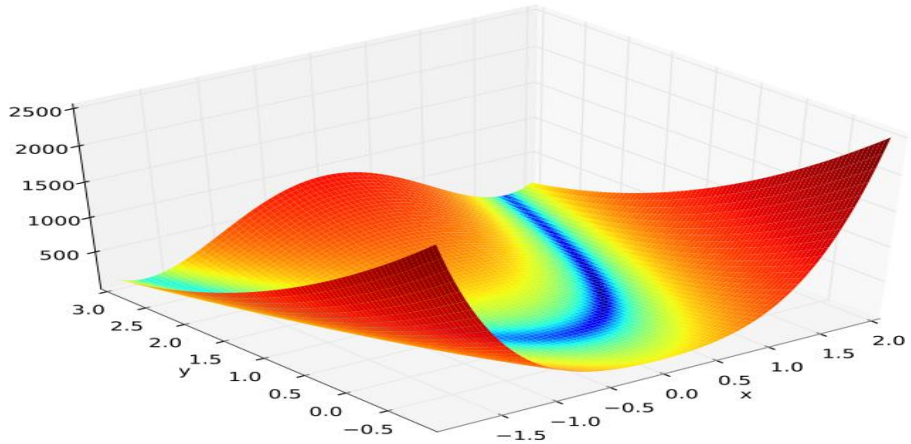

Fig. 3. An animation revealing the iterations of the gradient descent in SAS/GIS applied to the spatiotemporal-sampled S. damnosum s.l. explanatory covariate coefficients.

An autoregressive model was then attained in SAS/GIS using $X_t = c + \sum_{i=1}^{p} \varphi_i X_{t-i} + \varepsilon_t.$ An autoregressive coefficient is essentially an all-pole infinite impulse response filter with some additional interpretation placed on it |]. Some constraints were necessary on the values of the parameters of this model in order that the residuals remained stationary. For example, processes in the autoregressive models generated at each 5km interval from the capture point with |ϕ1| ≥ 1 were not stationary. The notation MA(q) was then also constructed to the moving average model of order q: $X_t = \mu + \varepsilon_t + \sum_{i=1}^{q} \theta_i \varepsilon_{t-i}$ where the θ1, ..., θq were the riverine parameters of the models, μ was the expectation of X_t (often assumed to equal 0), and the ε_t, ε_{t-1} ,...were , white noise error terms. The moving-average model is essentially a finite impulse response filter with some additional interpretation placed on it (Toe et al., 1997).

We then considered an array of nonlinear predictive equations: $\begin{cases} 3x_1 - \cos(x_2 x_3) - \frac{3}{2} = 0 \\ 4x_1^2 - 625x_2^2 + 2x_2 - 1 = 0 \\ \exp(-x_1 x_2) + 20x_3 + \frac{10\pi - 3}{3} = 0 \end{cases}$ employing different functions $G(\mathbf{x}) = \begin{bmatrix} 3x_1 - \cos(x_2 x_3) - \frac{3}{2} \\ 4x_1^2 - 625x_2^2 + 2x_2 - 1 \\ \exp(-x_1 x_2) + 20x_3 + \frac{10\pi - 3}{3} \end{bmatrix}$ where $\mathbf{x} = \begin{bmatrix} x_1 \\ x_2 \\ x_3 \end{bmatrix}$ and the objective function $F(\mathbf{x}) = \frac{1}{2} G^{\mathrm{T}}(\mathbf{x}) G(\mathbf{x})$

$= \frac{1}{2}((3x_1 - \cos(x_2 x_3) - \frac{3}{2})^2 + (4x_1^2 - 625x_2^2 + 2x_2 - 1)^2 + (\exp(-x_1 x_2) + 20x_3 + \frac{10\pi - 3}{3})^2)$ $\mathbf{x}^{(0)} = \begin{bmatrix} x_1 \\ x_2 \\ x_3 \end{bmatrix} = \begin{bmatrix} 0 \\ 0 \\ 0 \end{bmatrix}$

$\mathbf{x}^{(1)} = \mathbf{x}^{(0)} - \gamma_0 \nabla F(x^{(0)})$ where $\nabla F(\mathbf{x}^{(0)}) = J_G(\mathbf{x}^{(0)})^{\mathrm{T}} G(\mathbf{x}^{(0)})$. A Jacobian matrix was then constructed using the time series dependent onchocerciasis endemic transmission –oriented explanatory covariate as $J_G(\mathbf{x}^{(0)})$

$J_G = \begin{bmatrix} 3 & \sin(x_2 x_3) x_3 & \sin(x_2 x_3) x_2 \\ 8x_1 & -1250x_2 + 2 & 0 \\ -x_2 \exp(-x_1 x_2) & -x_1 \exp(-x_1 x_2) & 20 \end{bmatrix}$. We then evaluated these terms at $\mathbf{x}^{(0)}$ rendered $J_G(\mathbf{x}^{(0)}) = \begin{bmatrix} 3 & 0 & 0 \\ 0 & 2 & 0 \\ 0 & 0 & 20 \end{bmatrix}$, $G(\mathbf{x}^{(0)}) = \begin{bmatrix} -2.5 \\ -1 \\ 10.472 \end{bmatrix}$ $\mathbf{x}^{(1)} = 0 - \gamma_0 \begin{bmatrix} -7.5 \\ -2 \\ 209.44 \end{bmatrix}$. and $F(\mathbf{x}^{(0)}) = 0.5((-2.5)^2 + (-1)^2 + (10.472)^2) = 58.456$. Surfaces are isosurfaces of $F(\mathbf{x}^{(n)})$ and $\mathbf{x}^{(n)}$,which can revealed the direction of descent(Boatin et al., 1997).

Given the spatiotemporal-sampled empirical endemic transmission-oriented explanatory covariate coefficients dataset set $\mathbf{y} = \mathbf{f}(\mathbf{x})$ of n equations in n variables x_1, ..., x_n, our models were written explicitly as $\mathbf{y} \equiv \begin{bmatrix} f_1(\mathbf{x}) \\ f_2(\mathbf{x}) \\ \vdots \\ f_n(\mathbf{x}) \end{bmatrix}$, or more explicitly as $\begin{cases} y_1 = f_1(x_1, \ldots, x_n) \\ \vdots \\ y_n = f_n(x_1, \ldots, x_n) \end{cases}$ using a Jacobian matrix . These models were defined by $\mathbf{J}(x_1, \ldots, x_n) = \begin{bmatrix} \frac{\partial y_1}{\partial x_1} & \cdots & \frac{\partial y_1}{\partial x_n} \\ \vdots & \ddots & \vdots \\ \frac{\partial y_n}{\partial x_1} & \cdots & \frac{\partial y_n}{\partial x_n} \end{bmatrix}$. The determinant of J was the Jacobian determinant and was denoted $J = \left| \frac{\partial(y_1, \ldots, y_n)}{\partial(x_1, \ldots, x_n)} \right|$. The Jacobian matrix and determinant for the predictive spatiotemporal S. damnosum s.l. endemic transmission-order model was computed using the Mathematica commands JacobianMatrix[f_List?VectorQ, x_List] : Outer[D, f, x] /; Equal@@(Dimensions/@{f,x} JacobianDeterminant[f_List?VectorQ, x_List] := Det[JacobianMatrix[f, x]] /; Equal @@ (Dimensions /@ {f, x}. Taking the differential $d\mathbf{y} = \mathbf{y}_\mathbf{x}\, d\mathbf{x}$ revealed that J was the determinant of the matrix $\mathbf{y}_\mathbf{x}$, for each distant-based model and therefore provided the ratios of n-dimensional volumes (contents) in y and x, $d y_1 \cdots d y_n = \left| \frac{\partial(y_1, \ldots, y_n)}{\partial(x_1, \ldots, x_n)} \right| d x_1 \cdots d x_n$.

In this research the notation ARMA (p, q) referred to the model with p autoregressive terms and q moving-average terms. This model contained the AR(p) and MA(q) models which was then expressed as: $X_t = c + \varepsilon_t + \sum_{i=1}^{p} \varphi_i X_{t-i} + \sum_{i=1}^{q} \theta_i \varepsilon_{t-i}$. The error terms ε_t were assumed to be independent identically distributed random variables (i.i.d.) sampled from a normal distribution with zero mean: ε_t~ N(0,σ2) where σ2 was the variance. The spatially-dependent models were then specified in terms of the lag operatorL. In these terms then the AR(p) models was provided by $\varepsilon_t = \left(1 - \sum_{i=1}^{p} \varphi_i L^i\right) X_t = \varphi X_t$ where φ represented the polynomial $\varphi = 1 - \sum_{i=1}^{p} \varphi_i L^i$. The MA(q) model was then given by the equation $X_t = \left(1 + \sum_{i=1}^{q} \theta_i L^i\right) \varepsilon_t = \theta \varepsilon_t$, where θ represented the polynomials. Finally, the combined ARMA(p, q) models were given by $\left(1 - \sum_{i=1}^{p} \varphi_i L^i\right) X_t = \left(1 + \sum_{i=1}^{q} \theta_i L^i\right) \varepsilon_t$, or more concisely, $\varphi X_t = \theta \varepsilon_t$.

Results from both a Poisson and a negative binomial (i.e., a Poisson random variable with a gamma distrusted mean) revealed that the explanatory covariate coefficients were highly significant, but furnished virtually no predictive power. In other words, the sizes of the population denominators were not sufficient to result in statistically significant relationships, while the detected relationships were inconsequential.

Next, an Autoregressive Integrated Moving Average (ARIMA) analysis of individual time-series related data feature attribute revealed a conspicuous but, not very prominent first-order temporal autoregressive structure in the sampled data. Therefore, a random effects term was specified with the monthly time series data. This random effects specification revealed a non-constant mean across the study site that were variable which represented a district-constant across time. This specification also represented a district-specific intercept term that was a random deviation from the overall intercept term as it was based on a draw from a normal frequency distribution. This random intercept represented the combined effect of all omitted seasonal covariate coefficients that caused some georeferenced interventional villages to be more prone to onchocerciasis prevalence than other villages. Inclusion of a random intercept assumed random heterogeneity in the riverine –based villages propensity or

underlying risk of onchocerciasis prevalence that persisted throughout the entire duration of the time sequence under study.

Table 1 presents the values for this random effects term, district-level for prevalence regressed on predicted prevalence rates. The Poisson mean response specification was mu = exp[a + re+ LN(population)] , Y ~Poisson(mu). The mixed-model estimation results included: a = = exp[-2.9147 + (random effect)i] where P(S-W) = 0.0005 and the Pseudo-R2 = 0.3103.This random effects term displayed no spatial autocorrelation, and failed to closely conform to a bell-shaped curve. Its variance implied a substantial variability in the prevalence of malaria across the sampled districts in the study site. The estimated model contained considerable overdispersion (i.e., excess Poisson variability): quasi-likelihood scale = = 69.565.Using this data a seasonal predictive S. damnosum s.l. – related map was constructed.

A spatial filter algorithm was then constructed where: $y = XB + E$ was written with a first-order spatially autocorrelated difference as :$y(l - \rho W) = (1 - \rho W)XB + E$; hence $y = XB + (1 - \rho W)^{-1}E$. The term: $(1 - \rho W)^{-1}$ was the spatial filter. Similarly, the mixed spatial lag model: $y = \rho Wy + XB + E$ was written with a first-order spatially autocorrelated difference as: $y(1 - \rho W) = XB + E$. A pure spatial autoregressive model simply consists of a spatially lagged version of the dependent variable (McCulloch and Searle, 2005). A typical stochastically autocorrelated spatial variable can then be modified by a spatially lagged autocorrelated variable (Jacob, et., 2012). Both PSA and NSA eigenvectors were then selected by a stepwise regression procedure. To expand the inferential basis with a random effect, a generalized linear mixed model (GLMM) was then used to account for latent non-spatial residual correlation. GLMM estimation was computed using PROC NLMIXED. Randomized effects in multivariate linear models can be estimated using PROC NLMIXED with an adaptive quadrature. Gaussian quadrature in PROC NLMIXED using georeferenced seasonal-sampled aquatic larval habitat observational explanatory predictor covariate coefficient estimates of S. damnosum s.l.. The estimated model enabled generating accurate forecasts of an arbitrary function by using the parameter estimates and the empirical Bayes estimates of the random effects. In this research, PROC NLMIXED fit the specified nonlinear mixed model by maximizing an approximation using the likelihood integrated over the random effects in the sampled S. damnosum s.l. data. The variances of the random-effects parameter estimators became the covariance parameters in the predictive autoregressive habitat distribution model. Additionally, PROC NLMIXED appointed the standard errors in the model using the first derivative of the function (i.e., delta method).

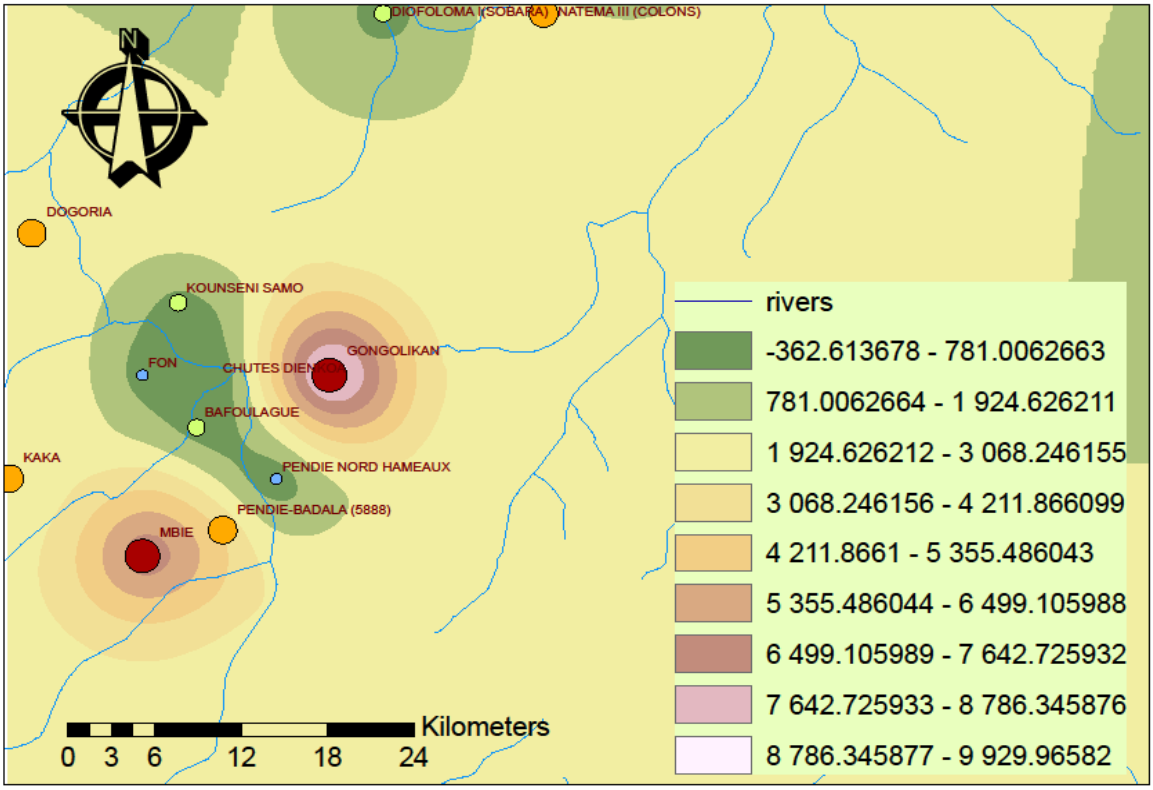

Fig. 4. A predicted autoregressive seasonal endemic S. damnosums.l. –related risk map.

Spatial autocorrelation was evaluated among the ecological datasets of the S. damnosum s.l. explanatory predictor covariate coefficient estimates sampled in the study site in order to evaluate the distribution of the georeferenced indicator variables to determine the randomness of the observed patterns. It was proposed to approximate the moments of Moran's I by means of incorporating the spatiotemporal-sampled riverine habitat parameter estimators into the covariance matrix of the model to obtain a less biased test. Covariance matrix is a square matrix whose diagonal entries are the variances and whose off-diagonal entries are the covariances between the row column labeling variable (Toe et al., 1997). Therefore, neighboring georeferenced S. damnosum s.l. habitats in the study site were identified based on the spatiotemporal field -sampled adult count values. The formulation for the Moran's index of spatial autocorrelation used in this research was: $I(x) = \frac{n\sum_{(2)} W_{ij}(x_i-\bar{x})(x_j-\bar{x})}{\sum_{(2)} W_{ij}\sum_{i=1}^{n}(x_i-\bar{x})^2}$ where $\sum_{(2)} = \sum_{i=1}^{n}\sum_{j=1}^{n}$ with $i \neq j$. The values W_{ij} were spatial weights stored in the symmetrical matrix [i.e., $W_{ij} = W_{ji}$] that had a null diagonal (W_{ii}). In this research, a Moran's Index value near +1.0 indicated clustering while an index value near -1.0 indicated dispersion. Moran's I value and a Z score can be used to evaluate the significance of the index value (Gosper et al., 1972). Z scores are measures of standard deviation that can help decide whether or not to reject the null hypothesis.

In this research, the weighted matrices was initially generalized to an asymmetrical matrix W where it was a stochastic matrix that expressed each observed seasonal sampled S. damnosum s.l. habitat value yi as a function of the average of habitat location i's nearby field-sampled counts which allowed a single autoregressive parameter, ρ, to have a maximum value of 1 [27]. Matrix W was generalized by a non-symmetric matrix W * by using $= (W^* + W^{*T})/2$. Usually, this matrix is symmetric (Wij=Wji), but it can be generalized to a non-symmetric matrix W by using $W = (W^* + W^{*T})/2$ [17]. Moran's I was then rewritten using the matrix notation: $I(x) = \frac{n}{1^t W 1}\frac{x^T HHWHHx}{x^T HHx} = \frac{n}{1^t W 1}\frac{x^T HWHx}{x^T Hx}$, (2.2) where $H = (I - 11^T/n)$ was an orthogonal projector verifying that $H = H^2$, i.e., H was independent.

In this research we quantified the heteroskedastic disturbances in the S. damnosum s.l. ArcGIS/SAS-based models using the model specification $\sum = \left[\left(I - <\rho>_{diag} W'\right)\left(I - <\rho>_{diag} W\right)\right]^{-1}\sigma^2$ (2.5) where the diagonal

matrix of autoregressive parameters, $<\rho>_{diag}$, contained two parameters: ρ_+ for those georeferenced habitat pairs at the riverine study site displaying positive spatial dependency, and ρ for those habitat pairs displaying negative spatial dependency. When a mixture of positive and NSA is present in the data, a more explicit representation of both effects leads to a more accurate interpretation of empirical results [17]. For example, letting $\sigma^2 = 1$ and employing a 2-by-2 regular square tessellation: $\sum = \left[\begin{pmatrix}1&0&0&0\\0&1&0&0\\0&0&1&0\\0&0&0&1\end{pmatrix} - \begin{pmatrix}\rho_+&0&0&0\\0&\rho_+&0&0\\0&0&\rho_-&0\\0&0&0&\rho_-\end{pmatrix}\begin{pmatrix}0&\frac{1}{2}&\frac{1}{2}&0\\\frac{1}{2}&0&0&\frac{1}{2}\\\frac{1}{2}&0&0&\frac{1}{2}\\0&\frac{1}{2}&\frac{1}{2}&0\end{pmatrix}\right]^2$ for the vector $\begin{pmatrix}y_1\\y_2\\y_3\\y_4\end{pmatrix}$, enabled posited a positive relationship between the seasonal-sampled S. damnosum s.l. habitats by the individual-sampled georeferenced observational explanatory predictor covariates coefficients, y_1 and y_2, a negative relationship between the sampled covariate coefficients, y_3 and y_4, and on no relationship between covariate coefficients y1 and y3 and between y_2 and y_4. This covariance matrix specification then yielded the expression$= \mu(I - \rho_+ Y < I_+ >_{diag} - \rho_- < I_- >_{diag})1 + (\rho_+ < I_+ >_{diag} + \rho_- < I_- >_{diag})WY + \varepsilon$ (2.6) where I_+ was a binary 0-1 indicator variable which denoted those georeferenced observational explanatory predictor variables displaying positive spatial dependency, and I_- was a binary 0-1 indicator variable denoting those habitats displaying negative spatial dependency, with $I_+ + I_- = 1$.

.

In this research if either $\rho_+ = 0$ and hence $I_+ = 0$ and $I_- = 0$) or $I_- = 0$ and $I_+ = I$, then equation (2.3) reduced to equation (2.1). This indicator variable classification was parsimoniously constructed in accordance with the quadrants of the corresponding Moran scatterplot in ArcGIS generated using the sampled georeferenced data attributes By graphically portraying the relationship between two quantitative sampled observational explanatory predictor covariate coefficients measured for the same habitat, a the scatterplot related the numerical value generated by a correlation coefficient formula. The Moran's scatterplot was based upon expression $P(Y_i = 1|X_i) = \exp(X_i\beta) / [1 + (X_i\beta)]$ (2.7), where β was the (K+1)-by-1 vector of non-redundant parameters and $P(Y_i = 0|X_i) = 1 - P(Y_i = 1|X_i)$. Independent Bernoulli outcomes were then denoted by $Y_i = 0$ or 1, taken at a sampled habitat locations i = 1, 2, …, n, at the study site .These indicator variables were then denoted by the spatiotemporal seasonal field and remote-sampled S. damnosum s.l. observational explanatory predictor variables using Xi, a 1-by-(K+1) vector of K covariate values and a 1(for the intercept term for i.). We also used the simplest form of this expression: $P(Y_i = 1|X_i) = P(Y_i = 1|\alpha) \exp(\alpha) / [1 + (\alpha)]$, for a constant α using a bivariate regression notation. The constant probability across the spatiotemporal seasonal -sampled riverine larval habitat georeferenced observational explanatory predictor covariate coefficient estimates was then described by β0 in a multiple regression notation, where $P(Yi = 1| \alpha) \to 0$ as $\alpha \to -\infty$, $P(Yi = 1| \alpha) \to 0.5$ as $\alpha \to 0$, and $P(Yi = 1| \alpha) \to 1$ as $\alpha \to \infty$

A Morans scatterplot was then generated based on The SAS/GIS spatial database consisted of the SAS data sets that contained the time series-dependent sampled S.damnosums.l. geocoordinates which identified information of seasonal attribute features in the ecological datasets. A spatial entry (i.e.,a SAS catalog entry of type GISSPA) identified which SAS datasets contained the spatial information. The spatial entry also stored the sampled elements based on the composites that defined how the riverine-sampled habitat explanatory predictor variables in the seasonal sampled spatial data defined the boundaries of area layers for constructing the predictive risk map (i.e;, polygonal indexes). A lattice hierarchy then defined which feature attributes in the seasonal S.damnosums.l. data were enclosed by the sampled covariates (i.e., the relationships among the S.damnosums.l. polygonal variables). The spatial entry alternatively contained references to the spatial entries that were subsequently merged into a single spatial database. A coverage entry (i.e., a SAS catalog entry of type GISCOVER) then selected a subset of the spatial data that was then available for display in a predictive autoregressive endemic risk map format. Thereafter, SAS catalog entries of type GISLAYER identified the time-series dependent S.damnosums.l. Seasonal features attributes that had common characteristics and, additionally, specified how they were displayed as layers in the predictive endemic risk map. We also used a SAS catalog entry of type GISMAP which specified which layers from a particular coverage were included in the autoregressive predictive risk map. The map entry then stored the names of the sampled feature attribute data variables that were associated with the predictive risk map, along with definitions of how the sampled variables were linked to the data and the name

of the SAS dataset that contained the labels for the mapped endemic features. Various GIS actions were then performed employing the seasonal mapped features data attributes which were then used for generating definitions for map legends values for display. We also created new SAS/GIS spatial databases from the sampled riverine-village based spatial data in other formats by interactively employing the GIS Spatial Data Importing window and then programmatically employing the SAS/GIS Batch Import process. Figure 5 portrays scatterplots of observed versus predicted prevalence rates for selected months, and reflects the considerable amount of noise in the MBR-related prevalence data feature attributes as well as the random effects term accounting for about a third of the variance in the space-time series of onchocerciasis prevalence. Based on the sampled district level random effects model was generated. As with most statistical procedures, the random effects term corresponded more closely with the data in the center of the time-series. This goodness-of-fit feature implied that although the random effects term can be used for predictive purposes, it is less effective for lengthy (e.g. > 1 year) forecasts for mapping endemicity up from 0 to 15km.After 15km the model revealed excessive noise indicating no endemicity.

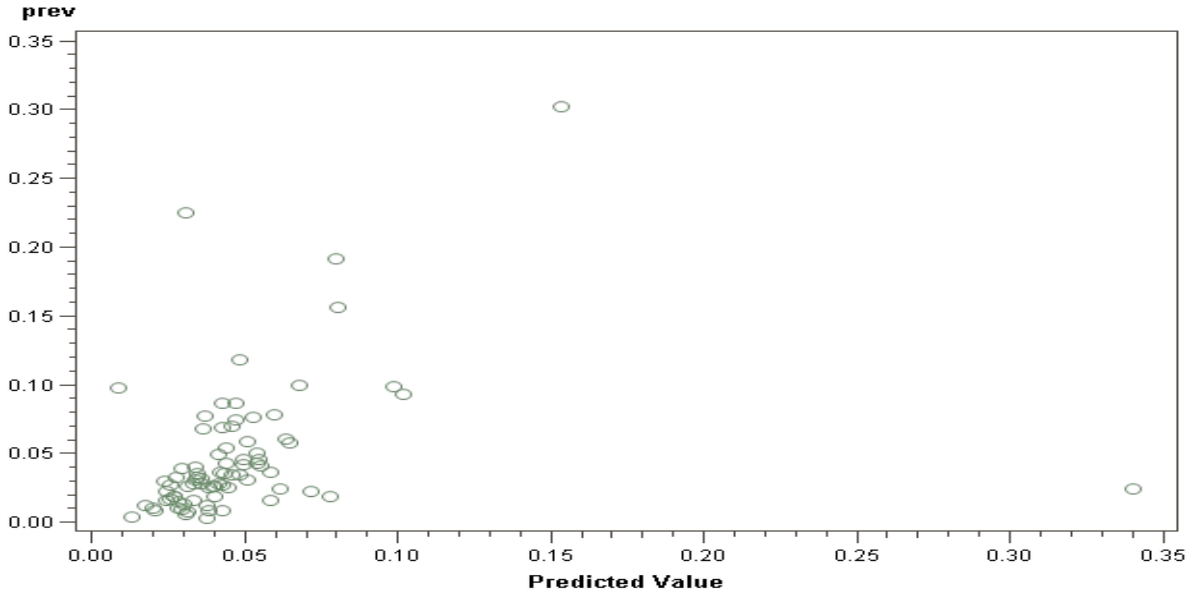

Fig. 5. Scatterplots of selected observed versus predicted S. damnosum s.l. endemic transmission-oriented values past 15km from the capture point.

The dependency in our model was then qualitatively assessed using random effect specifications. Random effects model specifications address samples for which independent observations are selected in a highly structured rather than random way, and involve repeated measures in frequentist analyses (Toe et al., 1997). This average, however, in this research, ignored both spatial and serial uncertainty correlation coefficients in the space-time series. A random effects model essentially works with these averages, adjusting them in accordance with the correlational structure latent in their parent space-time series, as well as their simultaneous estimation (Boatin et al., 1997). For example, in this research, the random effects model specification was achieved by fitting a distribution with as few parameter estimators as possible (e.g., a mean and a variance for a bell-shaped curve), rather than n means (i.e., fixed effects) for the n sampled riverine study site georferenced locational attributes (e.f., village stratified prevalence rates) . Consequently, a relationship existed between the time-series means and the random effects in the predictive seasonal S.damnosums.l. model (Figure 6.a). This random effects specification included n indicator variables, each for a separate specific district local intercept (i.e., one local intercept was arbitrarily set to 0 to eliminate perfect multicollinearity with the global mean). Here, the local mean for was set to 0. The estimated global mean was -3.6723, the mean of the random effects term was -0.0010, and the mean of the local means was 0.4837; the sum of these three values was -[-2.9147] which in this research was exactly the same as the random effects global mean. The scatterplot of the random effects versus the local intercepts corresponded to a straightly line with no dispersion about it. By using a random effect specification we were able to predict onchocerciasis prevalence rates and seasonal-sampled S. damnosums.l., throughout the riverine study site. The

following predictive equation was then employed to forecast the expected value of the prevalence of onchocerciasis for the surrounding interventional villages: prevalence= exp[-[-2.9147 + (random effect)i] .

4. Discussion

Initially, we constructed a Poisson and a negative binomial regression models in PROC GEN MOD for examining all latent autocorrelation error coefficients in a spatiotemporal S. damnosum s.l. endemic risk transmission-oriented model for a riverine study site in Burkina Faso. In the endemic transmission-oriented ArcGIS/SAS-based model risk model, a discrete stochastic prevalence-oriented predictor variable was defined to have a Poisson distribution with parameter λ>0, if for k = 0, 1, 2, (e.g., spatiotemporal-sampled S.damnosum s.l. capture point Euclidean-count values) while the pmf was provided by: $f(k;\lambda) = \Pr(X = k) = \frac{\lambda^k e^{-\lambda}}{k!}$ where e is the base of the natural logarithm (e = 2.71828...) and k! was the factorial of k.. In probability theory and statistics, the pmf is a function that gives the probability that a discrete random variable is exactly equal to some value (Toe et al., 1997). The mode of a Poisson-distributed multiseasonal -sampled S. damnosum s.l.-related randomized explanatory predictor variables with a non-integer λ was then be equal to $\lfloor \lambda \rfloor$, which would then essentially be the largest integer less than or equal to λ in the model. Hence, all of the cumulants of the Poisson distribution in the geopredictive onchocerciasis endemic transmission-oriented model would be equal to the expected value λ calculated at each sampled interventional study site regardless of location or the value of the Poison multi-seasonal-sampled count data. By so doing, the seasonal-sampled explanatory predictor covariate coefficients of variation in the Poisson-specified multi-seasonal S. damnosum s.l. related regression risk-based model could be quantitated as $\lambda^{-1/2}$ while the index of dispersion was be 1. Thereafter, the mean deviation about the mean in the model was expressed as $\mathrm{E}\,|X - \lambda| = 2\exp(-\lambda)\frac{\lambda^{\lfloor\lambda\rfloor}}{\lfloor\lambda\rfloor!}$ for determining the statistical significance of the regressed explanatory covariate coefficients.

The PROC GENMOD procedure estimated the sampled parameters of the model numerically through an iterative fitting process. The dispersion parameter ϕ was then estimated by MLE thereafter by tabulating the residual deviance by Pearson's chi-square and dividing by the degrees of freedom (d.f). The deviance for our spatiotemporal onchocerciasis endemic transmission-oriented predictive linear risk map model (e.g.,M0) based on an empirical dataset (i.e., y) was then defined as $D(y) = -2\Big(\log\left(p(y|\hat{\theta}_0)\right) - \log\left(p(y|\hat{\theta}_s)\right)\Big)$. Here $\hat{\theta}_0$ denoted the fitted values of the sampled parameter estimators in the endemic-transmission-oriented model M0, while $\hat{\theta}_s$ denoted the fitted parameters for the "full model" (i.e., "saturated model"). If we let κ be a finite or infinite cardinal number and M a model in some first-order language, then M is called κ-saturated if for all subsets A ⊆M of cardinality less than κ, M realizes all complete types over A(Nielsen, 1897) The model M is called saturated if it is |M|-saturated where |M| denotes the cardinality of M (Toe et al., 1997) In our research, fitted values were implicitly functions of the sampled endemic transmission-oriented explanatory covariate coefficient indicator observational values (i.e., y). Here the full model was a model with a parameter for every sampled S. damnosum s.l. observation so that the data were fitted exactly. This expression was simply −2 times the log-likelihood ratio of the reduced model compared to the full model. The deviance was then used to construct various GLMs where it performed a similar role to the residual variance commonly derived from linearly quantitating the time series dependent S. damnosum s.l. ANOVA in linear models (RSS).Interestingly our GLM, had two nested sub- models, M1 and M2. M1 contained the parameters in M2, and k additional sampled S. damnosum s.l. related parameters. As such, under the null hypothesis that M2 was the true model, the difference between the deviances for the predictive l endemic transmission model followed an approximate chi-squared distribution with k-degrees of freedom. It is important to note that although usage of the term "deviance"[i.e., $-2\log\left(p(y|\hat{\theta}_0)\right)$s]. By so doing we were able to generate viable covariances, standard errors, and p-values while computing the sampled observational predictor based on the asymptotic normality of the MLE.

Fortunately, in our model construction process, a simple recursive method was useful for linearally characterizing Poisson process functionals which required only the use of conditional probability in the robust spatiotemporal S. damnosum -related regression based risk model distribution. A simple recursive method is useful for characterizing Poisson -derived process functionalism solely employing the conditional probability estimates

(Jacob, et., 2012). By so doing, the generating function of the Touchard polynomials in the spatiotemporal S. damnosum s.l. predictive endemic regression-based risk model was expressed as $\sum_{n=0}^{\infty} \frac{T_n(x)}{n!} t^n = e^{x\left(e^t-1\right)}$. Thereafter, the contour-integral representation of the seasonal-sampled parameter estimators was summarized for optimizing the residual parameter uncertainty estimation employing $T_n(x) = \frac{n!}{2\pi i} \oint \frac{e^{x(e^t-1)}}{t^{n+1}}\, dt$. In the future, Touchard polynomials may be used for constructing spatiotemporal linear predictive S. damnosum s.l. regression risk ArcGIS/SAS-based model building employing the real part of the integral, to an non-integer order by intuitively applying: $T_n(x) = \frac{n!}{\pi} \int_0^{\pi} e^{x\left(e^{\cos(\theta)} \cos(\sin(\theta))-1\right)} \cos\left(x e^{\cos(\theta)} \sin(\sin(\theta)) - n\theta\right) \mathrm{d}\theta$ [see 2].

A SAR and a spatial filter model specification was then constructed to help describe selected Gaussian and Poisson random variables rendered from the linear-based S.damnosum s.l. model residuals. When coupled with regression equations and a normal probability model, an autoregressive specification can result in a covariation term characterizing autocorrelation uncertainty components in empirical datasets of field and remote-sampled georeferenced explanatory covariate coefficient estimates (Boatin et al., 1997). A eigenfunction decomposition spatial filtering analysis was then performed by constructing a linear combination of a subset of the eigenvectors of a modified geographically weighted matrix. We attempted to generate a subset of eigenvectors by selecting a stepwise regression procedure. In this research, the SAR used a response variable, Y, as a function of nearby sampled Y riverine village-level values [i.e., an autoregressive response], and/or the model residuals of Y was a function of nearby Y sampled model covariate coefficient estimate [i.e., spatial error specification].

In this research we defined a right eigenvector as a column vector $\mathbf{X}_R$ for satisfying $\mathsf{A}\,\mathbf{X}_R = \lambda_R\,\mathbf{X}_R$, where A was the seasonal predictive S. damnosum s.l. autoregressive matrix, so $(\mathsf{A} - \lambda_R\,\mathsf{I})\,\mathbf{X}_R = \mathbf{0}$, which meant the right eigenvalues rendered had zero determinants, [i.e., $\det(\mathsf{A} - \lambda_R\,\mathsf{I}) = 0$.] Similarly, we defined a left eigenvector as a row vector $\mathbf{X}_L$ satisfying $\mathbf{X}_L\,\mathsf{A} = \lambda_L\,\mathbf{X}_L$. Taking the transpose of each side in the risk model $(\mathbf{X}_L\,\mathsf{A})^{\mathrm{T}} = \lambda_L\,\mathbf{X}_L{}^{\mathrm{T}}$, we then re-wrote the autoregressive equation as $\mathsf{A}^{\mathrm{T}}\,\mathbf{X}_L{}^{\mathrm{T}} = \lambda_L\,\mathbf{X}_L{}^{\mathrm{T}}$. Thereafter, we rearranged the endemic transmission-orienetd model and obtained $\left(\mathsf{A}^{\mathrm{T}} - \lambda_L\,\mathsf{I}\right)\mathbf{X}_L{}^{\mathrm{T}} = \mathbf{0}$, which meant $\det\left(\mathsf{A}^{\mathrm{T}} - \lambda_L\,\mathsf{I}\right) = 0$. By rewriting the endemic transmission-oriented model the spatiotemporal-sampled residuals also rendered $0 = \det\left(\mathsf{A}^{\mathrm{T}} - \lambda_L\,\mathsf{I}\right) = \det\left(\mathsf{A}^{\mathrm{T}} - \lambda_L\,\mathsf{I}^{\mathrm{T}}\right) = \det(\mathsf{A} - \lambda_L\,\mathsf{I})^{\mathrm{T}} = \det(\mathsf{A} - \lambda_L\,\mathsf{I})$, where the last step after quantitating a viable identity was $\det(\mathsf{A}) = \det\left(\mathsf{A}^{\mathrm{T}}\right)$. Equating ($\diamondsuit$) and $\det(\mathsf{A}) = \det\left(\mathsf{A}^{\mathrm{T}}\right)$. in the seasonal S. damnosum s.l. risk model revealed that they were both equal to 0 for arbitrary A and X , therefore the predictive autoregressive framework required that $\lambda_R = \lambda_L \equiv \lambda$, (i.e., left and right eigenvalues had to be equivalent which was not true for the eigenvectors in the model). We then let $\mathbf{X}_R$ be a matrix formed by the columns of the right eigenvectors and $\mathbf{X}_L$ be a matrix formed by the rows of the left eigenvectors. Thereafter, we let $\mathsf{D} \equiv \begin{bmatrix} \lambda_1 & \cdots & 0 \\ \vdots & \ddots & \vdots \\ 0 & \cdots & \lambda_n \end{bmatrix}$. By so doing, $\mathsf{A}\,\mathbf{X}_R = \mathbf{X}_R\,\mathsf{D}$ and $\mathbf{X}_L\,\mathsf{A} = \mathsf{D}\,\mathbf{X}_L$ and $\mathbf{X}_L\,\mathsf{A}\,\mathbf{X}_R = \mathbf{X}_L\,\mathbf{X}_R\,\mathsf{D}$ and $\mathbf{X}_L\,\mathsf{A}\,\mathbf{X}_R = \mathsf{D}\,\mathbf{X}_L\,\mathbf{X}_R$, thus $\mathbf{X}_L\,\mathbf{X}_R\,\mathsf{D} = \mathsf{D}\,\mathbf{X}_L\,\mathbf{X}_R$. But this equation was not of the form CD=DC where D was a diagonal matrix , so thus we could not achieve $\mathsf{C} \equiv \mathbf{X}_L\,\mathbf{X}_R$. In particular since A was a symmetric matrix then the left and right eigenvectors rendered from the S. damnosums.l. risk model were not transposed and as such A was not a self-adjoint matrix (i.e., Hermitian) and the left and right eigenvectors were not adjoint matrices where D was a diagonal matrix. If A is a symmetric matrix, then the left and right eigenvectors are simply each other's transpose, and if A is a self-adjoint matrix (i.e., it is Hermitian), then the left and right eigenvectors are adjoint matrices (Toe et al., 1997).In mathematics, an Hermitian matrix is a square matrix with complex entries that is equal to its own conjugate transpose – that is, the element in the i-th row and j-th column is equal to the complex conjugate of the element in the j-th row and i-th column, for all indices i and j: $a_{ij} = \overline{a_{ji}}$. Fortunately, the Hermitian property in this research was written concisely as $A = A^{\dagger}$. Our model revealed that that if the conjugate transpose of a spatially autoregressive seasonal predictive S. damnosum s.l. –related matrix A can be denoted by $A^{\dagger}$ covariate significance levels can be attained. Further,

since every Hermitian S. damnosum s.l. –related matrix is a normal matrix, and then the finite-dimensional spectral theorem can be applied for targeting endemic regions.

The spectral theorem states that if we let A be an operator on a finite-dimensional inner product space A is said to be normal if A* A = A A*.(McCulloch and Searle, 2005) Therefore, an infectious disease vector ecologist or local abatement district manager can show that A is normal if and only if it is unitarily diagonalizable by employing the Schur decomposition, The Schur decomposition reads as follows: if A is a n × n square matrix with complex entries, then A can be expressed as $A = QUQ^{-1}$ where Q is a unitary matrix . Therefore the inverse Q−1 would be conjugate transpose Q* of Q , in a spatiotemporal predictive S. damnosum s.l. –related endemic transmission-oriented model where U is an upper triangular matrix, (e.g., Schur form of A) (Toe et al., 1997).This U would be similar to A in the endemic model since it would have the same multiset of eigenvalues, and since it is triangular, those eigenvalues are the diagonal entries of U. The Schur decomposition implies that there exists a nested sequence of A-invariant subspaces {0} = V0 ⊂ V1 ⊂ ... ⊂ Vn = Cn, and that there exists an ordered orthonormal basis (for the standard Hermitian form of Cn) such that the first i basis vectors span Vi for each i occurring in the nested sequence(McCulloch and Searle, 2005). Phrased somewhat differently, the first part of the theoreum states that an operator T on a complex finite-dimensional vector space stabilizes a complete flag (V1,...,Vn). Therefore T must be diagonal in the S. damnosum s.l. regression-based model since normal upper triangular matrices would be diagonal. The converse can also be quantitated. For example, A is normal in a time series S. damnosum s.l. geopredictive model if, and only if, there exists a unitary matrix U such that $A = UDU^*$ where D is a diagonal matrix. Then, the entries of the diagonal of D would be the eigenvalues of A. The column vectors of U would then be the eigenvectors of A and they are orthonormal. Unlike the Hermitian case, the entries of D need not be real.

While an n x n matrix from a seasonal S. damnosum s.l. risk model always has n eigenvalues, some or all of which may be degenerate. For example, traditionally in autoregressive vector arthropod-borne seasonal predictive models (e.g., S. damnosums.l. risk ArcGIS/SAS model) the matrix $\begin{bmatrix} 1 & 1 \\ 0 & 1 \end{bmatrix}$ has only the single eigenvector $(1, 0)$. Eigenvectors may be computed using eigenvectors that are not linearly independent which then can be returned as zero vectors. Eigenvectors and eigenvalues can then be used for risk based endemic transmission-oriented modeling for delineating important onchocerciasis transmission zones based on prolific MBR prevalence related rates. For example; given a spatiotemporal S. damnosum s.l. risk-based 2x2 matrix A with eigenvectors $\mathbf{x}_1$, $\mathbf{x}_2$, and $\mathbf{x}_3$ and corresponding eigenvalues λ_1, λ_2, and λ_3, then an arbitrary vector $\mathbf{y}$ can be written $\mathbf{y} = b_1 \mathbf{x}_1 + b_2 \mathbf{x}_2 + b_3 \mathbf{x}_3$. Applying the matrix $\mathbf{A}$, $\mathbf{A}\,\mathbf{y} = b_1 \mathbf{A}\,\mathbf{x}_1 + b_2 \mathbf{A}\,\mathbf{x}_2 + b_3 \mathbf{A}\,\mathbf{x}_3 = \lambda_1 \left(b_1 \mathbf{x}_1 + \frac{\lambda_2}{\lambda_1} b_2 \mathbf{x}_2 + \frac{\lambda_3}{\lambda_1} b_3 \mathbf{x}_3 \right)$, then $\mathbf{A}^n \mathbf{y} = \lambda_1^n \left[b_1 \mathbf{x}_1 + \left(\frac{\lambda_2}{\lambda_1} \right)^n b_2 \mathbf{x}_2 + \left(\frac{\lambda_3}{\lambda_1} \right)^n b_3 \mathbf{x}_3 \right]$. If, $\lambda_1 > \lambda_2, \lambda_3$, and $b_1 \neq 0$, therefore follows in the seasonal predictive autoregressive model residuals that that $\lim_{n \to \infty} \mathbf{A}^n \mathbf{y} = \lambda_1^n b_1 \mathbf{x}_1$, so repeated application of the matrix to an arbitrary vector would result in a vector proportional to the eigenvector with largest eigenvalue. By so doing, a heirachary of covariates maybe generated from a S. damnosums.l.risk map remotely targeting specific pathogen transmission zones (e.g., hyperendemic regions).

In this research, we utilized a function which defined all the spatiotemporal-sampled predictive S. damnosum s.l. endemic transmission model residuals which were Lipschitz continuous with the Lipschitz constant K = 1, as it was differentiable and the absolute value of the derivative was bounded above by 1. Likewise, the sine function was Lipschitz continuous and its derivative, the cosine function, was bounded above by 1 in the absolute value estimation in the endemic model. The function f(x) = |x| was then defined then on the sampled endemic transmission-oriented model which were Lipschitz continuous with the Lipschitz constant equal to 1, by the reverse triangle inequality. The reverse triangle inequality is an elementary consequence of the triangle inequality that gives lower bounds instead of upper bounds. For plane geometry the statement is: Any side of a triangle is greater than the difference between the other two sides.(Haight, 1967) In the case of a normed vector space, the statement is: $\Big| \|x\| - \|y\| \Big| \leq \|x - y\|$, or for metric spaces, | d(y, x) − d(x, z) | ≤ d(y, z). This implies that the norm ||−|| in our predictive spatiotemporal S. damnosum s.l. riverine endemic transmission-oriented model as

well as the distance function d(x, –) were Lipschitz continuous with Lipschitz constant 1, and therefore were in particular uniformly continuous.

The proof for the reverse triangle employs the regular triangle inequality,and $\|y-x\| = \|-1(x-y)\| = |-1|\|x-y\| = \|x-y\|$
$\|x\| = \|(x-y)+y\| \leq \|x-y\| + \|y\| \Rightarrow \|x\| - \|y\| \leq \|x-y\|,$
$\|y\| = \|(y-x)+x\| \leq \|y-x\| + \|x\| \Rightarrow \|x\| - \|y\| \geq -\|x-y\|.$ (McCulloch and Searle, 2005) Combining

$$-\|x-y\| \leq \|x\| - \|y\| \leq \|x-y\| \Rightarrow \Big|\|x\| - \|y\|\Big| \leq \|x-y\|.$$

these two statements, however, renders :
which interestingly is a Lipschitz continuous function that may not be differentiable in a spatiotemporal-sampled predictive S. damnosum s.l. endemic transmission model. More generally, a norm on a vector space is Lipschitz continuous with respect to the associated metric in the endemic transmission model with the Lipschitz constant would equal to 1.But , a differentiable function in the model,(e.g., g : R → R) would be Lipschitz continuous (with K = sup |g′(x)|) if, and only if, it has bounded first derivative; one direction follows from the mean value theorem. In particular, any continuously differentiable function is locally Lipschitz, as continuous functions in a spatiotemporal-sampled predictive S. damnosum s.l. endemic transmission model are locally bounded so its gradient would also be locally bounded as well. A Lipschitz function g : R → R is absolutely continuous and therefore is differentiable almost everywhere, that is, differentiable at every point outside a set of Lebesgue measure zero(Haight, 1967). Its derivative in the predictive S. damnosum s.l. endemic transmission model residual would then be essentially bounded in magnitude by the Lipschitz constant, and for a < b, the difference g(b) − g(a) which then would be equal to the integral of the derivative g′ on the interval [a, b]. Conversely, if ƒ : I → R is absolutely continuous and thus differentiable almost everywhere in the endemic model residuals, and satisfies |ƒ′(x)| ≤ K for almost all x in I, then ƒ is Lipschitz continuous with Lipschitz constant at K. More generally, Rademacher's theorem would extend the differentiability result to Lipschitz mappings between Euclidean spaces: a Lipschitz-related spatiotemporal-sampled predictive S. damnosum s.l. endemic transmission risk map ƒ : U → Rm, where U is an open set in Rn, is almost everywhere differentiable. Moreover, if K is the best Lipschitz constant of ƒ, then $\|Df(x)\| \leq K$ whenever the total derivative Dƒ exists in the model.

There is a version of Rademacher's theorem that holds for Lipschitz functions from a Euclidean space into an arbitrary metric space in predictive S. damnosum s.l. endemic transmission model in terms of metric differentials instead of the usual derivative For example, suppose that $\{f_n\}$ is a sequence of Lipschitz spatiotemporal S. damnosum s.l. model continuous mappings between two Euclidean-distance -based metric spaces, and that all f_n have Lipschitz constant bounded by some K. If fn converges to a model for endemic mapping ƒ uniformly, then ƒ is also Lipschitz, with Lipschitz constant bounded by the same K. In particular, this implies that the set of real-valued functions in the model would be a compact metric space with a particular bound for the Lipschitz constant which would be a closed and convex subset of the Banach space of continuous functions in the model. This result will not hold however, for sequences in which the functions in the spatiotemporal-sampled endemic transmission model may have unbounded Lipschitz constants. In fact, the space of all Lipschitz functions in such a model would have an impact on a compact metric space which then would be i dense in the Banach space of continuous functions which in turn would be an elementary consequence of the Stone–Weierstrass theorem. The statement of the approximation theorem as originally is as follows: Suppose ƒ is a continuous complex-valued function defined on the real interval [a,b] (Toe et al., 1997). For every ε > 0, there exists a polynomial function p over C such that for all x in [a,b], we have | ƒ(x) − p(x) | < ε, or equivalently, the supremum norm || ƒ − p || < ε. If ƒ is real-valued, the polynomial function can be taken over R(McCulloch and Searle, 2005).

As a consequence of the Weierstrass approximation theorem, an infectious disease vector ecologist or local abatement district manager can show that the space C[a,b] is separable spatiotemporal-sampled predictive S. damnosum s.l. endemic transmission risk model when the polynomial functions are dense, and each polynomial function is uniformly approximated by one with rational coefficients. Unfortunately, there are only countably many polynomials with rational coefficients which may delineate onchocercsis endemic transmission zones .For example Since C[a,b] is Hausdorff and separable it follows that C[a,b] has cardinality equal to $2^{\aleph_0}$ — the same cardinality as the cardinality of the reals (sampled. riverine endemic transmission-oriented estimators) may be applicable in a spatiotemporal-sampled predictive S. damnosum s.l. risk map. A version of the Stone–Weierstrass theorem may also be also true when X in the endemic model is only locally compact. If we let C0(X, R) be the space of real-

valued continuous functions on X which vanish at infinity; that is, a continuous function f is in C0(X, R) if, for every ε > 0, there exists a compact set K ⊂X such that f < ε on X \ K.(Nielsen, 1897) C0(X, R) is a Banach algebra with the supremum norm(Toe et al., 1997). Also A subalgebra A of C0(X, R) is said to vanish nowhere if not all of the elements of A simultaneously vanish at a point; that is, for every x in X, there is some f in A such that f(x) ≠ 0. The theorem would then generalize as follows in spatiotemporal-sampled predictive S. damnosum s.l. endemic transmission-oriented risk map: Suppose X is a locally compact Hausdorff space and A is a subalgebra of C0(X, R) in the endemic model then A would be considerably dense in C0(X, R) given the topology of uniform convergence if and only if it separates georeferenced points (village stratified prevalence data). This version clearly implies the previous version in the case when X is compact, since in that case C0(X, R) = C(X, R) in the predictive S. damnosum s.l. model. In topology and related branches of mathematics, a Hausdorff space, separated space or T2 space is a topological space in which distinct points have disjoint neighborhoods(Toe et al., 1997). Of the many separation axioms that can be imposed on a topological space, the "Hausdorff condition" (T2) is the most frequently used and discussed as It implies the uniqueness of limits of sequences, nets, and filters (Nielsen, 1897).

Additionally, the Stone–Weierstrass theorem can be used to prove the following two statements which go beyond Weierstrass's result in spatiotemporal-sampled predictive S. damnosum s.l. endemic transmission risk map. For example, if f is a continuous real-valued function defined on the set [a,b] × [c,d] and ε > 0, then there exists a polynomial function p in two of the sampled endemic transmission explanatory predictor variables such that | f(x,y) − p(x,y) | < ε for all x in [a,b] and y in [c,d]. Additionally, if X and Y are two compact Hausdorff spaces and f : X×Y → R in the endemic transmission model which is a continuous function, then for every ε > 0 there exist n > 0 and continuous functions f1, f2, …, fn on X and continuous functions g1, g2, …, gn on Y such that || f − ∑figi || < ε. The theorem may also have other applications to analysis, including: Fourier series whereby a set of linear combinations of functions in spatiotemporal-sampled geopredictive onchocerciasis endemic transmission-oriented risk ArcGIS SAS-based map en(x) = e2πinx, n ∈Z is dense in C([0,1]/{0,1}). In such circumstances we can identify the endpoints of the interval [0,1] to obtain a circle. An important consequence of this would that the en in the model would be an orthonormal basis of the space L2([0,1]) of square-integrable functions on [0,1]. Additionally, every Lipschitz spatiotemporal-sampled geopredictive endemic transmission model continuous map would be uniformly continuous, and hence a fortiori continuous. More generally, a set of functions with bounded Lipschitz constant would forms an spatiotemporal-sampled predictive S. damnosum s.l. endemic transmission model equicontinuous dataset.

Further, the Arzelà–Ascoli theorem would imply that if $\{f_n\}$ is a uniformly bounded sequence of functions with bounded Lipschitz constant, in spatiotemporal-sampled predictive S. damnosum s.l. endemic transmission risk map then it would aslo may have a convergent subsequence. In simplest terms, the theorem can be stated as follows: Consider a sequence of real-valued continuous functions (ƒn)n∈N defined on a closed and bounded interval [a, b] of the real line. If this sequence is uniformly bounded and equicontinuous, then there exists a subsequence (ƒnk) that converges uniformly. As such , the limit function would also be Lipschitz, with the same bound for the Lipschitz constant spatiotemporal-sampled predictive S. damnosum s.l. endemic transmission model equicontinuous dataset. . In particular the set of all real-valued Lipschitz functions on a compact metric space X having Lipschitz constant ≤ K is a locally compact convex subset of the Banach space C(X). F

Many aspects of this research merit future research for constructing robust spatiotemporal-sampled predictive S. damnosum s.l. endemic transmission risk map especially involving the Banach space. For example, in this research a Banach space of bounded continuous functions $f(x) = f(x^1, ..., x^n)$ was defined on a set E of an n-dimensional Euclidean space in the predictive spatiotemporal S . damnosum s.l. riverine model .The residuals revealed that our model was able to satisfy a Hölder condition on E. but only if the Hölder space was calculated as $C_m(E)$, when $m \geq 0$ based on the sample endemic transmission-oriented explanatory covaraite coefficient integer- based values consisting of the functions that were m times continuously differentiable on E (i.e., continuous for m=0). Thus in the future, Hölder space in the model can be described by $C_{m+\alpha}(E), 0 < \alpha \leq 1$, where $m \geq 0$ is a spatiotemporal sampled predictive S . damnosum s.l. riverine ArcGIS/SAS endemic transmission-oriented model, consisting of the functions that are $m$times continuously differentiable (e.g., continuous for dry season m=0 counts) and whose m -th derivatives satisfy the Hölder condition with index α. The bounded E a norm could then theoretically be introduced in $C_m(E)$and $C_{m+\alpha}(E)$as follows:

$|f|_m = \|f, E\|_m = \sum_{|k|=0}^{m} \sup_{x \in E} |f^{(k)}(x)| f|_{m+\alpha} = \|f, E\|_{m+\alpha} = |f|_m + \sum_{|k|=m} \|f^{(k)}, E\|_\alpha, \quad k = (k_1, ..., k_n) k_j \geq 0$

$|k| = k_1 + \ldots + k_n, \quad f^{(k)}(x) = \frac{\partial^{|k|} f(x)}{\partial x_1^{k_1} \ldots \partial x_n^{k_n}}$. where, the sampled integer can be formally calculated employing The fundamental properties of Hölder spaces for a bounded connected domain in the time series dependent S. damnosum s.l. riverine endemic transmission-oriented model parameters (i.e., E is the closure of E) where: 1) $C_{m+\beta}(E)$ is imbedded in $C_{k+\alpha}(E)$ if, $0 \leq k + \alpha \leq m + \beta$, where k and m are the time series sampled covariate coefficient integers values $0 < \alpha \leq 1$, $0 \leq \beta \leq 1$ Here $|f|_{k+\alpha} \leq A|f|_{m+\beta}$ and the constant A would be independent of $f \in C_{m+\beta}(E)$. The unit sphere of $C_{m+\beta}(E)$ would be then compact for $C_{m+\alpha}(E)$ if, $0 < \alpha < \beta$. Consequently, any bounded set of functions in the endemic transmission-oriented predictive model residuals from $C_{m+\beta}(E)$ would contain a sequence of functions that converges in the metric of $C_{m+\alpha}(E)$ or, to a function of $C_{m+\alpha}(E)$. This would also hold for scalar functions on a compact metric space X in the predictive S. damnosum s.l. endemic transmission-oriented risk model for satisfying a Hölder condition with respect to the metric on X which then would delineate all ArcGIS-Euclidean distance –based endemic transmission-oriented explanatory covariate coefficients.

In gradient-descent methods, the parameter vector is a column vector with a fixed number of real valued components, $\vec{\theta}_t = (\theta_t(1), \theta_t(2), \ldots, \theta_t(n))^T$ (the T here denotes transpose), and $V_t(s)$ is a smooth differentiable function of $\vec{\theta}_t$ for all $s \in \mathcal{S}$. (se 5) Thus, if an infectious disease vector ecologist assumes that on each step t, a new S. damnosum s.l. endemic transmission-oriented parameter for, example $s_t \mapsto V^\pi(s_t)$ may be observed in the residuals. These states might be successive states from an interaction with the riverine environment. Even though the exact, correct values, $V^\pi(s_t)$ could be quantitated for each s_t, there would be still a difficult problem because our function approximator may have limited resources and thus limited resolution. In particular, there is generally no $\vec{\theta}$ that gets all the states, or even all the examples, exactly correct in a spatiotemporal onchocerciasis. endemic transmission-oriented model .

We may assume that states appear in examples with the same distribution, P, over which we are trying to minimize the MSE as given by in the spatiotemporal onchocerciasis endemic transmission-oriented model . A good strategy may then be to try to minimize error on the observed samples. A robust Gradient-descent methods would do this by adjusting the parameter vector in the endemic transmission model a by a small amount in the direction that would most reduce the error on that sample {e.g., $\vec{\theta}_{t+1} = \vec{\theta}_t - \frac{1}{2}\alpha \nabla_{\vec{\theta}_t} \left[V^\pi(s_t) - V_t(s_t)\right]^2 = \vec{\theta}_t + \alpha \left[V^\pi(s_t) - V_t(s_t)\right] \nabla_{\vec{\theta}_t} V_t(s_t)$, where α is a positive step-size parameter, and $\nabla_{\vec{\theta}_t} f(\vec{\theta}_t)$, for any function f, denotes the vector of partial derivatives, $(\frac{\partial f(\vec{\theta}_t)}{\partial \theta_t(1)}, \frac{\partial f(\vec{\theta}_t)}{\partial \theta_t(2)}, \ldots, \frac{\partial f(\vec{\theta}_t)}{\partial \theta_t(2)})^T$. This derivative vector would be then the gradient of f with respect to $\vec{\theta}_t$. in the onchocerciasis endemic transmission-oriented model . This is kind of gradient descent because the overall step in $\vec{\theta}_t$ is proportional to the negative gradient of the example's squared error. This may also be the direction in which the error falls most rapidly in the endemic model.

This research has revealed the values of specific calculus based functions for geomapping onchocerciasis endemic trasnmission zones based on emperical datasets of field and remote sampled S. damnsoum s.l. riverine larval habitat data attributes and local neighboring village prevalance rates. For example, generally, for spatiotemporal-sampled real-valued functions calculated from empirical seasonal datasets of georeferenced S. damnosum s.l. explanatory predictor variables, functions holds if, and only if ,the absolute value of the slopes of all secant lines are bounded by K. The set of lines of slope K passing through a point on the seasonal S. damnosum s.l. graph of the function (e.g., sampled georeferenced capture point) then would form the tip of a circular cone. Thereafter, a function could be classified as a Lipschitz in an endemic transmission-oriented model but, the graph of the function must lie completely outside of this cone. A function is called locally Lipschitz continuous if, for every x in X there exists a neighborhood U of x such that f restricted to U is Lipschitz continuous (Nielsen, 1897).

Equivalently, if X is a locally compact metric space in the geopredictive onchocerciasis endemic transmission-oriented model , then ƒ would be locally Lipschitz if, and only if, it is Lipschitz continuous on every compact subset of X. In spaces that are not locally compact in a endemic transmission-oriented model this would be necessary but not a sufficient condition. More generally, a function f defined on X would be classified as be Hölder continuous or, to satisfy a Hölder condition of order [e.g., α > 0 on X] in the spatiotemporal geopredictive.endemic transmission model, if there exists a constant M > 0 such that $d_Y(f(x), f(y)) \leq M d_X(x, y)^\alpha$ for all x and y in X in the residual forecasts.

Importantly if there exists a K ≥ 1 with $\frac{1}{K} d_X(x_1, x_2) \leq d_Y(f(x_1), f(x_2)) \leq K d_X(x_1, x_2)$ then f in a onchocerciasis endemic transmission oriented georpedictive model is bilipschitz A bilipschitz onchocerciasis related endemic transmission mapping is injective, and is in fact a homeomorphism onto its image. This bilipschitz function in the endemic transmission model would be the same as an injective Lipschitz function whose inverse function is also Lipschitz. Additionally, the surjective bilipschitz functions generated from this model would be isomorphic in metric spaces.

Further, the inequality would only be trivially satisfied in a spatiotemporal geopredictive onchocerciasis endemic transmission oriented model ArcGIS/SAS-based model at best especially if, x1 = x2. Otherwise, the vector ecologist is forced to equivalently define a function to be Lipschitz continuous but, this can only occur in the endemic model forecasts if, and only if, there exists a constant K ≥ 0 in the empirical time series dataset such that, for all x1 ≠ x2, [e.g., $\frac{d_Y(f(x_1), f(x_2))}{d_X(x_1, x_2)} \leq K$ A metric space then could be defined as an ordered pair (M, d) where M is a set and d is a metric on M, (i.e., a function $d\colon M \times M \to \mathbb{R}$ such that for any $x, y, z \in M$, the following holds: $d(x, y) \geq 0$ (non-negative), $d(x, y) = 0$ iff $x = y$ (i.e., identity of indiscernibles), $d(x, y) = d(y, x)$ (symmetry) and $d(x, z) \leq d(x, y) + d(y, z)$ (i.e., triangle inequality) . In a spatiotemporal onchocercisis endemic transmission-oriented model the first condition may then follow from the any other three, since $2d(x, y) = d(x, y) + d(y, x) \geq d(x, x) = 0$ .The function d (i.e., distance function) would be the most important criteria for determining and mapping onchocerciasis endemicity in ArcGIS. These methods are typically slower than gradient descent however they may aid in regressing ArcGIS Euclidean-distance based measurements for seasonally geographically mapping onchocerciasis endemicity

Introductio In this research we used the Lerch transcendent to express the Dirichlet beta function[1.e., $\beta(s) = \sum_{k=0}^{\infty} (-1)^k (2k+1)^{-s} = 2^{-s}\, \Phi\left(-1, s, \frac{1}{2}\right)$.] in the geopredictive spatiotemporal onchocerciasis endemic transmission-oriented model. In the future , a special case can be given by $\Phi(z, n, 1) = \frac{\mathrm{Li}_n(z)}{z}$, (7,8), where $\mathrm{Li}_n(z)$ is the polylogarithm. Special cases giving simple constants in a geopredictive endemic transmission-oriented model include $\Phi\left(-1, 2, \frac{1}{2}\right) = 4K$, $\frac{\partial \Phi}{\partial s}(-1, -1, 1) = \ln\left(\frac{A^3}{2^{1/3}\, e^{1/4}}\right)$, $\frac{\partial \Phi}{\partial s}(-1, -2, 1) = \frac{7\zeta(3)}{4\pi^2}$, $\frac{\partial \Phi}{\partial s}\left(-1, -1, \frac{1}{2}\right) = \frac{K}{\pi}$ where K is Catalan's constant, $\zeta(3)$ is Apéry's constant, and A is the Glaisher-Kinkelin constant.(McCulloch and Searle, 2005). This predictive endemic model outcome may provide the integrals of the Fermi-Dirac distribution $\int_0^\infty \frac{k^s\, dk}{e^{k-\mu} + 1} = e^\mu\, \Gamma(s+1)\, \Phi(-e^\mu, s+1, 1) = -\Gamma(s+1)\, \mathrm{Li}_{1+s}(-e^\mu)$, where $\Gamma(z)$ is the gamma function and $\mathrm{Li}_n(z)$ is the polylogarithm and Bose-Einstein distribution $\int_0^\infty \frac{k^s\, dk}{e^{k-\mu} - 1} = e^\mu\, \Gamma(s+1)\, \Phi(e^\mu, s+1, 1) = \Gamma(s+1)\, \mathrm{Li}_{1+s}(e^\mu)$. Thereafter, double integrals involving the Lerch transcendent could include $\int_0^1 \int_0^1 \frac{x^{u-1}\, y^{v-1}}{1 - x\, y\, z} [-\ln(x\, y)]^s\, dx\, dy$

$$= \Gamma(s+1)\,\frac{\Phi(z, s+1, v) - \Phi(z, s+1, u)}{u - v} \qquad \int_0^1 \int_0^1 \frac{(x\,y)^{u-1}}{1 - x\,y\,z}\,[-\ln(x\,y)]^s\,dx\,dy$$

$$= = \Gamma(s)\,\Phi(z, s+2, u),$$

where $\Gamma(z)$ is the gamma function(Toe et al., 1997). These formulas led to a variety of special cases of unit square integrals in the predictive spatiotemporal S. damnosum s.l. endemic transmission-oriented model. The residuals were then used to evaluate Dirichlet L-series. In mathematics, a Dirichlet L-series is a function of the form $L(s,\chi) = \sum_{n=1}^{\infty} \frac{\chi(n)}{n^s}.$ where χ is a Dirichlet character and s is a complex variable with real part greater than 1 (Jacob, et., 2012). By analytic continuation, this function may even be extended to a meromorphic function in a S. damnosum s.l. endemic transmission-oriented model on the whole complex Euclidean-distance based plane, (i.e., a Dirichlet L-function).

n

In conclusion results from both a Poisson and a negative binomial regression (i.e., a Poisson random variable with a gamma distrusted mean) revealed that the village-level seasonal-sampled explanatory covariate coefficients were highly significant, but furnished virtually no predictive power. In other words, the sizes of the population denominators were sufficient to result in statistically significant relationships, while the detected relationships were inconsequential. Inclusion of indicator variables denoting the time sequence and the district geolocation spatial structure was then articulated with Thiessen polygons which also failed to reveal meaningful estimates. Unfortunately, the presence of additional noise in the data did not allow for forecasting the seasonal-sampled S.damnosum s.l data employing an eigendecomposition spatial filter algorithm. Thereafter, an ARIMA analysis of the sampled related time-series revealed a conspicuous but not very prominent first-order temporal autoregressive structure in the data. As such, a random effects term was specified with the monthly time series. This random intercept represented the combined effect of all omitted covariates that caused some of the georefernced villages to be more prone to the onchocerciasis prevalence than other villages. The random effects term displayed no spatial autocorrelation, and failed to closely conform to a bell-shaped curve. The variance, however, implied a substantial variability in the prevalence of onchocerciasis across districts. The estimated model contained considerable overdispersion (i.e., excess Poisson variability).The following equation was then generated to forecast the expected value of the prevalence of malaria for district: prevalence =exp [-[-2.9147 + (random effect)i] .The goodness-of-fit feature implied that the random effects term can be used for forecasting purposes. The model however, also indicated the autoregressive residuals were less effective for forecasting purposes especially for a relatively lengthy time. Compilation of additional data can allow continual updating of the random effects term estimates, allowing rolling in new-data informed resulted to bolster the quality of the predictions for future time-series dependent S. damnosum s.l. -related seasonal modeling efforts. The asymptotic distribution of the resulting residual adjusted predictor error autocovariate uncertainty coefficients were then established while estimates of the asymptotic variance lead to the construction of approximate confidence intervals for accurately targeting productive S. damnosum s.l. habitats based on spatiotemporal field-sampled count data. Varying and constant coefficient regression models, , sub-meter resolution satellite imagery, a robust residual intra-cluster diagnostic test, eigendecomposition spatial filter algorithms, and Bayesian matrices could enable accurate autoregressive estimation of latent uncertainty affects and other residual error probabilities (i.e. heteroskedasticity) for testing correlations between georeferenced S. damnosum s.l. riverine larval habitat estimators.

References

Boatin, B., Molyneux, D.H., Hougard, J.M., Christensen O.W., Alley, E.S., Yaméogo, L., Seketeli, A., Dadzie, K.Y., 1997. Patterns of epidemiology and control of onchocerciasis in West Africa. J. Helminthol., 71 (7), 91–101.

de la Vallée Poussin, C., 1898. Sur les valeurs moyennes de certaines fonctions arithm´etiques, Annales de la soci´et´e sci. Bruxelles., Vol. 22, , 84–90.

Gosper, W., Beeler, M., Gosper, R.W., eds, S., 1972. MIT Artificial Intelligence Laboratory, Memo AIM-239, Cambridge. Massachussetts., pp. 55.

Griffith, D.A., 1897. Spatial autocorrelation and spatial filtering: Gaining understanding through theory and scientific visualization," Springer-Verlag, Berlin, 2003.N.Nielsen, EenRaekke for Euler's Konstnat, Nyt.Tidssfor Math., Vol.8B, pp.10-12.

Haight, F.A., 1967. Handbook of the Poisson Distribution, Wiley Press, New York.

Jacob, B.G., Novak R.J., Toe, L., Sanfo, S.M., Afriyne, A.N., Ibrahim, Mohammed G.D.A., Unnasch T.R., 2012. Quasi-likelihood techniques in a logistic regression equation for identifying Simulium damnosum sl. larval habitats intra-cluster covariates in Togo. Geo-spat. Inform. Sci., 15(2), p. 117-133.

McCulloch, C.E., Searle, S.R., 2005. Generalized, Linear and Mixed Models; Wiley-Interscience: New York, NY.

Nielsen, N., 1897. Een Raekke for Euler's Konstant. Nyt. Tidss. for Math., 8B, 10-12.

Sondow, Zudilin, W., 2006. Euler's Constant, q -Logarithms, and Formulas of Ramanujan and Gosper, Ramanujan J., Vol. 12, pp. 225-244.

Toe, L., Tang, J., Back, C., Katholi, C.R., Unnasch, T.R., 1997. Vector-Parasite Transmission Complexes for Onchocerciasis in West Africa. Lancet., 349, 163–166.